Responses of mouse skeletal muscle to endurance exercise

Functional, metabolic, and genomic adaptations

Maartje de Snoo

Cover design Anton van Woerkom
Lay out Maartje de Snoo
Printed by Atalanta Drukwerkbemiddeling, Houten

de Snoo, M.W. Responses of mouse skeletal muscle to endurance exercise. Functional, metabolic, and genomic adaptations.
PhD thesis, Faculty of Veterinary Medicine, Utrecht University, 2009

ISBN 978-90-393-5090-4

Responses of mouse skeletal muscle to endurance exercise

Functional, metabolic, and genomic adaptations

Het effect van duurtraining op skeletspieren van de muis

Functionele, metabole en genetische aanpassingen

(met een samenvatting in het Nederlands)

Proefschrift

ter verkrijging van de graad van doctor aan de
Universiteit Utrecht op gezag van de
rector magnificus, prof. dr. J.C. Stoof, ingevolge het besluit van het
college voor promoties in het openbaar te verdedigen op
woensdag 24 juni 2009 des middags te 4.15 uur

door

Maartje Willemijn de Snoo

geboren op 13 mei 1978
te Groningen

Promotor: Prof. dr. M.E. Everts

Table of contents

Chapter I

General introduction

SKELETAL MUSCLE constitutes 30-50% of total body mass -the largest organ system of the body-, and plays an important role in posture maintenance and locomotion. During physical activity it becomes the major determinant of energy use. Regular physical activity is known to improve common well-being and is associated with changes in skeletal muscle in response to the enhanced physical demand. Adaptations in skeletal muscle in response to endurance exercise include improved oxygen utilization capacity and improved energy metabolism, all improving fatigue resistance. The molecular basis of these adaptations in skeletal muscle is still largely unclear, despite extensive research on skeletal muscle adaptation. The present thesis focuses on functional, metabolic and genomic adaptations of endurance exercised mouse skeletal muscle.

1.1 Skeletal muscle anatomy and physiology

One skeletal muscle is build up of multiple bundles containing several muscle fibers themselves. One muscle fiber, in turn, is made up from myofibrils. Skeletal muscles can be roughly divided into two categories; 1) Muscles that generate high power for a limited period. 2) Muscles that generate low force but with high endurance capacity. The total constitution of muscle fibers in one muscle determines its function [1].

Myofibrils, multinucleated cylindrical cells, constitute the major contractile proteins: actin and myosin [2]. Sliding of these filaments will result in shortening of the myofibril [3]. Shortening of all, or at least a majority, myofibrils will induce a contraction of the muscle. Myosins are the active sliding filaments, and have a head, neck and a tail domain. The head domain is linked to actin and is hydrolyzed under influence of ATP which results in moving of the head, and thus, shortening of the myofibril. Myosin contains two 'heavy' chains that constitute the head and tail domain. Four 'light' chains bind the head and neck domain in the neck domain. Myosin heavy chain (MyHC) is the largest protein of skeletal muscle, accounting for approximately 40% of total protein content [4].

Adult MyHC can be distinguished as type I and type II [1, 5], based on histochemical staining properties. Fibers composed of type I are typically slow contracting, have low force output, and have a high endurance capacity [1]. Type II fibers have high shortening velocities, high force production, but are limited fatigue resistant. Based on mATPase histochemical and immunohistochemical staining properties, MyHC II can further be specified as IIa, IIX, and IIb; IIb being the fastest, IIa the slowest [1]. Muscles mainly composed of type I fibers are so-called slow-oxidative. They are well suited for endurance exercise, and are well supplied by blood vessels to provide oxygen to the muscle [1]. Hence, they are also referred to as red skeletal muscles. Muscles mainly composed of type IIb fibers are fast-glycolytic. They can generate very high power, but have only limited time to sustain this performance [1]. They are also referred to as white muscles due to the poor blood supply. Most muscles, however, are a mixture of all fibers to fulfill specific demands.

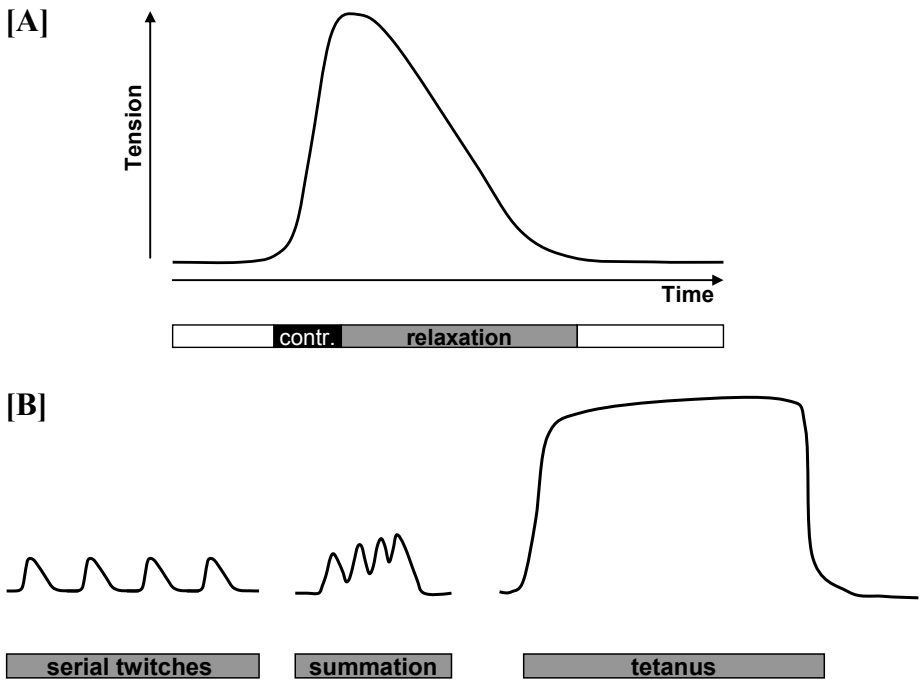

Figure 1.1 A A muscle twitch is the response of skeletal muscle to a single short threshold stimulus. The contraction time is the time during which tension is developed, while the relaxation time comprises the time needed to fully relax. **B** At low stimulation frequencies, serial twitches can be observed. More rapid stimulations –before termination of the first twitch- causes a subsiding twitch at higher force than the previous one. Complete tetanus is reached when the firing frequency is thus high that a decrease in tension can not be observed. It results in the highest power output of a skeletal muscle.

1.2 Muscle contraction

A group of muscle fibers is innervated by one motoneuron. The complex of one motoneuron and its related fibers is called a motor unit. A stimulus from the central nervous system leads to an action potential from the motoneuron, resulting in release of acetyl choline (Ach) from the neuron. ACh binds to ACh-receptors on the skeletal muscle membrane which induces depolarization. Depolarization of the membrane initializes Ca^{2+} release from the sarcoplasmic reticulum (SR), a Ca^{2+} store within the skeletal muscle fiber through the ryanodine receptor (RyR) [6]. The released Ca^{2+} ions combine with troponin C which forces tropomyosin to roll off the actin filament

active sites, exposing myosin [5]. Subsequently, myosin forms a cross-bridge with actin, pulls the actin and thus shortens the actin-myosin complex [7]. Repeating these steps will lead to shortening of the muscle. The 'walking' of myosin over actin is performed under hydrolysis of ATP, the main energy storage and transfer molecule. More specifically, myosin binds to actin due to the increased intracellular Ca^{2+} concentration. The bending of the myosin head pulls the actin and generates force. Only when ATP is hydrolyzed to ADP + P_i the myosin head can bend back to its initial state and the cycle can be repeated.

After contraction, Ca^{2+} is removed from the filaments and actively pumped back into the SR by SR Ca^{2+} ATPase (SERCA) [8]. For every two Ca^{2+} ions that are pumped back, one ATP needs to be hydrolyzed. The intracellular Ca^{2+} concentration drops, and tropomyosin rolls back over the actin filament, relieving the binding of actin and myosin. This terminates the contraction and thus induces relaxation. In skeletal muscle, two isoforms of SERCA exist; SERCA1 is the typical isoform present in fast-twitch fibers, while SERCA2 is predominantly expressed in slow-twitch muscle fibers [9-11]. PLB inhibits SERCA2 function while phosphorylation of PLB relieves the inhibitory effect [12, 13]. On the other hand, SLN is described to inhibit both SERCA1 as well as SERCA2 [14, 15].

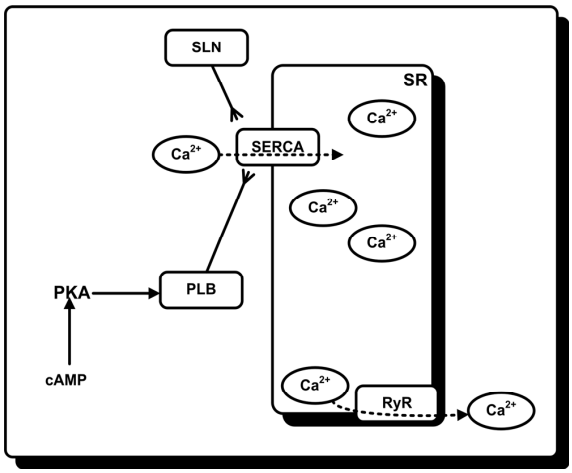

Figure 1.2 Schematic overview of Ca^{2+} handling in the sarcoplasmic reticulum (SR). Upon stimulation, Ca^{2+} is released from the SR through the ryanodine receptor (RyR). The release of Ca^{2+} induces contraction, and activates several other signaling pathways. Contraction is ended when Ca^{2+} is pumped back into the SR through SERCA. SERCA is inhibited by sarcolipin (SLN) and phospholamban (PLB). Phosphorylation of these regulatory proteins relieves the inhibitory effect, and thus promotes SERCA function.

1.3 Energy metabolism

ATP plays a crucial role in skeletal muscle contraction, and is the most important energy transfer molecule in mammals. It consists of one adenosine molecule with three phosphate groups. Hydrolysis of one ATP phosphate group results in production of ADP and P_i and provides the energy needed for skeletal muscle to contract. During exercise, ATP is produced by phosphorylation of ADP. Three pathways can be distinguished for the production of ATP [16].

1) The most direct, and thus fastest, form of ADP phosphorylation into ATP results from creatine phosphate in the myoplasm. Creatine phosphate availability is restricted and thus it only provides a very limited source of ATP production. As such, this pathway functions as a buffer to provide ATP only directly after onset of contractions. 2) A second pathway for ATP production results from anaerobic glycolysis. It uses glucose -produced from glycogen- as a substrate for ADP phosphorylation under non-aerobic circumstances. The resultant production of ATP further leads to production of lactate from pyruvate. Muscle glycogen stores are quickly depleted limiting this pathway. However, this pathway provides a rapid energy source for the contracting skeletal muscle, and is typically seen in the fast-twitch MyHC IIb fibers. 3) Finally, ATP can be produced from ADP by oxidative phosphorylation. The main energy source for this pathway comes from fatty acid oxidation. This is the most efficient way to produce ATP, and, albeit a slow process, it can be sustained for extended periods. As stated, this pathway depends on the supply of oxygen which takes place in the mitochondria. It is the typical ATP source in the slow-twitch MyHC I fibers.

Role of cytokines

Cytokines are a class of regulatory proteins involved in the immune response. However, cytokines have also been demonstrated to play a role during exercise without muscle damage [17-19], thus under noninflammatory conditions. In this respect, interleukin-6 has well been documented; it is suggested that endurance exercise promotes production of IL-6 in skeletal muscle, which is subsequently released into the circulation, promoting lipolysis and glucose output from adipose tissue and liver [reviewed in 20]. Direct effects on skeletal muscle would increase fatty acid and glucose uptake

and utilization. As such, it serves a beneficial role in energy metabolism by providing additional substrates during exercise.

1.4 Exercise

Exercise is defined as: 'physical activity that is planned, structured, and repetitive for the purpose of conditioning any part of the body'. Roughly, two types of exercise can be distinguished; strength and endurance exercise. The first is associated with increased muscle strength and mass, and includes resistance and high-speed sprint training [21, 22]. The latter improves cardiac output and endurance performance and is known to improve common well-being. More specifically, it is associated with the prevention and treatment of cardiac disorders, diabetes, obesity, etc [23-25]. Endurance exercise is an aerobic form of exercise meaning that the extensive duration capacity relies on oxygen supply to the skeletal muscle. It demands low power output, but the activity can normally be performed for an extensive time period. Typical forms of endurance exercise include running, cycling, swimming, and rowing, all of which require total body performance.

1.5 Skeletal muscle plasticity

Development

During embryonic development, skeletal muscles are formed by fusion of primary and secondary myotubes. Each of these two populations induces MyHC isoform expression. The first isoform expressed is embryonic MyHC, which is replaced by a neonatal isoform around birth [1]. During early development of mammals, neonatal MyHC expression is reduced, while adult MyHC expression (i.e. I, IIa, IIx, and IIb) is upregulated [26, 27]. The resultant MyHC phenotype of each skeletal muscle is a mixture of type I and II fibers.

Further changes during postnatal maturation include transitions in myosin light chain expression, and Ca^{2+} regulatory proteins [1]. One of these is SERCA: the predominant isoform expressed during late fetal and early neonatal skeletal muscle is SERCA2 [28]. This isoform is gradually replaced by the SERCA1 in muscles developing fast-twitch properties, while it remains in slow-twitch muscles. Changes in maturing skeletal muscle do not necessarily occur in synchrony, and may proceed or follow MyHC development.

Exercise

As stated before, slow-oxidative muscles are well designed for endurance exercise, while fast-glycolytic muscles are well suited for strength exercise. Skeletal muscle phenotype is genetically determined and establishes one's exercise capabilities. However, skeletal muscle shows an enormous plasticity to adapt to stimuli.

Endurance exercise is dependent on oxygen supply to the muscle. One of the first adaptations to regular endurance exercise thus typically leads to an increase in blood supply to the muscle fiber, as well as an increase in mitochondria to increase oxygen supply [29-31]. Likewise, glycogenolysis is stimulated in order to increase the energy pool to the skeletal muscle [31, 32]. Further, an increase in Ca^{2+} ATPase is responsible for skeletal muscle's capacity to relax after contraction which is associated with increases in SERCA concentration [33, 34]. The time and extend to which these changes occur depend on duration, length, and extension of the exercise [35].

An extreme regime might further result in fiber type shifting; strenuous endurance exercise leads to a fiber shift from MyHC type II to type I [35, 36], while a slow-to-fast (type I to II) fiber type shift is observed during weight restriction in e.g. space flights and long-term bed rest [37, 38].

High intensity sprinting exercise has been regarded as high power exercise associated with a slow-to-fast fiber type transformation. However, high intensity *interval* sprint training in human has been demonstrated to induce an endurance-exercise type adaptation [39, 40], suggesting that repetitive bouts of sprint exercise compare to endurance-type training.

Molecular regulation of skeletal muscle adaptation

The precise mechanisms how skeletal muscle adapts toward enhanced physiological demands are still largely unknown. Extensive research has revealed several pathways that are related to these changes. A rise in intracellular Ca^{2+} is essential to generate force in the skeletal muscle [41]. Further, adaptational changes in skeletal muscle have also been attributed to increases in intracellular Ca^{2+}. The elevation of Ca^{2+} during repeated contractions results in the activation of two key downstream Ca^{2+}/calmodulin (CaM)-dependent signaling pathways. The first is regulated through activation of calcineurin (CnA), also known as protein phosphatase 2B, while the second is modulated by calcium/CaM-dependent protein kinase II (CaMKII).

Activation of CnA regulates nuclear factor of activated T cells (NFAT) and myocyte enhancer factor 2 (MEF2) [42, 43], both of which result in activation of target proteins that encode oxidative-type muscle protein and proteins responsible for muscle growth.

Activation of the CnA/NFAT signaling pathway is associated with prolonged low-frequency Ca^{2+} transients [44], typically associated with slow-twitch fibers [45]. Activation of CaMKII in response to increases in $[Ca^{2+}]_i$ induces mitochondrial biosynthesis through activation of proliferator-activated receptor gamma co-activator 1 (PGC-1) [46-48]. Conversely, CaMKII activity has also been demonstrated during hypertrophic growth and muscle atrophy [49].

The relation of these two pathways to each other and to other pathways is still not completely understood, as downstream target genes might have controversial effects on skeletal muscle signaling.

1.6 Models of investigation

Extensive research has focused on skeletal muscle adaptation. Traditionally, the fast-to-slow transition has been induced by evoking chronic low-frequency stimulation in *in situ* fast-twitch muscles [50]. Most frequently used models for these studies are larger laboratory animals, like rabbits. Under anesthesia, the tibialis anterior is prepared so that the tendons at the distal end can be attached to a force transducer while the remainder of the muscle itself is still connected to the animal. This system provides a reproducible and standardized program of contractions where the contralateral muscle can serve as a standardized control. Furthermore, the blood –and thus oxygen- supply, is provided by the animal itself due to the *in situ* situation. Unfortunately, this protocol does not compare to the *in vivo* situation.

Other options to study the mechanism of skeletal muscle adaptation include biopsies taken from exercising objects [51-54]. This is usually performed in human subjects, before, during, and after the exercise protocol. These experiments have the advantage of a controlled *in vivo* situation that can study short-term as well as long-term effects. Typical examples include knee-bending or controlled cycling experiments, respectively [52, 55]. Especially during cycling experiments, the power output can be controlled by the observer. However, biopsies have to be taken, associated with inconvenience by the study subject. Further, results of these studies may display

large differences between subjects due to heterogeneity of the human population. Therefore, one-legged experiments are sometimes performed so that the contralateral leg can serve as a control [52], although this differs from natural movement patterns.

Studies in smaller rodents -rats and mice-, have proven an excellent model to study the adaptation processes associated with endurance exercise [56, 57]. These animals can easily be handled due to their small size, and can easily be trained in treadmills or running wheels or even in water by swimming [58]. Furthermore, these animals reproduce quickly providing an easy opportunity to work with homogenous groups. Finally, the advent of transgenic technology and its vast potential to study the involvement of specific genes and their splice products put the mouse as a favorable animal to investigate the mechanistic basis for these adaptations [59-62] .

1.7 Rodent hindlimb muscles

Mouse hindlimbs constitute five major muscles; the tibialis anterior and extensor digitorum longus (EDL) comprise the shin muscles, used for dorsiflexion and inversion of the foot. The gastrocnemius, soleus, and plantaris muscles form the calf muscles that are plantar-flexors of the foot. The tibialis anterior is the largest shin muscle and consists of a mixture of myofibers [63, 64]. The EDL, on the other hand, is a very small muscle typically consisting of fast-twitch fibers [65]. Of the calf muscles, the gastrocnemius is the largest. It has two distinct 'heads', one red –slow-twitch- and one white –fast-twitch. The plantaris is located between the gastrocnemius and soleus muscle and is mostly formed of fast-twitch fibers [66]. The soleus is typically regarded as a slow-twitch muscle, composed of a large portion of MyHC I fibers [65]. Like the EDL muscle, it is a very small muscle.

Mouse EDL and soleus muscles have been intensively investigated in skeletal muscle adaptation studies as typical fast-twitch versus slow-twitch muscles. Their dimensions and geometry make them highly suitable for superfused stimulation experiments of isolated muscle [67-69].

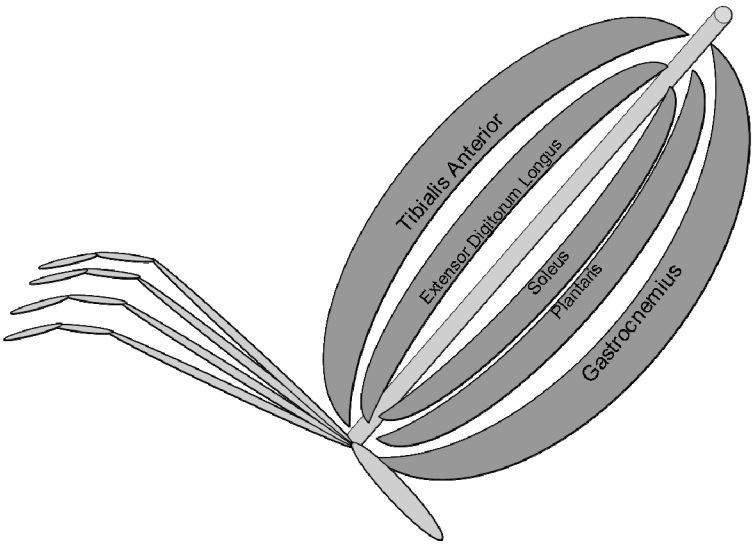

Figure 1.3 Schematic overview of mouse hindlimb muscles

1.8 Aims of the study

The aim of the present study was to obtain better understanding of skeletal muscle adaptation in exercising mice. This was performed by combining a six week *in vivo* exercise protocol with physiological contraction parameters of *in vitro* skeletal muscle, as well as with biochemical analysis of skeletal muscle proteins.

The following questions were addressed:

1) Both treadmill and running wheel exercise are associated with endurance-type running, although they typically consist of different running patterns. The question is how these exercise modalities affect skeletal muscle mechanical performance, and which of these has the greatest influence on this performance?
2) Mice with access to a running wheel device can run voluntarily and thus at their own pace, while during treadmill running mice are forced to run for a sustained period. In order to understand running wheel exercise-induced skeletal muscle adaptation, the question is: What is the running pattern of voluntarily running mice?
3) Many studies –including our own- on mouse skeletal muscle adaptation are performed in young animals that are still developing. The

question is whether aging affects skeletal muscle adaptation and if running wheel exercise influences these results.

4) What genes, or subset of genes, are affected by running wheel exercise? Can we reveal which of the two main signaling pathways (CaN/NFAT or CaMKII) is activated in fast-twitch or in slow-twitch muscle?

1.9 Outline of this thesis

Chapter two compares the effects of forced treadmill and voluntary wheel running exercise. Mice were sacrificed after the six-week experimental period. Contraction parameters and oxygen consumption of isolated EDL muscles were determined during serial stimulation. These data were combined with analysis of MyHC profile.

Chapter three gives a detailed analysis of the running pattern of mice during six weeks of voluntary running wheel exercise. Mice were sacrificed after the experimental period and the slow-twitch soleus muscle was dissected. Data on serial twitch contraction parameters were combined with analysis of MyHC profile and of SERCA and its regulators.

In chapter four the developmental changes in mouse soleus and EDL muscle were analyzed during aging and running wheel exercise. The particular focus was on SERCA distribution and of its regulatory proteins. Mice were sacrificed at the age of 4 weeks, and at 8 and 10 weeks with or without running wheel exercise.

Chapter five focuses on the genetic profile of skeletal muscle. Mice were subjected to six weeks of running wheel exercise, and soleus and EDL muscles were isolated. A whole genome wide microarray was performed on RNA from these muscles and genes were ordered based on the probability that they were indeed affected by running wheel exercise.

In chapter six the role of interleukin-6 (IL-6) in running wheel-exercised mice was elucidated. Blood samples were collected from mice during the experimental period, and IL-6 plasma levels were determined. Hindlimb muscles isolated from the animals after the experimental period were tested on IL-6 mRNA levels.

Chapter seven integrates all findings from the previous chapters and provides answers to the questions raised in this thesis.

1.10 References

1. Pette, D. and R.S. Staron, *Mammalian skeletal muscle fiber type transitions*. Int Rev Cytol, 1997. **170**: p. 143-223.
2. Cooke, R., *Actomyosin interaction in striated muscle*. Physiol Rev, 1997. **77**(3): p. 671-97.
3. Patel, T.J. and R.L. Lieber, *Force transmission in skeletal muscle: from actomyosin to external tendons*. Exerc Sport Sci Rev, 1997. **25**: p. 321-63.
4. Warrick, H.M. and J.A. Spudich, *Myosin structure and function in cell motility*. Annu Rev Cell Biol, 1987. **3**: p. 379-421.
5. Schiaffino, S. and C. Reggiani, *Molecular diversity of myofibrillar proteins: gene regulation and functional significance*. Physiol Rev, 1996. **76**(2): p. 371-423.
6. Fill, M. and J.A. Copello, *Ryanodine receptor calcium release channels*. Physiol. Rev., 2002. **82**(4): p. 893-922.
7. Oosawa, F., *The unit event of sliding of the chemo-mechanical enzyme composed of myosin and actin with regulatory proteins*. Biochem Biophys Res Commun, 2008. **369**(1): p. 144-8.
8. Wu, K.D., et al., *Localization and quantification of endoplasmic reticulum Ca(2+)-ATPase isoform transcripts*. Am J Physiol, 1995. **269**(3 Pt 1): p. C775-84.
9. Brandl, C.J., et al., *Two Ca2+ ATPase genes: homologies and mechanistic implications of deduced amino acid sequences*. Cell, 1986. **44**(4): p. 597-607.
10. Korczak, B., et al., *Structure of the rabbit fast-twitch skeletal muscle Ca2+-ATPase gene*. J Biol Chem, 1988. **263**(10): p. 4813-9.
11. Zarain-Herzberg, A., D.H. MacLennan, and M. Periasamy, *Characterization of rabbit cardiac sarco(endo)plasmic reticulum Ca2(+)-ATPase gene*. J Biol Chem, 1990. **265**(8): p. 4670-7.
12. James, P., et al., *Nature and site of phospholamban regulation of the Ca2+ pump of sarcoplasmic reticulum*. Nature, 1989. **342**(6245): p. 90-2.
13. Jorgensen, A.O. and L.R. Jones, *Localization of phospholamban in slow but not fast canine skeletal muscle fibers. An immunocytochemical and biochemical study*. J Biol Chem, 1986. **261**(8): p. 3775-81.
14. Tupling, A.R., M. Asahi, and D.H. MacLennan, *Sarcolipin overexpression in rat slow twitch muscle inhibits sarcoplasmic reticulum Ca2+ uptake and impairs contractile function*. J Biol Chem, 2002. **277**(47): p. 44740-6.
15. Vangheluwe, P., et al., *Sarcolipin and phospholamban mRNA and protein expression in cardiac and skeletal muscle of different species*. Biochem J, 2005. **389**(Pt 1): p. 151-9.
16. Berne, R.M. and M.N. Levy, *Skeletal Muscle Physiology, chapter 18*. Physiology, 3rd edt, 1993: p. 292-308.
17. Steinacker, J.M., et al., *New aspects of the hormone and cytokine response to training*. Eur J Appl Physiol, 2004. **91**(4): p. 382-91.
18. Febbraio, M.A. and B.K. Pedersen, *Muscle-derived interleukin-6: mechanisms for activation and possible biological roles*. FASEB J., 2002. **16**(11): p. 1335-1347.
19. Croisier, J.L., et al., *Effects of training on exercise-induced muscle damage and interleukin 6 production*. Muscle Nerve, 1999. **22**(2): p. 208-12.

20. Glund, S. and A. Krook, *Role of interleukin-6 signalling in glucose and lipid metabolism.* Acta Physiol (Oxf), 2008. **192**(1): p. 37-48.
21. Young, W.B., *Transfer of strength and power training to sports performance.* Int J Sports Physiol Perform, 2006. **1**(2): p. 74-83.
22. Fry, A.C., *The role of resistance exercise intensity on muscle fibre adaptations.* Sports Med, 2004. **34**(10): p. 663-79.
23. Sharman, J.E. and M. Stowasser, *Australian Association for Exercise and Sports Science Position Statement on Exercise and Hypertension.* J Sci Med Sport, 2009.
24. Vella, C.A. and R.A. Robergs, *A review of the stroke volume response to upright exercise in healthy subjects.* Br J Sports Med, 2005. **39**(4): p. 190-5.
25. Ascensao, A., R. Ferreira, and J. Magalhaes, *Exercise-induced cardioprotection--biochemical, morphological and functional evidence in whole tissue and isolated mitochondria.* Int J Cardiol, 2007. **117**(1): p. 16-30.
26. Agbulut, O., et al., *Myosin heavy chain isoforms in postnatal muscle development of mice.* Biology of the Cell, 2003. **95**(6): p. 399-406.
27. Adams, G.R., et al., *Time course of myosin heavy chain transitions in neonatal rats: importance of innervation and thyroid state.* Am J Physiol Regul Integr Comp Physiol, 1999. **276**(4): p. R954-961.
28. Arai, M., et al., *Regulation of sarcoplasmic reticulum gene expression during cardiac and skeletal muscle development.* Am J Physiol, 1992. **262**(3 Pt 1): p. C614-20.
29. Sexton, W.L., *Vascular adaptations in rat hindlimb skeletal muscle after voluntary running-wheel exercise.* J Appl Physiol, 1995. **79**(1): p. 287-96.
30. Salmons, S. and J. Henriksson, *The adaptive response of skeletal muscle to increased use.* Muscle Nerve, 1981. **4**(2): p. 94-105.
31. Holloszy, J.O. and E.F. Coyle, *Adaptations of skeletal muscle to endurance exercise and their metabolic consequences.* J Appl Physiol, 1984. **56**(4): p. 831-8.
32. Suh, S.H., I.Y. Paik, and K. Jacobs, *Regulation of blood glucose homeostasis during prolonged exercise.* Mol Cells, 2007. **23**(3): p. 272-9.
33. Kubo, H., et al., *Differential effects of exercise training on skeletal muscle SERCA gene expression.* Med Sci Sports Exerc, 2003. **35**(1): p. 27-31.
34. Schertzer, J.D., et al., *Mechanisms underlying increases in SR Ca^{2+}-ATPase activity after exercise in rat skeletal muscle.* Am J Physiol Endocrinol Metab, 2003. **284**(3): p. E597-610.
35. Demirel, H.A., et al., *Exercise-induced alterations in skeletal muscle myosin heavy chain phenotype: dose-response relationship.* J Appl Physiol, 1999. **86**(3): p. 1002-8.
36. Kariya, F., et al., *Effects of prolonged voluntary wheel-running on muscle structure and function in rat skeletal muscle.* Eur J Appl Physiol, 2004. **92**(1-2): p. 90-7.
37. Stein, T.P. and C.E. Wade, *Metabolic consequences of muscle disuse atrophy.* J Nutr, 2005. **135**(7): p. 1824S-1828S.
38. Stelzer, J.E. and J.J. Widrick, *Effect of hindlimb suspension on the functional properties of slow and fast soleus fibers from three strains of mice.* J Appl Physiol, 2003. **95**(6): p. 2425-33.
39. Gibala, M.J., et al., *Short-term sprint interval versus traditional endurance training: Similar initial adaptations in human skeletal muscle and exercise performance.* J Physiol, 2006.
40. Allemeier, C.A., et al., *Effects of sprint cycle training on human skeletal muscle.* J Appl Physiol, 1994. **77**(5): p. 2385-90.

41. Berchtold, M.W., H. Brinkmeier, and M. Muntener, *Calcium ion in skeletal muscle: its crucial role for muscle function, plasticity, and disease.* Physiol Rev, 2000. **80**(3): p. 1215-65.
42. Wu, H., et al., *Activation of MEF2 by muscle activity is mediated through a calcineurin-dependent pathway.* EMBO J., 2001. **20**(22): p. 6414-6423.
43. Schulz, R.A. and K.E. Yutzey, *Calcineurin signaling and NFAT activation in cardiovascular and skeletal muscle development.* Developmental Biology, 2004. **266**(1): p. 1-16.
44. Liu, J., K. Arai, and N. Arai, *Inhibition of NFATx activation by an oligopeptide: disrupting the interaction of NFATx with calcineurin.* J Immunol, 2001. **167**(5): p. 2677-87.
45. Hennig, R. and T. Lomo, *Firing patterns of motor units in normal rats.* Nature, 1985. **314**(6007): p. 164-6.
46. Lehman, J.J., et al., *Peroxisome proliferator-activated receptor gamma coactivator-1 promotes cardiac mitochondrial biogenesis.* J Clin Invest, 2000. **106**(7): p. 847-56.
47. Ikeda, S., et al., *Muscle type-specific response of PGC-1 alpha and oxidative enzymes during voluntary wheel running in mouse skeletal muscle.* Acta Physiol (Oxf), 2006. **188**(3-4): p. 217-23.
48. Wu, H., et al., *Regulation of mitochondrial biogenesis in skeletal muscle by CaMK.* Science, 2002. **296**(5566): p. 349-52.
49. Chin, E.R., *Role of Ca2+/calmodulin-dependent kinases in skeletal muscle plasticity.* J Appl Physiol, 2005. **99**(2): p. 414-23.
50. Pette, D. and G. Vrbova, *Adaptation of mammalian skeletal muscle fibers to chronic electrical stimulation.* Rev Physiol Biochem Pharmacol, 1992. **120**: p. 115-202.
51. Leek, B.T., et al., *Effect of acute exercise on citrate synthase activity in untrained and trained human skeletal muscle.* Am J Physiol Regul Integr Comp Physiol, 2001. **280**(2): p. R441-7.
52. Pilegaard, H., B. Saltin, and P.D. Neufer, *Exercise induces transient transcriptional activation of the PGC-1alpha gene in human skeletal muscle.* J Physiol, 2003. **546**(Pt 3): p. 851-8.
53. Harmer, A.R., et al., *Skeletal muscle metabolic and ionic adaptations during intense exercise following sprint training in humans.* J Appl Physiol, 2000. **89**(5): p. 1793-803.
54. Ostrowski, K., et al., *Evidence that interleukin-6 is produced in human skeletal muscle during prolonged running.* J Physiol (Lond), 1998. **508**(3): p. 949-953.
55. Putman, C.T., et al., *Effects of strength, endurance and combined training on myosin heavy chain content and fibre-type distribution in humans.* Eur J Appl Physiol, 2004.
56. Fitzsimons, D.P., et al., *Effects of endurance exercise on isomyosin patterns in fast- and slow-twitch skeletal muscles.* J Appl Physiol, 1990. **68**(5): p. 1950-5.
57. Friedman, W.A., T. Garland, Jr., and M.R. Dohm, *Individual variation in locomotor behavior and maximal oxygen consumption in mice.* Physiol Behav, 1992. **52**(1): p. 97-104.
58. Baar, K., et al., *Adaptations of skeletal muscle to exercise: rapid increase in the transcriptional coactivator PGC-1.* Faseb J, 2002. **16**(14): p. 1879-86.
59. Akimoto, T., et al., *Skeletal muscle adaptation in response to voluntary running in Ca^{2+}/calmodulin-dependent protein kinase IV (CaMKIV) deficient mice.* Am J Physiol Cell Physiol, 2004. **287**(5): p. C1311-9.

60. Kemi, O.J., et al., *Intensity-controlled treadmill running in mice: cardiac and skeletal muscle hypertrophy.* J Appl Physiol, 2002. **93**(4): p. 1301-9.
61. Nair-Shalliker, V., et al., *Myofiber adaptational response to exercise in a mouse model of nemaline myopathy.* Muscle Nerve, 2004. **30**(4): p. 470-80.
62. Wang, Y.X., et al., *Regulation of muscle fiber type and running endurance by PPARdelta.* PLoS Biol, 2004. **2**(10): p. e294.
63. Allen, D.L., et al., *Cardiac and skeletal muscle adaptations to voluntary wheel running in the mouse.* J Appl Physiol, 2001. **90**(5): p. 1900-1908.
64. LaFramboise, W.A., et al., *Effect of muscle origin and phenotype on satellite cell muscle-specific gene expression.* J Mol Cell Cardiol, 2003. **35**(10): p. 1307-18.
65. James, R.S., J.D. Altringham, and D.F. Goldspink, *The mechanical properties of fast and slow skeletal muscles of the mouse in relation to their locomotory function.* J Exp Biol, 1995. **198**(Pt 2): p. 491-502.
66. Waters, R.E., et al., *Voluntary running induces fiber type-specific angiogenesis in mouse skeletal muscle.* Am J Physiol Cell Physiol, 2004. **287**: p. C1342-8.
67. Leijendekker, W.J. and G. Elzinga, *Metabolic recovery of mouse extensor digitorum longus and soleus muscle.* Pflugers Arch, 1990. **416**(1-2): p. 22-7.
68. Crow, M.T. and M.J. Kushmerick, *Chemical energetics of slow- and fast-twitch muscles of the mouse.* J Gen Physiol, 1982. **79**(1): p. 147-66.
69. ter Veld, F., J.A. Jeneson, and K. Nicolay, *Mitochondrial affinity for ADP is twofold lower in creatine kinase knock-out muscles. Possible role in rescuing cellular energy homeostasis.* Febs J, 2005. **272**(4): p. 956-65.

Chapter II

Treadmill but not wheel running improves fatigue resistance of isolated Extensor Digitorum Longus muscle in mice

Acta Physiol 2007; ***190(2)****: 151-161*

J.A.L. Jeneson
M.W. de Snoo
N.A.T. Verlinden
B.J.L.J. Joosten
A. Doornenbal
A. Schot
M.E. Everts

ABSTRACT - The present study is the first to compare the physiological impact of either forced treadmill or voluntary wheel running exercise on hindlimb muscle in mice. Male C57BL/6 mice were subjected to either six weeks of forced treadmill or voluntary wheel running exercise. Mice in the treadmill running exercise group (TRE; n=8) ran 1.9 km/day at a speed of 16 m/min against an uphill incline of 11°. In the running wheel exercise group (RWE; n=8) animals ran 8.8 ± 0.2 km per day (average speed 42 ± 2 m/min). After the experimental period, animals were sacrificed and mechanical performance and oxygen consumption of isolated extensor digitorum longus (EDL) muscle were determined during serial electrical stimulation at 0.5, 1 and 2 Hz. Steady-state half-width time (HWT) of twitch contraction at 0.5 Hz was significantly shorter in TRE and RWE than controls (CON) (41.3 ± 0.2 s, 41.3 ± 0.1 s and 44.3 ± 0.1 s, respectively; $P<0.05$). The rate of fatigue development and HWT lengthening at 2 Hz was the same in RWE and CON but lower in TRE (1.2-fold and 2-fold, respectively; $P<0.05$). EDL oxygen consumption, mitochondrial content and myosin heavy-chain (MyHC) composition were not different between the groups. These results indicate that both exercise modalities have an effect on a hindlimb fast-twitch muscle in mice, with the greatest impact seen with forced treadmill running.

2.1 Introduction

Endurance exercise is commonly known to improve skeletal muscle performance with respect to fatigue resistance [1]. The adaptive responses typically concern a fast-to-slow fibre type transformation involving an increase of oxidative capacity (i.e., mitochondrial density) and energetic efficiency (i.e., shift in myosin heavy chain (MyHC) composition towards slower isoforms; [2-4]). These processes were originally studied in laboratory animals employing classic cross-innervation and chronic motor nerve stimulation experiments [4-6]. In time, treadmill and running wheel exercise modalities became more popular due to their ability to study adaptation processes in a minimally invasive, *in vivo* situation.

In this respect, mouse skeletal muscle adaptations have been extensively investigated, mainly due to the increasing availability of transgenic animals [7-10]. In studies on this animal, treadmill and wheel running exercise are considered to induce adaptations associated with endurance exercise [e.g. 8, 10, 11]. However, in the case of wheel running, the animal has free access to the exercise modality resulting in a running pattern which consists of bouts of high speed running [12]. This specific exercise compares roughly to interval training in humans. Treadmill running, on the other hand, forces the animal to run for a sustained period in spite of its natural running behaviour. This particular running activity should therefore rather be compared to endurance running in human (e.g. marathon running) and has been classically regarded as the physiological stimulus to induce fast-to-slow skeletal muscle transformation. Despite this significant difference between the two exercise regimen, no studies in mice have directly compared skeletal muscle adaptations in response to either forced treadmill running or voluntary running wheel exercise.

Here, we studied the physiological impact of six weeks of forced treadmill (TRE) and voluntary running wheel (RWE) exercise on the fast-twitch extensor digitorum longus (EDL) muscle in C57Bl/6 mice. Physiological endpoints to test mechanical performance after the experimental period were twitch contraction half-width time (HWT), and tension-time integral (TTI) during serial contraction. The former is an index of cellular calcium handling [13] while the latter corresponds to total force produced per twitch. The rate of muscle fatigue may be defined as the rate of TTI decline [13]. Two hypotheses were tested: (i) EDL muscles in both groups would show improved mechanical performance compared to sedentary controls,

and (ii) the greatest improvement of mechanical performance would be found in the TRE rather than the RWE group, due to the forced running load.

2.2 Materials and methods

Animals

Four-week old male C57Bl/6 mice were randomly assigned to a treadmill exercise group (n=8; TRE), a running wheel exercise group (n=8; RWE) or a control (n=8; CON) group. Animals were placed at room temperature on a 12:12-h light-dark cycle with food and water provided *ad libitum*. Phenotypically and mechanically, we found no differences between CON mice housed individually or in groups (data not shown). For animal well fare considerations, we therefore decided to group CON as well as TRE mice four to a cage.

Animals in RWE group were housed individually. Cages (28.8 cm x 28.8 cm x 24.5 cm) were custom built and made from Plexiglas. Mice were weighed every week during the six week experimental period.

Training protocol

Cages of the RWE group were equipped with in-house made running wheels with a diameter of 12.1 centimetres. For each cage, the running wheel was equipped with a small magnet and a bicycle speedometer (Hema, Amsterdam, the Netherlands) attached on the outside of the cage to measure total accumulated running distance and average running speed. Data points were collected three times per week.

Animals in the TRE group ran five days per week for two hours on a motor-driven treadmill (custom built) in two separate bouts of 60 min (first bout in the morning; second bout in the afternoon) during the dark cycle, at a speed of 16 m min^{-1} against an uphill inclination of 11° using manual and/or auditory stimulation. These settings were chosen to build on previous work by other groups [14, 15]. Since mice are nocturnal animals, treadmill running was performed during the dark cycle.

Experiments were performed in accordance with institutional and governmental guidelines after approval of the Animal Experimentation Ethics Committee, Utrecht University.

Muscle dissection

Mice were sacrificed by cervical dislocation at the age of ten weeks, i.e. six weeks after the start of the exercise protocol. The extensor digitorum longus (EDL) muscle of the right hindlimb was ligated at the proximal and distal tendons with 5.0 silk sutures and placed in an organ bath for physiological characterization. Contralateral EDL and soleus (SOL) muscles were dissected, snap frozen in liquid nitrogen and stored at -80°C for further biochemical experiments.

Physiological measurements

Isolated EDL muscles were mounted in holders custom-built to fit the glass chambers of a dual-chamber Cyclobios oxygraph apparatus (A. Paar KG, Graz, Austria) and characterized with respect to mechanical performance and respiration as described elsewhere [13]. Briefly, EDL muscles were mounted by attaching tendons to a fixed support at one end and to the lever of a Harvard Apparatus model 60-2995 isometric force transducer (Harvard Apparatus, South Natick, MA, USA) at the other end. The holders were fitted with platinum wire electrodes over the top and bottom tendon positions for electrical stimulation of the muscles. The chambers were equipped with a Clarke-type oxygen electrode (Orbisphere Model 2120, Orbisphere Laboratories, Vésenaz, Switzerland) and a magnetic stirrer, and were embedded in an insolated copper block with integrated Peltier heat pump thermostat for temperature control [16]. After each experiment, muscles were carefully blotted and weighted after removal of the tendons. The volume of the chambers was determined gravimetrically (~ 5 ml).

All experiments were performed at 20° C in a bicarbonate Ringer solution (116 mM NaCl, 4.6 mM KCl, 1.16 mM KH_2PO_4, 2.5 mM $CaCl_2$, 1.16 mM $MgSO_4$, and 25.3 mM $NaHCO_3$) equilibrated with 95% O_2 - 5% CO_2 (pH 7.4). Oxygen partial pressure (PO_2) of the medium was >450 Torr during all experiments, which is above the critical PO_2 at which diffusive flux of O_2 could be rate limiting for oxidative phosphorylation for muscles of this size at this temperature (350-450 Torr; [17]). The stirring rate in each chamber was 600 rpm, resulting in a response time constant of the electrode of 4 sec.

Twitch contractions were evoked using supramaximal single pulses (0.5 msec duration at 8-12 V) delivered by a Grass model S88 dual channel stimulator (Astro-Med, Warwick, RI, USA). The analogue transducer output (volts) was recorded both using a Grass model 2400 dual channel recorder as well as digitally (1 kHz sampling) using Labview software, and

stored on a PC. The output of the oxygen electrode was likewise digitized (1 kHz sampling) using this software and stored on a PC. The electrodes were calibrated prior to each experiment using a two point method (zero oxygen, obtained by addition of dithionite solution, and atmospheric PO_2; atmospheric pressure was recorded for each experiment).

Stimulation protocol

Prior to measurements, both muscle length as well as stimulation voltage were adjusted (typically 18 mm (tendon-to-tendon) and 8-12 V, respectively) to yield maximal twitch force. Next, isometric twitch and tetanic contractions were characterized with respect to kinetics and force. Three tetanic contractions were evoked at 90 Hz, which was the typical fusion frequency at 20 °C. Finally, muscles were serially stimulated for 6 minutes at 0.5, 1.0 and 2.0 Hz in a ramp protocol. The latter frequency range was chosen based on previous work [13, 18];. The concern during serial stimulation for a period of minutes was adequacy of oxygen delivery by superfusion. To limit metabolic rate during contractions, a lower temperature (20 °C rather than 37 °C) as well as low stimulation frequencies were chosen. No evidence for development of an anoxic muscle core under these conditions was found by ^{31}P NMRs [19].

Data analysis

The mechanics of EDL muscle contraction were analyzed on a twitch-per-twitch basis with respect to two mechanical force parameters (baseline force and contraction amplitude, respectively; dimension: N), three contraction time parameters (rise time, relaxation time and half-width time, respectively; dimension: ms) and the hybrid parameter tension-time integral (dimension: N s) using standard LabView subroutines [13]. Changes in TTI during stimulation at 1 and 2 Hz were quantified for each muscle by scaling to its stationary value at 0.5 Hz (= sTTI; [13]). Oxygen concentration in the chambers was calculated as described elsewhere [16]. Absolute muscle respiratory rates were computed as the derivative of the time course of chamber oxygen content using Origin 6.0 (Microcal Software Inc., Northampton, MA, USA).

Citrate synthase

Citrate synthase enzyme activity of EDL muscle homogenate was determined to characterize Krebs cycle activity, as described by Srere, 1969 [20]. Citrate synthase of CON soleus muscle was included as a positive control.

Briefly, muscle samples removed of connective tissue were homogenized, followed by sonication to further disrupt the mitochondrial membrane. After centrifugation, the resulting supernatant was decanted and assayed for enzyme activity. Activity was determined spectrophotometrically (412 nm; 30°C) by measuring the production of CoA-SH (acetyl-CoA + oxaloacetate + $H_2O \leftrightarrow$citrate + CoA-SH + H^+ (side reaction: CoA-SH + DTNB $\rightarrow$ mercaptide ion)). Readings were taken at 20-s intervals for 2-2.5 min to measure acetyl-CoA deacylase activity. Samples were assayed in duplicate, and samples from all animals were assayed on the same day to further reduce variation. Total protein in the homogenate was assayed by using the technique described by Bradford [21].

MyHC profiling

Skeletal myosin heavy chain (MyHC) composition of EDL muscles was analyzed by separating the various isoforms using sodium dodecyl-sulphate polyacrylamide gel electrophoresis (SDS-PAGE) according to Talmadge and Roy [22]. Briefly, EDL muscle samples were homogenized in a solution containing 250 mM sucrose, 100 mM KCl, 5 mM EDTA, and 20 mM Tris base, and protein concentration was determined by the method of Bradford [21]. Next, 800 ng of protein sample was run on an 8% running gel for 48 hours at 70 V at 4 °C to quantify MyHC composition in EDL muscles after exercise. MyHC bands were visualized by silver staining (Biorad; Hercules, CA, USA), and quantified (as percentage of total) using AlphaEase FC software (San Leandro, CA, USA).

Statistics

Data are presented as arithmetic means ± standard error (SE), unless stated otherwise. All the data were analyzed with SPSS 12.0.1 for Windows (SPSS Inc., Chicago, IL, USA). One-way ANOVAs were used to examine the differences between CON, TRE, and RWE groups, with Bonferroni as post-hoc test. $P<0.05$ was considered statistically significant. (Non)linear curve fitting analysis of time courses of variables was conducted using Origin 6.0 (Microcal Software Inc., Northampton, MA, USA).

2.3 Results

Animals and running activity

Body weights and EDL muscle weights were the same for animals in all three groups after the six week experimental period (Table 2.1). Mice in the TRE group daily ran 1.9 km at an imposed constant speed of 16 m min^{-1}. Mice in the RWE group ran 8.8 ± 0.2 km per day (n=8; range: 7.7 – 9.6 km) during the dark cycle at an average speed of 2.5 ± 0.1 km h^{-1}, or 42 ± 2 m min^{-1}. This distance was constant for an individual mouse in the RWE group for the duration of the study. Total distance run was significantly higher in the RWE than in the TRE group (P<0.05).

	CON	TRE	RWE
General parameters	**n=8**	**n=8**	**n=8**
Body weight (g)	26.6 ± 0.8	23.1 ± 0.3	24.0 ± 0.4
EDL muscle (mg)	10.1 ± 0.3	9.6 ± 0.3	11.0 ± 0.3
EDL/Body weight ratio (mg/g)	0.38 ± 0.01#	0.42 ± 0.01#	0.46 ± 0.01#
Twitch	**n=6**	**n=6**	**n=8**
Force (N)	42 ± 3	45 ± 3	41 ± 4
Force (N/g muscle)	4.2 ± 0.3	4.8 ± 0.4	3.7 ± 0.6*
Rise time (ms)	12.7 ± 0.1	12.6 ± 0.2	13.4 ± 0.8
Relaxation time (ms)	97 ± 10	78 ± 29	74 ± 36
Tetanus	**n=6**	**n=6**	**n=8**
Force (N)	258 ± 22	234 ± 22	213 ± 19*
Force (N/g muscle)	25.4 ± 1.5	24.5 ± 2.0	19.4 ± 1.7*
Rise time (ms)	226 ± 10	195 ± 47	138 ± 33*
Relaxation time (ms)	63 ± 6	58 ± 6	68 ± 4

Table 2.1 Mouse and EDL muscle characteristics at age 10 weeks for mice in control (CON), treadmill (TRE) and running wheel (RWE) groups. Mechanical and kinetic parameters of single isometric twitch and tetanic contractions of isolated EDL muscles in the CON, TRE and RWE groups (CON: n=6; TRE: n=6; RWE: n=8). * P<0.05 RWE vs CON and TRE; # P<0.0.5 CON vs TRE vs RWE.

Mechanical performance

Tetanic force and rise time of RWE EDL muscle were significantly lower than of CON and TRE muscle (P<0.05; Table 2.1). Likewise, normalized twitch and tetanic force per gram of RWE EDL muscle were significantly lower than those of CON and TRE muscle (P<0.05; Table 2.1). Other iso-

metric twitch and tetanic EDL contraction characteristics were not different between groups (Table 2.1). Figure 2.1 shows a typical recording of isometric EDL twitch contractions during serial stimulation at 0.5, 1 and 2 Hz, respectively (single muscle; CON group). As observed previously [13], the amplitude of twitch contraction typically remained near-constant during stimulation at 0.5 Hz, declined by a third during stimulation at 1 Hz, and two-thirds during stimulation at 2 Hz (Figure 2.1). Twitch force fully recovered within 3 min following the protocol (not shown).

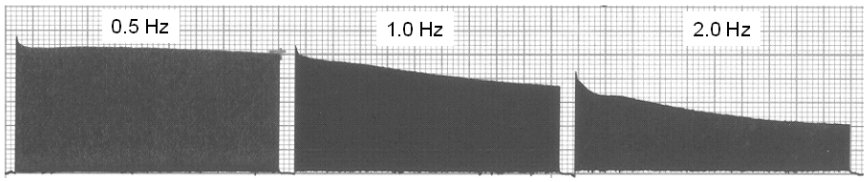

Figure 2.1 Typical recording of isometric twitch force (in V) of EDL contraction during serial stimulation at 0.5, 1 and 2 Hz, respectively (single muscle; CON group). One vertical unit (V) corresponds to 0.15 g of force; one horizontal unit (s) corresponds to 7.5 s.

Serial stimulation at 0.5 Hz

Figure 2.2a shows the average time course of TTI of EDL twitch contraction during serial stimulation at 0.5 Hz (pooled data, n=8; CON). As observed previously [13], TTI dropped rapidly after the second contraction reaching a stationary value within 90 s after onset of stimulation that was 40% lower than TTI of the first contraction (Figure 2.2a). This drop was much larger than that observed for twitch amplitude (Figure 2.1).

Figure 2.2b shows the average time course of the half-width time of twitch contraction during serial stimulation at 0.5 Hz for each group. Analogous to the time course of TTI shown in Figure 2.2a, HWT dropped rapidly after onset of stimulation and attained a stationary value typically within 90 s. Quantitative analysis of the time course was performed by nonlinear curve-fitting of a biexponential decay function for each group. Time constants were not different between groups (tau1 10 ± 1 s, tau2 42 ± 5 s; mean ± SE from regression). Stationary HWT for EDL muscles in the exercise groups was significantly shorter than CON (44.3 ± 0.1 s (CON) versus 41.3 ± 0.2 s (TRE; $P<0.05$) and 41.3 ± 0.1 s (RWE; $P<0.05$), respectively; mean ± SE from regression).

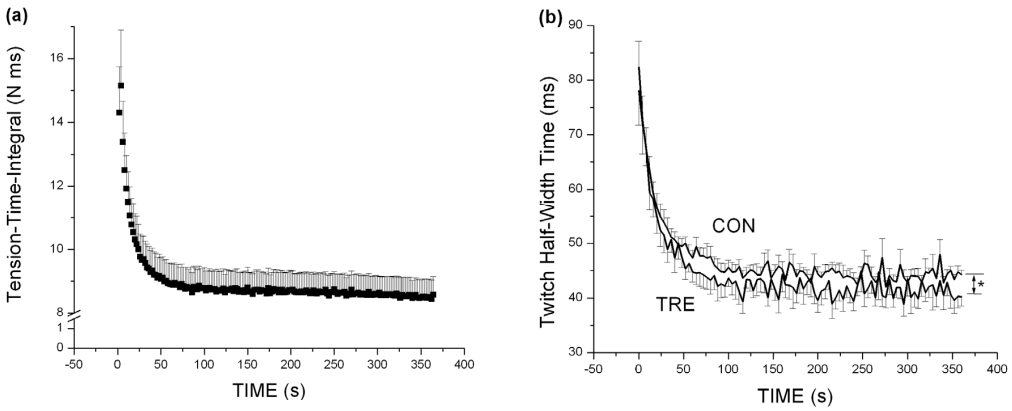

Figure 2.2 A Time course of tension-time-integral (TTI; in N ms) of EDL twitch contraction during serial stimulation at 0.5 Hz (pooled results CON group; n=8 muscles). Error bars represent SE. **B** Time course of EDL twitch contraction half-width (in ms) during serial stimulation at 0.5 Hz for CON (upper trace) and TRE (lower trace) groups (pooled results of n=8 muscles for each group). Error bars represent SE. Lines connecting subsequent data points rather than the data points themselves are shown for clarity of presentation. For clarity of presentation, the time course for RWE is not shown as it is superimposed on TRE. Further, every 4th data point is presented of the CON and TRE groups. * P<0.05 for CON vs TRE and RWE

Serial stimulation at 1 and 2 Hz

Mechanical performance of EDL muscles in the two exercise groups compared to controls was tested by analysis of the time course of TTI and HWT. Specifically, for each individual muscle absolute TTI (in N g^{-1} s) at each timepoint was scaled to its stationary TTI value determined during preceding serial stimulation at 0.5 Hz (see Figure 2.1b) yielding scaled TTI (sTTI). Any effects of random variation in muscle mass and dissection damage on the outcome of the analysis were thus minimized [13]. The second parameter, HWT (in ms) is in itself scaled to absolute twitch amplitude. Serial stimulation at 1 Hz did not reveal any differences with respect to TTI or HWT time course between the three groups (data not shown). Figure 2.3a shows the net change in sTTI of isometric twitch contraction of EDL muscle relative to the first contraction of the 2 Hz series (= (sTTI(t)-sTTI(t=0)). In all three groups, sTTI fell rapidly after the first contraction before approaching a steady-state during the ensuing 90 s (Figure 2.3a). At t=90 s, the net change in sTTI tended to be less in the TRE group than CON (-0.27 ± 0.05 (n=4) versus -0.34 ± 0.02 (n=8), respectively) although not significantly. In the RWE group, this initial timecourse followed a slightly different decay function in that no stationary state was approached

(Figure 2.3a). After 90 s, the net drop in sTTI of RWE equalled that of the CON group (Figure 2.3a). In all three groups, sTTI dropped monotonically during the remainder of the stimulation period but less so in the TRE group. Specifically, (sTTI(t)-sTTI(t=0)) dropped at a constant fatigue rate of 3% min^{-1} in both CON and RWE groups. In the TRE group, this rate was 20% lower. As a result, sTTI of isometric twitch contraction of EDL muscles in the CON and RWE groups had dropped by as much as half of its initial value after 6 min of serial stimulation at 2 Hz, twofold more than in the TRE group (Figure 2.3a).

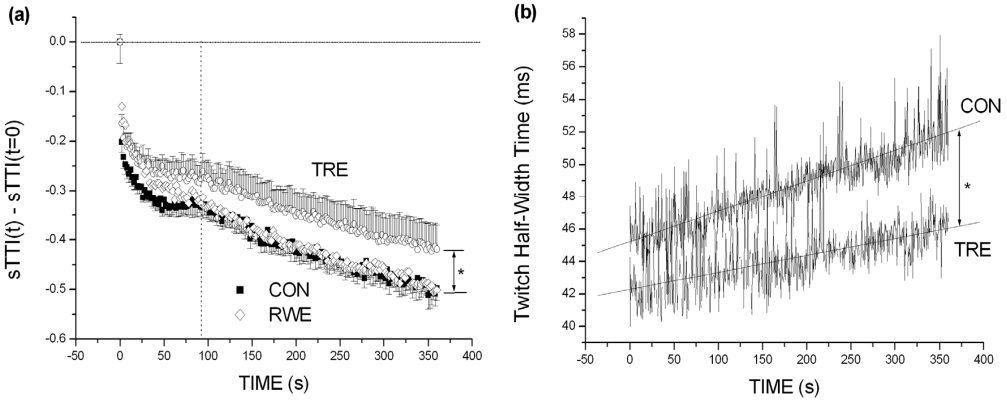

Figure 2.3 A Time course of net change in scaled tension-time integral (sTTI) relative to first contraction of EDL twitch contraction during serial stimulation at 2 Hz (pooled results for each group). Solid squares: CON group (n=8); circles: TRE group (n=4); diamonds: RWE group (n=8). Error bars represent SE. For clarity of presentation, error bars for the RWE were omitted. * $P<0.05$ for TRE vs CON and RWE **B** Time course of half-width of EDL twitch contraction (in ms) during serial stimulation at 2Hz (pooled results for each group). Lines connecting subsequent data points rather than the data points themselves are shown for clarity of presentation. CON group (n=8); black trace. RWE group (n=8); grey trace. TRE group (n=4); black trace. Solid lines (CON and TRE) and dashed line (RWE) represent fits of linear functions to the data for each group. For clarity of presentation, HWT of the RWE group is not shown as it is near-coincided with the CON group. * $P<0.05$ for TRE vs CON and RWE

Figure 2.3b shows the time course of HWT of isometric twitch contraction of EDL muscle for each group. In all three groups, HWT increased monotonically after the first contraction during the remainder of the protocol. However, analogous to the result for TTI, EDL muscles from the CON and RWE groups were identical with respect to this parameter, and were outperformed by the TRE group. Quantitative analysis of the time course by linear curve-fitting revealed that HWT of the first isometric contraction

of EDL muscles in the CON and RWE groups was the same (45.2 ± 0.1 and 44.6 ± 0.1 s, respectively; mean ± SE from regression) and already significantly longer than for the TRE group (42.3 ± 0.1; mean ± SE from regression; TRE vs CON or RWE: $P<0.05$). Subsequently, HWT in groups CON and RWE increased at a twofold faster rate than in the TRE group (1.2 ± 0.1 versus 0.6 ± 0.1 ms min^{-1}, respectively; $P<0.05$). As a result, HWT after 6 min of serial stimulation at 2 Hz was 52 ± 3 ms in the CON and RWE groups, versus 46 ± 4 ms in the TRE group ($P<0.05$ (TRE vs. CON and RWE); Figure 2.3b).

Oxygen consumption during serial contractions

Figure 2.4a shows a typical time course of the net change in chamber oxygen content during the stimulation experiment. This net change was calculated by subtraction of the constant background oxygen consumption of the chamber and EDL muscle. In this particular experiment, this background rate was measured for 25 min (t=0-1500s) after which the stimulation protocol commenced. With each increment of the stimulation frequency, the slope of additional oxygen consumption above background increased. After cessation of stimulation, oxygen consumption returned to initial background rate (Figure 2.4a).

Figure 2.4b shows the average additional oxygen consumption in nmol min^{-1} g^{-1} at each stimulation frequency for each group. To determine the maximal oxygen consumption rate for EDL muscles in the CON group at 20 °C, an arbitrary hyperbolic function was fitted to the variation of oxygen consumption with stimulation frequency (Figure 2.4b, solid line; r^2 0.99) yielding an estimate of 8.86 ± 0.4 nmol min^{-1} g^{-1} and a half-maximal stimulation frequency of 0.7 ± 0.1 Hz (mean ± SE from regression). EDL oxygen consumption during serial stimulation at 0.5, 1 and 2 Hz in the exercise groups was not different from control.

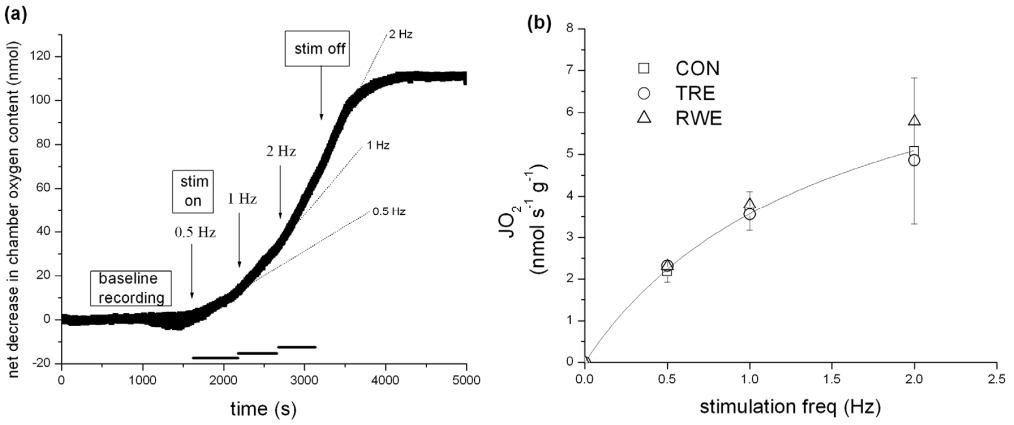

Figure 2.4 A Typical time course of the net change in chamber oxygen content (in nmol) during a rest-stimulation-recovery experiment (single EDL muscle; CON group). Chamber oxygen content and net change during the experiment was computed as described in Methods. Arrows indicate change of contraction duty cycle. Horizontal bars indicate length of each set of serial stimulations at a frequency (typically 360 s). Dashed lines are extrapolations of the slope of the curve for each stimulation frequency, where the slope corresponds to the absolute oxygen consumption rate (in nmol s^{-1}) **B** Oxygen consumption rate above chamber plus muscle background (in nmol s^{-1} g^{-1} muscle) as a function of stimulation frequency. Open squares: CON (n=5). Open circles: TRE (n=3). Open triangle: RWE (n=4). The solid line represents the fit of a rectangular hyperbolic function to the data of the CON group.

Citrate synthase

Figure 2.5 shows the CS activity in homogenate of soleus and EDL muscles from the CON group, versus the CS activity in homogenate of EDL muscles from the TRE and RWE groups, respectively. CON soleus CS activity was 2.8-fold higher than CON EDL (0.42 ± 0.03 (n=5) versus 0.15 ± 0.01 (n=8) μmol min^{-1} g^{-1} protein, respectively; $P<0.01$) (Figure 2.5). CS activity in EDL muscle homogenate from the two exercise groups was not different than in CON EDL (TRE: 0.11 ± 0.01 (n=5) μmol min^{-1} g^{-1} protein; RWE: 0.18 ± 0.01 (n=8) μmol min^{-1} g^{-1} protein; Figure 2.5).

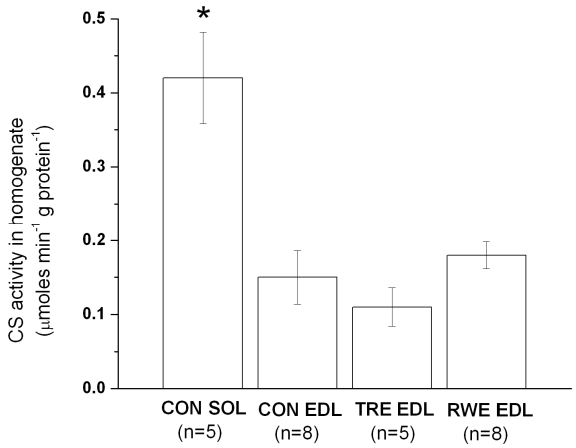

Figure 2.5 Bar graph of CS activity (in μmol min^{-1} g^{-1} protein) of soleus and EDL muscle of mice in the CON group (n=5 and n=8 muscles, respectively), EDL muscle in the TRE group (n=5 muscles) and EDL muscle in the RWE group (n=8 muscles). CS activity was assayed in duplo in muscle homogenates as described in Methods. * $P<0.05$ for CON soleus vs. all EDL groups.

MyHC composition

Figure 2.6 shows the MyHC gel electrophoresis result for EDL muscle homogenate of the TRE and CON groups. A similar result was obtained for RWE (data not shown). The mean results are given in table 2.2. EDL muscle was composed of 65% type IIb and 35% type IIx fibers in all three groups. Neither of the exercise protocols thus induced a shift in MyHC composition.

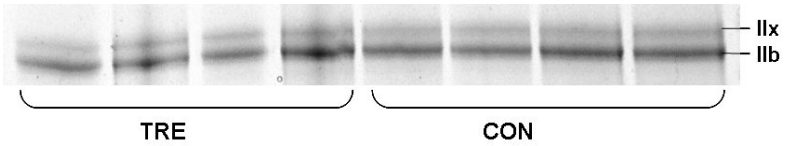

Figure 2.6 SDS-PAGE gel showing myosin heavy chain (MyHC) profile of EDL muscles in the CON group (n=4 muscles) and TRE group (n=4 muscles). The two bands correspond to the IIx (upper band) and IIb (lower band) MyHC isoforms expressed in this fast-twitch muscle.

	CON	TRE	RWE
Type IIa/x	35.5 ± 1.9 %	34.6 ± 1.4 %	35.0 ± 1.2 %
Type IIb	64.5 ± 1.9 %	65.4 ± 1.4 %	65.0 ± 1.2 %

Table 2.2 MyHC composition of C57Bl/6 mouse EDL muscles after the 6 week experimental period. n=4 for each group.

2.4 Discussion

The present study compared the impact of either forced treadmill or voluntary wheel running exercise on a fast-twitch dorsal toe flexor muscle in C57Bl/6 mice. This research has yielded two main findings. At the physiological level, we found evidence for adaptations in cellular calcium handling in both groups. This effect was the largest in the TRE group. At the protein level, however, our results confirmed previous observations that mouse hindlimb muscles are phenotypically remarkably robust to chronically elevated activity with respect to MyHC composition and mitochondrial volume [11, 23-26] compared to larger rodents such as rat [27, 28]. Below, the experimental design of the study and these main findings are discussed.

Design of the study

The physiological studies in isolated, superfused intact muscle in the present investigation were conducted on the EDL muscle for several reasons. First, this particular hindlimb muscle is highly suited for these particular measurements and conditions because of its dimensions and geometry. Secondly, the EDL muscle is a fast-twitch muscle. If any, a fast-twitch muscle is more prone to adjust its phenotype in response to endurance exercise than slow-twitch muscle since the latter is supposed to be yet near-optimized to endurance exercise. Thirdly, extensive information exists on mechanical performance and metabolic scope of superfused isolated mouse EDL muscle at 20°C both from our own work and others [13, 17] allowing for carefully controlled and verifiable experiments. For example, the particular experimental protocol for the serial electrical stimulation studies used prior knowledge of the mechanical and energetic properties of isolated mouse EDL muscles superfused at 20° C [13]. Absolute values of respiration during serial stimulation and estimated V_{max} in that study were similar to the rates measured in the present study.

Adaptations of EDL muscle to chronic exercise in C57BL/6 mice

Measurements of isometric twitch and tetanic contraction force in the RWE group revealed that per g muscle, both were significantly lower than in CON and TRE groups (Table 2.1). This result cannot be explained by altered myosin composition of the EDL muscle in the RWE group (Table 2.2). Possible mechanistic explanations include lower sarcoplasmic reticular (SR) calcium release, lowered calcium sensitivity of the myofilaments and

higher calcium buffering [review: 29]. Since no data were obtained on any of these variables, any discussion on which of these changes may underlie these results would be entirely speculative. Future measurements in EDL muscle of the RWE group are therefore warranted to further elucidate the mechanistic basis for these results.

The results of the physiological studies of EDL contractile performance after training indicated that a subtle adaptive change had occurred, confirming our first hypothesis. Specifically, it was found during serial stimulation at 0.5 Hz that HWT of isometric contraction attained a stationary value in both running groups that was significantly shorter than in controls (Figure 2.2b). Since the drop in twitch amplitude during serial stimulation at 0.5 Hz is typically small (Figure 2.1, first block), the large drop in TTI during serial stimulation at 0.5 Hz commonly observed in wild-type mice [13] is largely due to HWT shortening, and in particular to faster relaxation (not shown). This apparent 'warm-up' effect has thus far not been described in excised muscle and remains to be properly explained. Our untested hypothesis is that some activation of SR calcium recovery underlies this phenomenon. In a fast-twitch muscle such as the EDL, the rate of relaxation is determined by the rate of calcium pumping across the SR membrane more than the rate of cross-bridge detachment [30, 31]. In this light, the results shown in Figure 2.2b suggest that cation handling in trained EDL muscles was activated by a small (10%) but significantly larger amount than in controls. This positive effect on 'recruitable' capacity for cation handling was the same for treadmill and wheel running exercise (Figure 2.2b).

The time course of sTTI and HWT during serial stimulation at 2 Hz, however, demonstrated a different, not similar training effect of treadmill running and wheel running on capacity for cation handling. Specifically, voluntary wheel running appeared not to have any beneficial effect on contractile performance of isolated EDL muscle compared to controls at this high mechanical load (Figures 2.3a and 2.3b). In contrast, EDL muscles in the TRE group outperformed muscles from the control group (Figures 2.3a and 2.3b). Both the initial drop after 90 s of serial stimulation as well as the subsequent linear fatigue rate of EDL muscles in the TRE group were 1.2-fold less than in CON and RWE groups (Figure 2.3a). Similarly, twitch contraction lengthening during serial stimulation at 2 Hz was twofold less in the TRE group than in CON and RWE (Figure 2.3b) suggesting significantly better calcium handling at this high workload in the TRE group. These results also confirmed our second hypothesis.

Oxygen consumption during isometric contractions was the same in all three groups at all contraction frequencies tested (Figure 2.4). A trivial explanation of this result would be that the sensitivity of the polarographic oxygen consumption measurement was not sufficient to detect a 10% change in rate. Alternatively, the result may indicate that the apparent improved capacity for SR calcium pumping in TRE muscles was not metabolically supported by extra mitochondrial ATP synthesis flux. If so, this would entail that TRE training in C57BL/6 mice enhanced the capacity for anaerobic glycogenolysis (and paradoxically not mitochondrial ATP synthesis; Figure 2.5) in EDL muscle. Future studies may test this hypothesis at the protein level by assay of glycogenolytic enzymes, or at the physiological level by assay of lactate production during electrical stimulation.

At the protein level, we found neither of the two hallmark adaptations of endurance-type muscle remodelling (i.e., MyHC and mitochondrial density changes) for any of the two exercise paradigms studied. In both the TRE and RWE groups, EDL MyHC composition and CS activity were unchanged from CON (Figures 2.5 and 2.6). Our numbers for MyHC composition as well as CS activity in homogenate of EDL muscle from unexercised WT C57BL/6 mice (Table 2.2 and Figure 2.5) agreed well with the literature [32, 33] and [34-36], respectively. The sensitivity of the CS assay was independently verified by determination of the CS activity ratio of soleus and EDL muscle in the CON group. The result (ratio 2.8) was in agreement with previous findings [37, 38].

The finding that EDL MyHC composition and mitochondrial density were not affected by chronic exercise confirmed and complemented results of previous studies of hindlimb muscle adaptation to wheel running in mouse gastrocnemius, soleus and tibialis anterior muscles [24, 39]. Only a single previous study reported significantly altered MyHC composition in response to RWE, notably in the anterior tibialis muscle [40]. Similarly, the significant and substantial MyHC fast-to-slow shift in EDL muscle of WT FVB/NJ mice after 4 weeks of treadmill running reported by Nair-Shalliker et al. remains the sole finding of classic endurance-type adaptation to that particular exercise paradigm [8]. It should, however, be noted that EDL MyHC composition in the FVB/NJ mice shifted during training towards the very same composition we (Table 2.2) and others [41] found for control WT C57BL/6 mice. As previously noted and demonstrated [15, 41], there is quite a genetic variability and associated broad range of phenotypes between inbred mouse strains that should be taken into account when comparing results of different studies.

The finding that EDL muscles in the TRE group outperformed the RWE group confirmed our second hypothesis. Six weeks of wheel running appeared to have no beneficial effect over relatively sedentary behaviour on EDL contractile performance stimulated at a high frequency (Figure 2.3). On an absolute scale, mice in the RWE group outran the TRE group fourfold with respect to distance (8.8 versus 1.9 km per 24 hr, and 7 days per week versus 5 days per week, respectively), and more than twofold with respect to maximal speed (42 versus 16 m min^{-1}, respectively). However, a clear qualitative distinction existed between these two exercise regimens. In wheel running, the animal controlled its own pace and activity pattern, while in treadmill running, both were imposed. The results of the present study together with existing literature suggest that the former, 'natural' activity does not result in any endurance-type changes of FT hindlimb muscle in mice, however long the distance run may be, while 'non-natural' treadmill running for a mere quarter of the daily wheel running distance did have a small but significant training effect in this animal.

2.5 Acknowledgements

The authors are grateful to RW Wiseman (Michigan State University) for sharing protocols for the biochemical assays, and to MJ Kushmerick (University of Washington) and R Gronka (University of Washington) for sharing Labview programs for analysis of the mechanics data.

2.6 References

1. Holloszy, J.O. and E.F. Coyle, *Adaptations of skeletal muscle to endurance exercise and their metabolic consequences.* J Appl Physiol, 1984. **56**(4): p. 831-8.
2. Fuller, P.M., K.M. Baldwin, and C.A. Fuller, *Parellel and divergent adaptations of rat soleus and plantaris to chronic exercise and hypergravity.* Am J Physiol Regul Integr Comp Physiol, 2005. **290**(2): p. R442-8.
3. Kariya, F., et al., *Effects of prolonged voluntary wheel-running on muscle structure and function in rat skeletal muscle.* Eur J Appl Physiol, 2004. **92**(1-2): p. 90-7.
4. Simoneau, J.A. and D. Pette, *Species-specific effects of chronic nerve stimulation upon tibialis anterior muscle in mouse, rat, guinea pig, and rabbit.* Pflugers Arch, 1988. **412**(1-2): p. 86-92.
5. Matsushita, S. and D. Pette, *Inactivation of sarcoplasmic-reticulum Ca^{2+}-ATPase in low-frequency-stimulated muscle results from a modification of the active site.* Biochem J, 1992. **285 (Pt 1)**: p. 303-9.
6. Sultan, K.R., et al., *Fiber type-specific expression of major proteolytic systems in fast- to slow-transforming rabbit muscle.* Am J Physiol Cell Physiol, 2001. **280**(2): p. C239-47.
7. Wang, Y.X., et al., *Regulation of muscle fiber type and running endurance by PPARdelta.* PLoS Biol, 2004. **2**(10): p. e294.
8. Nair-Shalliker, V., et al., *Myofiber adaptational response to exercise in a mouse model of nemaline myopathy.* Muscle Nerve, 2004. **30**(4): p. 470-80.
9. Akimoto, T., et al., *Skeletal muscle adaptation in response to voluntary running in Ca^{2+}/calmodulin-dependent protein kinase IV (CaMKIV) deficient mice.* Am J Physiol Cell Physiol, 2004. **287**(5): p. C1311-9.
10. Kemi, O.J., et al., *Intensity-controlled treadmill running in mice: cardiac and skeletal muscle hypertrophy.* J Appl Physiol, 2002. **93**(4): p. 1301-9.
11. Pellegrino, M.A., et al., *Effects of voluntary wheel running and amino acid supplementation on skeletal muscle of mice.* Eur J Appl Physiol, 2005. **93**(5-6): p. 655-64.
12. De Bono, J.P., et al., *Novel quantitative phenotypes of exercise training in mouse models.* Am J Physiol Regul Integr Comp Physiol, 2005. **290**(4): p. R926-34.
13. Ter Veld, F., K. Nicolay, and J.A. Jeneson, *Increased resistance to fatigue in creatine kinase deficient muscle is not due to improved contractile economy.* Pflügers Arch, 2006. **452**(3): p. 342-348.
14. Nakamura, A., et al., *Up-regulation of mitogen activated protein kinases in mdx skeletal muscle following chronic treadmill exercise.* Biochim Biophys Acta, 2005. **1740**(3): p. 326-31.
15. Billat, V.L., et al., *Inter- and intrastrain variation in mouse critical running speed.* J Appl Physiol, 2005. **98**(4): p. 1258-63.
16. Haller, T., M. Ortner, and E. Gnaiger, *A respirometer for investigating oxidative cell metabolism: toward optimization of respiratory studies.* Anal Biochem, 1994. **218**(2): p. 338-42.
17. Crow, M.T. and M.J. Kushmerick, *Chemical energetics of slow- and fast-twitch muscles of the mouse.* J Gen Physiol, 1982. **79**(1): p. 147-66.

18. Jeneson, J.A.L., R.W. Wiseman, and M.J. Kushmerick, *The dynamic range of steady-state mitochondrial oxygen consumption at 20°C is the same in mouse fast- and slow-twitch muscle.* J Muscle Res Cell Motility, 2002. **23**(1): p. 22.
19. Jeneson, J.A., R.W. Wiseman, and M.J. Kushmerick, *Non-invasive quantitative 31P MRS assay of mitochondrial function in skeletal muscle in situ.* Mol Cell Biochem, 1997. **174**(1-2): p. 17-22.
20. Srere, P.A. and G.C. Brooks, *The circular dichroism of glucagon solutions.* Arch Biochem Biophys, 1969. **129**(2): p. 708-10.
21. Bradford, M.M., *A rapid and sensitive method for the quantitation of microgram quantities of protein utilizing the principle of protein-dye binding.* Anal Biochem, 1976. **72**: p. 248-54.
22. Talmadge, R.J. and R.R. Roy, *Electrophoretic separation of rat skeletal muscle myosin heavy-chain isoforms.* J Appl Physiol, 1993. **75**(5): p. 2337-40.
23. Pette, D. and G. Vrbova, *Adaptation of mammalian skeletal muscle fibers to chronic electrical stimulation.* Rev Physiol Biochem Pharmacol, 1992. **120**: p. 115-202.
24. Zhan, W.Z., et al., *Effects of genetic selection and voluntary activity on the medial gastrocnemius muscle in house mice.* J Appl Physiol, 1999. **87**(6): p. 2326-33.
25. Momken, I., et al., *Voluntary physical activity alterations in endothelial nitric oxide synthase knockout mice.* Am J Physiol Heart Circ Physiol, 2004. **287**(2): p. H914-20.
26. Houle-Leroy, P., et al., *Effects of voluntary activity and genetic selection on muscle metabolic capacities in house mice Mus domesticus.* J Appl Physiol, 2000. **89**(4): p. 1608-1616.
27. Taylor, E.B., et al., *Endurance training increases skeletal muscle LKB1 and PGC-1alpha protein abundance: effects of time and intensity.* Am J Physiol Endocrinol Metab, 2005. **289**(6): p. E960-8.
28. Demirel, H.A., et al., *Exercise-induced alterations in skeletal muscle myosin heavy chain phenotype: dose-response relationship.* J Appl Physiol, 1999. **86**(3): p. 1002-8.
29. Rome, L.C., *Design and function of superfast muscles: new insights into the physiology of skeletal muscle.* Annu Rev Physiol, 2006. **68**: p. 193-221.
30. Baylor, S.M. and S. Hollingworth, *Sarcoplasmic reticulum calcium release compared in slow-twitch and fast-twitch fibres of mouse muscle.* J Physiol, 2003. **551**(Pt 1): p. 125-38.
31. Rudolf, R., et al., *In vivo monitoring of Ca^{2+} uptake into mitochondria of mouse skeletal muscle during contraction.* J Cell Biol, 2004. **166**(4): p. 527-36.
32. Agbulut, O., et al., *Myosin heavy chain isoforms in postnatal muscle development of mice.* Biology of the Cell, 2003. **95**(6): p. 399-406.
33. Yu, F., et al., *Effects of thyroid hormone receptor gene disruption on myosin isoform expression in mouse skeletal muscles.* Am J Physiol Regul Integr Comp Physiol, 2000. **278**(6): p. R1545-1554.
34. Nakao, C., et al., *Effects of swimming training on three superoxide dismutase isoenzymes in mouse tissues.* J Appl Physiol, 2000. **88**(2): p. 649-54.
35. Anflous, K., D.D. Armstrong, and W.J. Craigen, *Altered mitochondrial sensitivity for ADP and maintenance of creatine-stimulated respiration in oxidative striated muscles from VDAC1-deficient mice.* J Biol Chem, 2001. **276**(3): p. 1954-60.
36. Oh-ishi, S., et al., *Effects of aging and/or training on antioxidant enzyme system in diaphragm of mice.* Respir Physiol, 1996. **105**(3): p. 195-202.

37. Woitaske, M.D. and R.J. McCarter, *Effects of fiber type on ischemia-reperfusion injury in mouse skeletal muscle.* Plast Reconstr Surg, 1998. **102**(6): p. 2052-63.
38. Moerland, T.S. and M.J. Kushmerick, *Contractile economy and aerobic recovery metabolism in skeletal muscle adapted to creatine depletion.* Am J Physiol, 1994. **267**(1 Pt 1): p. C127-37.
39. Pellegrino, M.A., et al., *Clenbuterol antagonizes glucocorticoid-induced atrophy and fibre type transformation in mice.* Exp Physiol, 2004. **89**(1): p. 89-100.
40. Allen, D.L., et al., *Cardiac and skeletal muscle adaptations to voluntary wheel running in the mouse.* J Appl Physiol, 2001. **90**(5): p. 1900-1908.
41. Lerman, I., et al., *Genetic variability in forced and voluntary endurance exercise performance in seven inbred mouse strains.* J Appl Physiol, 2002. **92**(6): p. 2245-55.

Chapter III

Running wheel exercise in mice: analysis of running pattern and physiological adaptations in soleus muscle

M.W. de Snoo
M.E. Everts
P.W.A. Cornelissen
B.J.L.J. Joosten
A. Doornenbal
A. Schot
J.A.L. Jeneson

ABSTRACT - Running wheels have been extensively used to study the beneficial effects of exercise in mice. To extrapolate these data to the human situation, it is necessary to understand the running pattern. We analyzed running pattern of voluntary exercising mice, with subsequent physiological characterization of the slow-twitch soleus muscle. Male C57Bl/6 mice were subjected to 6 weeks of voluntary wheel running exercise. The running wheel exercise group (RWE; n=12) and the sedentary control group (SED; n=8) had same body and soleus muscle weights after the experiment. Running pattern was investigated using Labview programs. After the experimental period, mice were killed and mechanical performance and oxygen consumption of isolated soleus muscle were determined during serial electrical stimulation at 3 Hz. Data were combined with analysis of MyHC profile and Ca^{2+} transport and regulatory proteins. RWE mice demonstrated an intermittent running pattern consisting of bouts at an average speed of 2.4 ± 0.1 km/h. Twitch and tetanic contractile parameters were unchanged. Residual force during serial stimulation was 1.3-fold higher in RWE muscle, associated with 1.3-fold higher oxygen consumption (both $P<0.05$). Peak of unstimulated force was significantly attenuated in RWE muscle ($P<0.05$). MyHC and CS activity were unchanged, as was total SERCA content. However, SERCA regulator phospholamban demonstrated a 50-60% decrease in mRNA and protein expression, while sarcolipin mRNA increased by 199% ($P<0.05$). This study demonstrates that the intermittent running pattern of voluntarily running mice improves fatigue resistance and affects Ca^{2+} regulation in the slow-twitch soleus muscle.

3.1 Introduction

Regular physical exercise is known to improve common well-being, and is associated with a.o. improved endurance capacity, cardiovascular function, and immune system. Changes in skeletal muscle associated with chronic endurance exercise include increases in oxidative capacity and energy production [1-4]. In rodents, the beneficial effects of exercise are traditionally studied using treadmill or running wheel devices [2, 3, 5]. We recently described and compared the effects of forced treadmill running and voluntary wheel running exercise on the function of mouse extensor digitorum longus (EDL) muscle [6]. Interestingly, treadmill running demonstrated the greatest improvement of EDL mechanical performance and fatigue resistance, despite larger distances and total time run during wheel running exercise [6].

Running wheels involve minimal animal handling and allow free running, and thus will hardly induce stress to the animal. As such, voluntary wheel running is today the preferred method to study functional improvements in skeletal and/or cardiac muscle in transgenic mice [7-9]. However, the precise exercise load associated with this type of training is still largely unknown, which is a prerequisite to extrapolate results to the human situation. To our knowledge, the voluntary running pattern in mice has only been described in two studies. The first provided details on running pattern and behavior in female mice on a large running wheel (diameter: 38 cm) [10], while the second investigated male mice using a special angled running track [11]. Although both studies focused on running behavior, however, there was no specific attention for resultant skeletal muscle performance.

The present study was undertaken to analyze voluntary running pattern of wild type C57Bl/6 mice. Subsequently, we investigated the impact of six weeks voluntary running wheel exercise on slow-twitch soleus muscle. Physiological end points were total produced active and unstimulated force during serial contractions and associated oxygen consumption. In addition, we questioned whether running wheel exercise affected MyHC composition and citrate synthase activity. As changes in active force are related to fatigue resistance [12], while those in unstimulated force are related to relaxation and/or Ca^{2+} transport [13, 14], the physiological data were combined with analysis of Ca^{2+} transport and regulatory proteins on mRNA and protein level.

3.2 Methods

Animals and exercise model

Four-week old male C57Bl/6 mice were randomly selected in a running wheel exercise (RWE; n=12) or a sedentary control (SED; n=10) group and housed individually on a 12:12-h light-dark cycle with food and water provided *ad libitum*.

Cages (28.8 cm x 28.8 cm x 24.5 cm) were custom built and made from Plexiglas. Cages of RWE group were equipped with in-house made running wheels with a diameter of 12.1 cm. Treads on the wheel were 1.2 cm apart. For each cage, the running wheel was equipped with a small magnet, and juxtaposed on the outside of the Plexiglas cage, a magnetic relais was attached and hooked up to a PC. The analogue output of the relais was sampled at a frequency exceeding 10 kHz using homebuilt Labview programs (National Instruments, Austin, TX, USA). Revolution times shorter than 0.2 seconds were excluded from analysis as these represented an artifact in the data due to the high sampling frequency. Ordinary bicycle speedometers (Hema, Amsterdam, the Netherlands) served as a backup control to measure total accumulated running distance.

Experiments were performed in accordance with institutional and governmental guidelines after approval of the Animal Experimentation Ethics Committee, Utrecht University.

Muscle preparation

Mice were sacrificed by cervical dislocation at the age of ten weeks, i.e. six weeks after the start of the protocol. Soleus muscles were ligated at the proximal and distal tendons with 5.0 silk sutures, removed from the hindlimbs and placed in organ baths immediately to recover. Muscle length and diameter were measured with a digital caliper. Contralateral soleus muscles were dissected, snap frozen in liquid nitrogen and stored at -80°C for further biochemical experiments.

Physiological studies of isolated soleus muscle

Physiological studies of mechanical function and oxygen consumption of isolated soleus muscles were conducted according to methods described previously [15]. Briefly, isolated soleus muscles were mounted in holders custom-built to fit the glass chambers of a Cyclobios oxygraph apparatus (A. Paar KG, Graz, Austria). This dual-chamber apparatus has been described

elsewhere [16]. Muscles were mounted by attaching tendons to a fixed support at one end and to the lever of a Harvard Apparatus model 60-2995 isometric force transducer (Harvard Apparatus, South Natick, MA, USA) at the other end. The holders were fitted with platinum wire electrodes over the top and bottom tendon positions for electrical stimulation of the muscles. The chambers were equipped with a Clarke-type oxygen electrode (Orbisphere Model 2120, Orbisphere Laboratories, Vésenaz, Switzerland) and a magnetic stirrer, and were embedded in an insulated copper block with integrated Peltier heat pump thermostat for temperature control [16]. After each experiment, muscles were carefully blotted and weighed after removal of the tendons. The volume of the chambers was determined gravimetrically (~ 5 ml).

All experiments were performed at 20 °C in a bicarbonate Ringer solution (116 mM NaCl, 4.6 mM KCl, 1.16 mM KH_2PO_4, 2.5 mM $CaCl_2$, 1.16 mM $MgSO_4$, and 25.3 mM $NaHCO_3$) equilibrated with 95% O_2 - 5% CO_2 (pH 7.4). Oxygen partial pressure (PO_2) of the medium was >450 Torr during all experiments, which is above the critical PO_2 at which diffusive flux of O_2 could be rate limiting for oxidative phosphorylation for muscles of this size at this temperature (350-450 Torr; [17]). The stirring rate in each chamber was 600 rpm, resulting in a response time constant of the electrode of 4 sec.

Twitch contractions were evoked using supramaximal single pulses (0.5 msec duration at 8-12 V) delivered by a Grass model S88 dual channel stimulator (Astro-Med, Warwick, RI, USA). The analogue transducer output was recorded both using a Grass model 2400 dual channel recorder as well as digitally (1 kHz sampling) using Labview software, and stored on a PC. The output of the oxygen electrode was likewise digitized (1 kHz sampling) using this software and stored on a PC. The electrodes were calibrated prior to each experiment using a two point method (zero oxygen, obtained by addition of dithionite solution, and atmospheric PO_2; atmospheric pressure was recorded for each experiment).

Stimulation protocol.

Prior to measurements the length of the muscle and stimulation voltage were adjusted to yield maximal twitch force upon stimulation. Next, twitch and tetanic contractions were characterized with respect to kinetics and force. Three tetanic contractions were evoked at 50 Hz, which was the typical fusion frequency at 20 °C. Subsequently, the muscle was serially stimulated at 3 Hz for a period of 6 minutes.

Data analysis.

The mechanics of muscle contraction were analyzed on a twitch-per-twitch basis with respect to four parameters: active force, unstimulated force, rise, and relaxation time using standard LabView subroutines. Changes in these parameters during the serial stimulation experiments in soleus muscles were quantified by scaling each to its initial value determined from the twitches recorded prior to the serial contraction protocol. The oxygen concentration in the chambers was calculated as described elsewhere [16]. Absolute muscle respiratory rates were calculated using Origin 6.0 (Microcal Software Inc., Northampton, MA, USA).

Biochemical studies

Citrate synthase assay

Citrate synthase enzyme activity of soleus homogenate was determined to characterize Krebs cycle activity as a measure of mitochondrial content, as described by Srere, 1969 [18]. Briefly, muscle samples free of connective tissue were homogenized, followed by sonication to further disrupt the mitochondrial membrane. Activity was determined spectrophotometrically (412 nm; 30 °C) by measuring the appearance of the CoA-SH (acetyl-CoA + oxaloacetate + $H_2O \leftrightarrow$citrate + CoA-SH + H^+ (side reaction: CoA-SH + DTNB $\rightarrow$ mercaptide ion)). Readings were taken at 20-s intervals for 2-2.5 min to measure acetyl-CoA deacylase activity. Samples were assayed in duplicate, and samples from all animals were assayed on the same day to reduce inter-assay variation. Total protein in the homogenate was assayed by using the technique described by Bradford [19].

MyHC profiling

Soleus muscle samples were homogenized in a solution containing 250 mM sucrose, 100 mM KCl, 5 mM EDTA, and 20 mM Tris base. Protein concentration was determined by the method of Bradford [19]. Skeletal MyHC composition was assessed by SDS-PAGE procedures, according to Talmadge and Roy [20]. In short, 800 ng of protein sample was run on an 8% running gel for 48 hours at 70 V at 4 °C to quantify MyHC composition in soleus muscles after running wheel exercise. MyHC bands were visualized by silver staining (Biorad), and quantified (as percentage of total) using AlphaEase FC software (San Leandro, CA, USA).

Ca^{2+} transport and regulatory proteins

Ca^{2+} ATPase content

The content of Ca^{2+} ATPase was determined by measurement of the Ca^{2+}-dependent steady-state phosphorylation from [γ-^{32}P]ATP in crude soleus muscle homogenates, as described previously [21]. Briefly, 180-200 µl aliquots of the homogenate were reacted for 30 s at 0 °C in a medium containing [γ-^{32}P] ATP (Specific activity 222 TBq/mmol; NEN Life Science Products Inc., Boston, MA, USA) as a tracer and 0.5 mM EGTA. In a parallel assay 0.55 mM $CaCl_2$ was added to the same medium, giving an estimated free Ca^{2+} concentration of 50 µM. All assays were performed in duplicate. The Ca^{2+} ATPase content was calculated as the difference between the ^{32}P incorporation in the presence and the absence of Ca^{2+}. It has been shown that this value represents a reproducible quantification of the concentration of total Ca^{2+}-dependent Mg^{2+}-ATPase of SR (both SERCA 1 and SERCA 2) [21].

RT-PCR

Total RNA was isolated from unstimulated soleus muscles using the Qiagen RNeasy fibrous tissue kit (Qiagen GmbH, Hilden, Germany). cDNA was prepared from 0.75 µg RNA in a total volume of 20 µl according to manufacturer's protocol (iScript cDNA synthesis kit; Biorad, Hercules, CA, USA). Primers were designed against SERCA 1, SERCA 2A, phospholamban, and sarcolipin (Table 3.1). RT-PCR was performed in a MyiQ cycler (Biorad) at an annealing temperature of 57°; input of cDNA was 50 ng and the concentration of the primers (forward and reverse) was 10 µM. Product specificity during PCR was verified by melting curve analysis of the products. For each amount of RNA tested, duplicate Ct values were obtained and averaged. Quantification was performed using a mathematical model of relative expression ratio in real-time PCR, the $^{-\Delta\Delta Ct}$-method [22, 23] and was calculated with help of the Genex-software (Biorad). GAPDH was used as a reference gene [24].

Western blot

Soleus muscle processing was done similarly to the method described above for MyHC profiling with the exception that homogenates were centrifuged and supernatant was collected in order to discard larger proteins like myosins. For SERCA 1 and SERCA 2, 10 µg of protein was run over a 10% running gel. For PLB, 25 µg of protein was run over a 12% running gel. Proteins were blotted to nitrocellulose membrane using a semi-dry blotting

apparatus (Biorad). Membranes were blocked for 1 hour in 5% BSA of 5% non-fat milk for SERCA and PLB, respectively. Membranes were incubated overnight at 4°C with first antibody (**SERCA 1** catalog# MA3-912, **SERCA 2** catalog# PA1-21904, **PLB** catalog number MA3-922; Affinity Bioreagents, Golden, CO, USA) in blocking solution. Incubation with second HRP-conjugated antibody was done for 1 hour at room temperature. Membranes were developed with ECL (Pierce, Rockford, IL, USA). Alpha-tubulin (Catalog# T5168; Sigma Aldrich, St Louis, MO, USA) served as a reference protein.

Statistics

Data are presented as arithmetic means ± standard error (SE). Statistical analyses were performed using a Student's unpaired *t*-test. Differences between SED and RWE muscles were considered significant if $P<0.05$.

Name	Sequence	Product length (bp)
SERCA 1	*For* ACA GGC AGG TGG ATA AGC *Rev* CCC GAA ATA GGA CAA ACA TTC	144
SERCA 2A	*For* TGC TGC TGG GAA AGC TAT GG *Rev* GTG TTC TCT CCT GTT CTG TTG C	101
PLB	*For* ACC GAA GCC AAG GTC TCC *Rev* CGA GCG AGT GAG GTA TTG C	149
SLN	*For* TTC ACA GTT GTC CTC ATC ACC *Rev* GCA CAC AGC AGT CAC TCC	101
GAPDH	*For* GAA GGT CGG TGT GAA CGC *Rev* TGA AGG GGT CGT TGA TGG	101

Table 3.1 SERCA 1, SERCA 2A, phospholamban, sarcolipin and GAPDH PCR-primers. The primer sequences are shown in 5' → 3' order. The length of the amplified product is indicated. Annealing temperature and number of cycles were 57°C and 40, respectively, for all primer sets. Product lengths are represented as numbers of base pairs.

3.3 Results

Animals and running activity

Mice with unlimited access to a running wheel typically ran 7.3 ± 0.5 km per day (n=12; range: 3.9 – 10.7 km) during the dark cycle. Food intake of mice in the exercise group was significantly higher than in the control group (RWE (n=10) 7.2 ± 0.5; SED (n=12) 6.1 ± 0.4 g per day; $P<0.01$),

with a significant correlation between running distance and food intake (r^2 0.8; data not shown). There were no differences in body weight between both groups, with both showing a progressive increase over the six-week experimental period (Table 3.2).

	Onset	Week 1	Week 2	Week 6
SED (n = 10)	18 ± 0.3	21 ± 0.4	22 ± 0.3	24 ± 0.3
RWE (n = 12)	18 ± 0.2	21 ± 0.1	22 ± 0.2	24 ± 0.3

Table 3.2 Weights (g) of C57Bl/6 mice during the six-week experimental period.

Figure 3.1a shows a typical two-day running recording from an individual mouse taken in the third experimental week. It is representative for the entire study from day 3 and onward. Coarse inspection of the recording suggests that the mouse continuously ran for nearly 12 hours. However, when focusing in on one hour of recordings, a discontinuous, intermittent running pattern is clearly discerned (figure 3.1b). Focusing further on only a single minute of the recording, short bursts of running activity can be distinguished (figure 3.1c).

The histogram of the time between subsequent passings of a running wheel through its magnetic relais during a 12 hour dark period typically showed two peaks (figure 3.2a): One sharp peak (peak #1) with a time between revolutions of 0.56 s and a second peak with an optimum at 1.6 s. Peak #1 represents actual periods of activity spent running on the wheel. With a peak at 0.56 s and a wheel circumference of 38 cm this accounts for an optimum speed of 0.67 m/s (2.4 km/h). This matched the running speed measured by the speedometers during running periods (data not shown). Peak #2 of figure 3.2a is most likely associated with the short periods of inactivity observed in figure 3.1c. Together, these data suggest an intermittent running pattern consisting of bouts of high speed running interspersed by nearly two-second periods of inactivity. Analysis of the histogram at day 2 (insert figure 3.2a) showed that peak #1 and #2 were not well separated. Typically, peak #1 of the histogram of day 2 had a higher optimum time between revolutions, indicative for a lower optimum running speed.

The box-plot in figure 3.2c represents running speed extracted from peak #1 in running histograms from all RWE mice (n=12). On the second day, mice ran with an average speed of 1.8 ± 0.1 km/h. During the rest of the experimental period, mice ran at an average speed of 2.5 ± 0.1 km/h, which was significantly higher than on the second day.

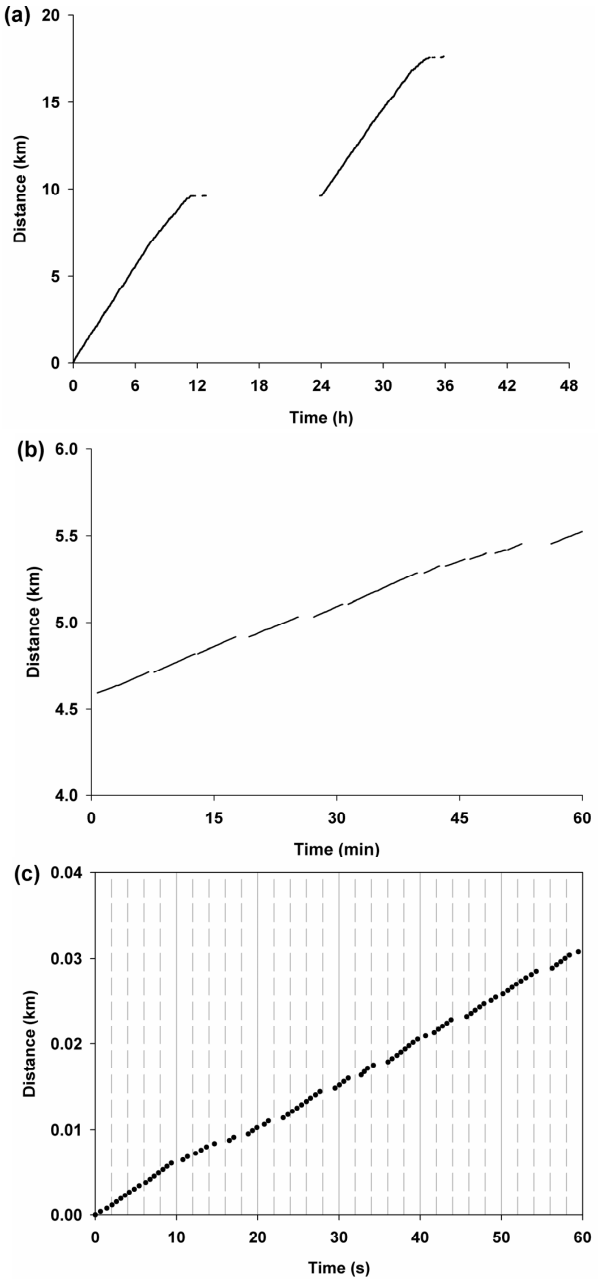

Figure 3.1: Running pattern of one mouse during the third week of the experimental period. **A:** Typical example of two days. **B:** detail of one hour running pattern between hours 5 and 6 on the first day, typically consisting of intermittent running. **C** detail of one minute during hours 5 and 6 on the first day demonstrating burst activity within the intermittent running.

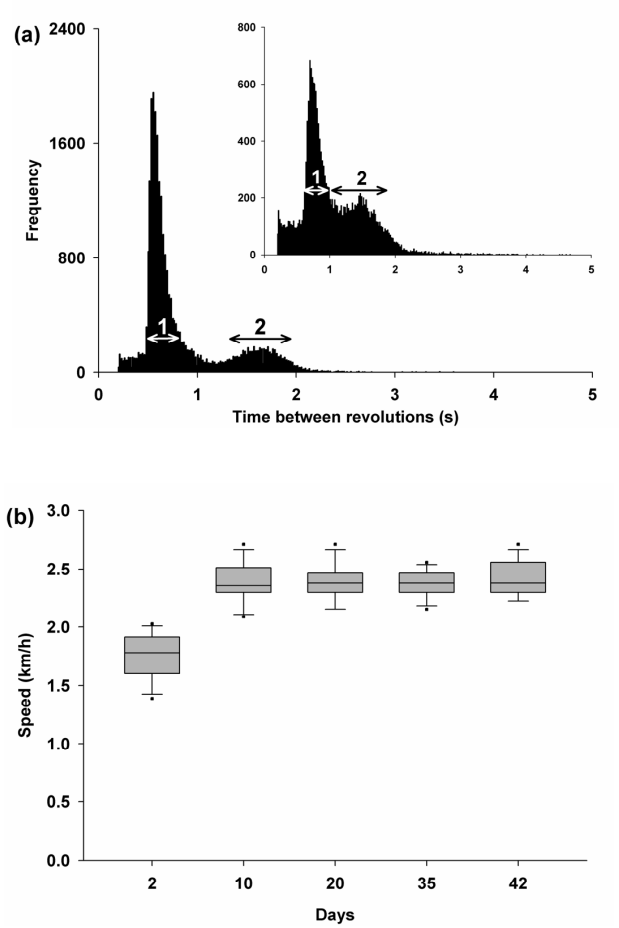

Figure 3.2 Analysis of the running pattern of the mouse shown in figure 1. **A:** histogram of the time between subsequent passings of a running wheel through its magnetic relais (recordings of one day). The x axis represents the time between wheel revolutions, whereas the y axis represents frequency. Two peaks are depicted by arrow bars and numbers; for clarity of presentation, periods between wheel revolutions longer than 5 s are excluded from the histogram. **Insert:** histogram of the same mouse at day two of the experimental period. **B** box-plot of average running speed analyzed from peak 1 from all animals (n=12). Running speed on day 2 was significantly lower than during the rest of the experimental period.

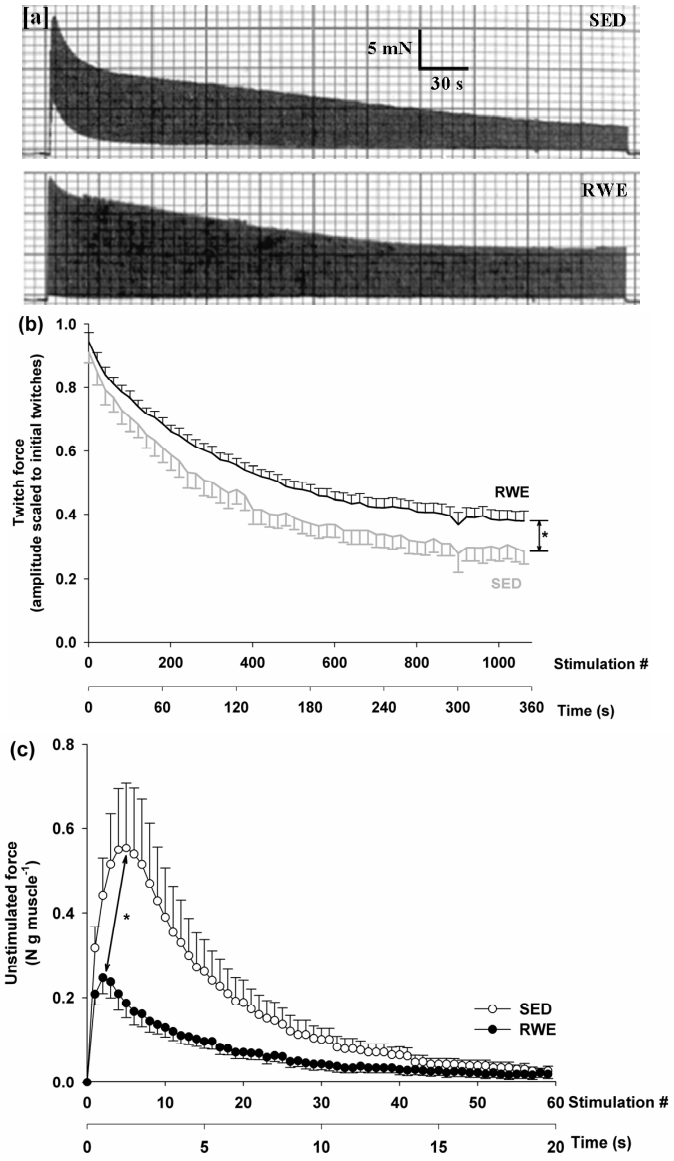

Figure 3.3 A Typical recording of twitch-force of a control (=SED; top) and exercised (=RWE; bottom) soleus muscle during serial stimulation at 3 Hz. Vertical bar corresponds to 5 mN of force. Horizontal bar corresponds to 30 s of time. **B** Residual twitch force (in scaled amplitude) of soleus muscles of SED (lower line; n=7) and RWE (upper line; n=12) mice, contracting at 3 Hz for 6 minutes. Force is significantly higher in RWE muscles compared to SED muscles, during the entire stimulation protocol. For clarity of presentation every twentieth error bar is shown. **C** Unstimulated force of SED (open symbols; n=7) and RWE (closed symbols; n=12) C57Bl/6 soleus muscle during the first 20 seconds of serial contractions at 3 Hz. Unstimulated force is represented as absolute force, since initial baseline force is zero. * $P<0.05$ RWE vs. SED.

Physiological studies of isolated soleus muscle

Soleus muscle lengths, weights, and cross sectional areas were not different between groups (Table 3.3). Also, no changes were found between the two groups in any of the parameters characterizing single twitch and tetanic contractions (Table 3.3).

	SED n=4	RWE n=6
General		
Weight (mg)	13.1 ± 1.3	13.0 ± 0.6
CSA (mm^2)	2.1 ± 0.2	2.2 ± 0.2
Length (tendon-to-tendon; mm)	9.9 ± 0.3	10.6 ± 0.5
Twitch		
Force (N/g muscle)	1.4 ± 0.2	1.6 ± 0.1
Rise time (ms)	36.0 ± 1.3	37.9 ± 2.5
Relaxation time (ms)	352 ± 19	335 ± 36
Tetanus		
Force (N/g muscle)	13.1 ± 2.0	11.9 ± 0.8
Rise time (ms)	455 ± 134	492 ± 88
Relaxation time (ms)	97 ± 11	114 ± 10

Table 3.3 Soleus muscle characterization.

Figure 3.3a shows typical strain recordings from control (upper trace) versus trained (lower trace) soleus muscles during serial electrical stimulation at 3 Hz. Combined results for active and unstimulated force are shown in figures 3.3b and 3.3c, respectively. Initial force was the same for both groups (Table 3.3). However, residual active twitch force produced by RWE muscles after 6 minutes of stimulation was 1.3-fold higher than by SED muscles ($P<0.05$; Figure 3.2b). Unstimulated force in SED muscles attained a maximum of 0.55 ± 0.15 N/g two seconds after onset of stimulation (figure 3.3c) before attaining the initial value (0 N/g) approximately 25 seconds later (not shown). In RWE soleus muscles, the time course of unstimulated force during serial stimulation at 3 Hz was qualitatively as well as quantitatively different: peak unstimulated force was already attained within one second after onset of stimulation and was twofold lower than in SED muscle (0.25 ± 0.04 N/g; $P<0.05$) (figure 3.3c). Unstimulated force re-

turned to initial –baseline- value after a similar time period as SED muscle (not shown).

Oxygen consumption during stimulation at 3 Hz attained steady-state approximately 180 seconds after onset of serial contractions in both SED and RWE muscle (not shown). The steady-state rate at this stimulation frequency was 1.3-fold higher in the RWE group than in the SED group (0.063 ± 0.004 nmol s^{-1} g^{-1} (n=9) versus 0.049 ± 0.004 (n=6) respectively; P<0.05) (figure 3.4a).

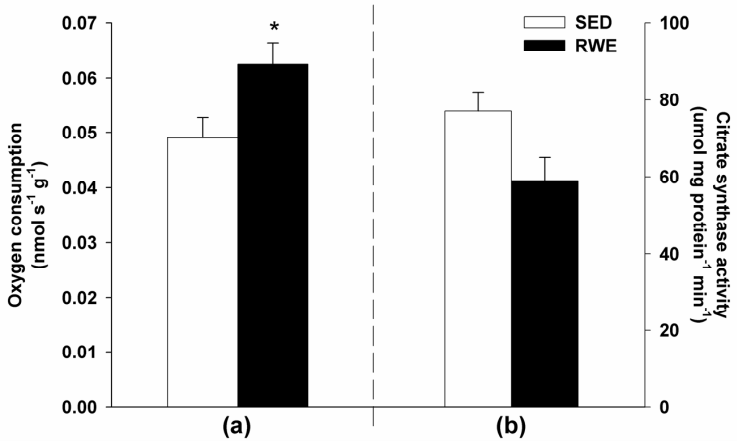

Figure 3.4 The left part of the figure (A) represents oxygen consumption of SED (n=6) versus RWE (n=9) mouse soleus muscles during stimulation at 3 Hz. The right part of the figure (B) represents citrate synthase activity in SED (n=9) versus RWE (n=5). * P<0.05 RWE vs. SED.

Biochemical assays

No effect of exercise was found on citrate synthase activity in soleus muscles (figure 3.4b). The mean results of MyHC composition in soleus muscles are presented in table 3.4. Although we were able to distinguish all four MyHC isoforms, complete separation of MyHC type IIa and IIx could not be achieved in every sample. Therefore we chose to combine these two types in the analysis. No significant changes were found in MyHC composition. If any, however, phenotype shifted towards the intermediate IIa/x isoform.

	SED (n=4)	RWE (n=4)
Type I	36.3 ± 2.3	35.4 ± 3.3
Type IIa/x	58.5 ± 4.4	60.3 ± 4.6
Type IIb	5.2 ± 5.4	4.3 ± 4.6

Table 3.4 MyHC composition (as %) of C57Bl/6 mouse soleus muscles, as detected by SDS-PAGE.

Ca^{2+} transport and regulatory proteins

Ca^{2+} ATPase content

There were no differences in Ca^{2+} ATPase content of the soleus between SED and RWE muscles (SED 10.4 ± 1.8 (n=3); RWE 10.9 ± 3.1 (n=3) nmol Ca^{2+} ATPase g $muscle^{-1}$).

mRNA

mRNA levels were calculated as expression values relative to GAPDH expression, for each individual gene. mRNA levels of SERCA 1 and SERCA 2A were unaffected in soleus muscle of the RWE group compared to the SED group (figure 3.5). However, phospholamban mRNA expression was reduced by up to 60% while sarcolipin mRNA expression was raised to 199% in the RWE group (n=8) compared to the SED group (n=8) (**PLB**: SED 100 ± 27; RWE 36 ± 7 %; $P<0.05$; **SLN**: SED 100 ± 14; RWE 199 ± 19 %; $P<0.05$).

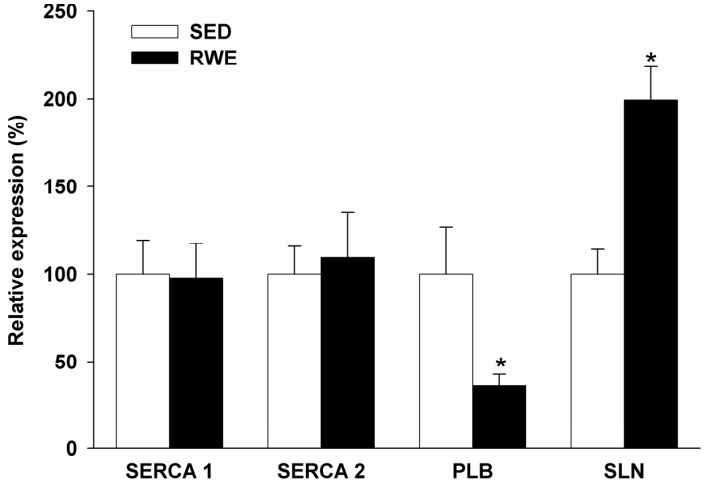

Figure 3.5 Relative mRNA expression of SERCA 1, SERCA 2, phospholamban (PLB), and sarcolipin (SLN) in soleus muscle, as detected by RT-PCR. n=8 for each group. * $P<0.05$ RWE vs. SED.

Protein

Protein levels were calculated as expression values relative to α-tubulin expression, which served as a loading control. Figure 3.6 demonstrates a typical example of western blots for SERCA 1, SERCA 2, PLB, and α-tubulin. No changes were seen in SERCA 1 and SERCA 2 protein levels in soleus muscle of the RWE group compared to the SED group (figure 3.7). Phospholamban protein expression was decreased by 40% (**PLB**: SED 1.0 ± 0.1 (n=6); RWE 0.57 ± 0.1 (n=6); $P<0.05$).

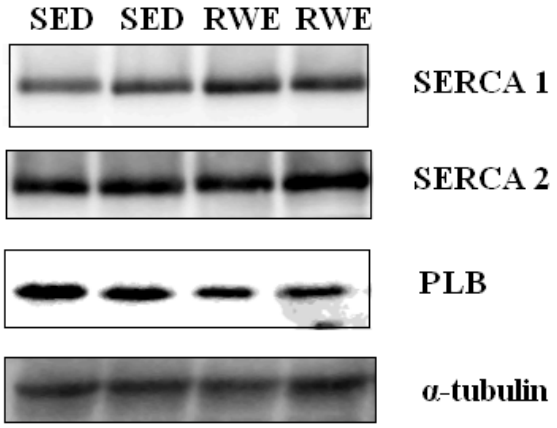

Figure 3.6 Typical example of western blot analysis of SERCA 1, SERCA 2, phospholamban, and α-tubulin, in soleus muscle homogenates. α-Tubulin served as a loading control.

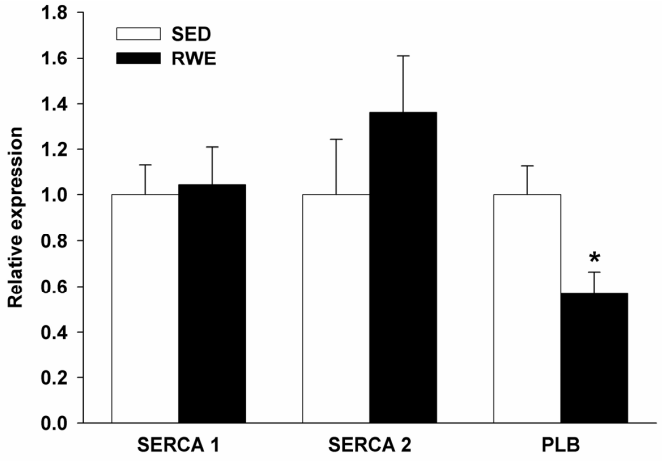

Figure 3.7 Relative protein expression of SERCA 1, SERCA 2, and phospholamban (PLB) in soleus muscle, detected by western blot analysis. n=6 for each group. * $P<0.05$ RWE vs. SED

3.4 Discussion

This work describes studies of voluntary wheel running exercise and ensuing adaptation of the slow-twitch soleus muscle. Analysis of running wheel revolution recordings revealed intermittent running activity consisting of bursts of high-speed running. Physiological measurements of soleus muscle demonstrated improved fatigue resistance and improved Ca^{2+} handling. No phenotypic changes were found in soleus muscle MyHC or SERCA content that could explain these improvements. However, significant changes were found in gene transcripts of the SERCA inhibitors PLB and SLN. Below, these results and how they impact our understanding of skeletal muscle plasticity in response to voluntary wheel running in this particular rodent model are discussed.

Running pattern characterization

Running wheels have been extensively used in order to study the beneficial effects of exercise on the outcome of disease. The mouse has proven to be the animal of choice mainly due to the availability of transgenic animals. In order to extrapolate these results to the human situation, however, it is necessary to understand the running pattern of this particular animal. Mice demonstrate an intermittent running pattern, rather than continuous running. Although this has long been known for rodents [25], the exact running pattern had not been described in detail until recently [10, 11], both using special running wheels. The first object of our study was therefore to characterize the running pattern of mice using running wheels, as these are the most common used devices [5].

Although it appeared as if the mouse ran continuously on the wheel (figure 3.1a), detailed analysis demonstrated an intermittent running pattern (figure 3.1b). These active periods were, in turn, interspersed by near-two seconds intervals (figure 3.1c). The running pattern was further analyzed by plotting the time between revolutions. This histogram (figure 3.2a) demonstrated two peaks. The first peak had a time of 0.56 s between revolutions corresponding to a speed 2.4 km/h. This speed matches the speed found in the study with horizontal running tracks [11] and corresponds to the maximum speed found by Allen et al. [5]. The second peak corresponded to the 'inactivity time' during periods of running, as seen in figure 3.1c, characterizing the burst activity seen in mice. The average time of this

peak was 1.7 s (data not shown), which was typically lower than the inter-bout pauses in the study by Girard et al. [10].

The burst activity was seen throughout the experimental period of 6 weeks, but mice clearly showed acclimatization. This was evident from the increase in time spent on the wheel, with a narrower range of speeds (peak 1, figure 3.2a) as well as a higher optimum speed after two days of running (figure 3.2b).

Soleus muscle adaptation

Six weeks of voluntary exercise did not induce any changes in soleus weight or size, nor in any of the twitch and tetanic contraction parameters (table 3.3) [26-28]. Differences were observed, however, during serial twitch contractions. SED muscles showed progressive decline in total produced force during six minutes of stimulation at 3 Hz (figure 3.1b). This is in agreement with previous *in vivo* studies in rat triceps surae muscle [29]. Likewise, studies in soleus muscle subjected to tetanic contractions demonstrated the same force reduction in mice [30] as well as in rats [31]. The decline was significantly smaller in RWE muscles, demonstrating improved fatigue resistance in exercised soleus muscles. Residual total force in RWE muscles was 1.3 fold higher than in SED muscle (figure 3.1b). An explanation for the higher residual force could be a fast-to-slow transformation of MyHC. However, no such change was found (table 3.4), similar to previous studies [26, 28]. Parallel to the higher residual force, oxygen consumption during serial contractions was 1.3-fold higher in RWE muscles (figure 3.4a). Apparently, this higher oxygen consumption could be sustained without an increase in mitochondrial content (figure 3.4b). This suggests that mitochondrial capacity was sufficient to ensure ATP production in both SED as well as RWE muscles.

As stated before, no changes were seen in relaxation times during individual twitches (table 3.3), indicating no major changes in Ca^{2+} transport capacity. Remarkably, unstimulated force dynamics during the first seconds of stimulation demonstrated a steep rise in SED muscles, slowly reaching baseline level after approximately 20 seconds (figure 3.2c). Unstimulated force is an index of free Ca^{2+} within the cell and, as such, a reflection of Ca^{2+} handling [13, 14]. The peak of unstimulated force in RWE was much lower and its return to baseline much faster than in SED muscle, suggesting improved Ca^{2+} handling during repeated contraction. This was not associated with an increase in total Ca^{2+} ATPase content, nor with changes in the absolute amounts of SERCA 1 and 2a isoforms (figures 3.5

and 3.7). Therefore, it is likely to suggest that proteins regulating SERCA activity could underlie the improved Ca^{2+} handling.

SERCA 2a is the predominant isoform in soleus muscle [32], which is regulated by phospholamban (PLB). While the activity of SERCA 2a is inhibited by PLB [33], phosphorylation of PLB relieves this inhibitory effect [34]. Both chronic PLB phosphorylation as well as downregulation of PLB expression would thus improve SERCA 2a activity. Indeed, a decrease of 60% in PLB mRNA expression was detected in RWE muscles compared to SED muscles (figure 3.5), which was associated with a 40% decrease in PLB protein expression.

Recently, sarcolipin (SLN) was proposed as a second major regulator of SERCA 2a, with a comparable inhibiting mechanism as PLB [32, 35]. Interestingly, we found an increase of 199% in SLN mRNA (figure 3.5). Unfortunately, we were not able to confirm this on protein level, due to a non-specific antibody. The increase in SLN mRNA expression suggests a compensatory effect for the decrease in PLB expression. This might be related to a difference in affinity for the SERCA pump between PLB and SLN and/or differences in response towards Ca^{2+} concentration; high levels of Ca^{2+} concentration are described to relieve the inhibitory effect of PLB [36], whereas SLN inhibits SERCA 2a activity even at high Ca^{2+} concentration [37, 38]. In support of this idea, SLN protein levels were upregulated in atria of PLB null mice [39] pointing to a similar compensatory mechanism as in the present study.

Impact of the study

This study has analyzed the running pattern of voluntary exercising mice in detail, demonstrating bursts of running at high speed in an intermittent pattern. Ensuing adaptations of the slow-twitch soleus muscle were found in SERCA regulators, rather than in classic fast-to-slow remodeling involving MyHC and mitochondrial content adaptation. To our knowledge, this particular adaptive strategy has hereto only been described for cardiac muscle after treadmill exercise [40, 41].

We hypothesize that our finding of downregulation of PLB gene expression constitutes 'hardwiring' of an apparent repetitive event in the mouse – i.e. phosphorylation of PLB as downstream effect of periodically Ca^{2+} activated cAMP signaling [42, 43]. This hypothesis is based on our observation that the steep rise of unstimulated force (representing a steep rise in free Ca^{2+} concentration) in SED muscles upon onset of electrical stimulation was less pronounced in RWE muscles (figure 3.2c). The analysis of volunta-

ry running pattern revealed an intermittent running pattern consisting of discontinuous peaks of high-speed running activity, as stated before. Therefore, we propose that voluntary running activity in mice is associated with repetitive bursts of free Ca^{2+} concentration increases ('frequency modulation'), which activate cAMP signaling pathway and its subsequent downstream events. In this light, it is of interest that continuous elevation of the cytosolic Ca^{2+} concentration ('amplitude modulation') in cultured myocytes results in mitochondrial biosynthesis [44, 45]. We did not find an increase in mitochondrial content after wheel running exercise (figure 3.4b), supporting the hypothesis of non-continuous Ca^{2+} elevations in our experimental model. Likely, voluntarily running mice do not run at their maximum capacity, and, as such, have sufficient mitochondrial capacity. The increased oxygen consumption seen with a reduced fatigability (figures 3.3b and 3.4a) can therefore be accommodated without any increase in mitochondrial content (figure 3.4b).

Taken together, we have shown that wheel running exercise induces fatigue resistance in mouse soleus muscle, and is associated with improved Ca^{2+} handling due to downregulation of PLB inhibition of SERCA 2a. Further investigation of the intracellular Ca^{2+} concentrations during serial contractions and the specific role of SLN in hindlimb muscle adaptation in this model will be necessary for a complete picture.

3.5 Acknowledgements

Valuable discussions and manuscript proofreading by dr Jean-Marc Renaud (Department of Cellular and Molecular Medicine, University of Ottawa, Canada) are gratefully acknowledged.

3.6 References

1. Pette, D. and G. Vrbova, *Adaptation of mammalian skeletal muscle fibers to chronic electrical stimulation.* Rev Physiol Biochem Pharmacol, 1992. **120**: p. 115-202.
2. Kariya, F., et al., *Effects of prolonged voluntary wheel-running on muscle structure and function in rat skeletal muscle.* Eur J Appl Physiol, 2004. **92**(1-2): p. 90-7.
3. Fuller, P.M., K.M. Baldwin, and C.A. Fuller, *Parellel and divergent adaptations of rat soleus and plantaris to chronic exercise and hypergravity.* Am J Physiol Regul Integr Comp Physiol, 2005. **290**(2): p. R442-8.
4. Simoneau, J.A. and D. Pette, *Species-specific effects of chronic nerve stimulation upon tibialis anterior muscle in mouse, rat, guinea pig, and rabbit.* Pflugers Arch, 1988. **412**(1-2): p. 86-92.
5. Allen, D.L., et al., *Cardiac and skeletal muscle adaptations to voluntary wheel running in the mouse.* J Appl Physiol, 2001. **90**(5): p. 1900-1908.
6. Jeneson, J.A., et al., *Treadmill but not wheel running improves fatigue resistance of isolated extensor digitorum longus muscle in mice.* Acta Physiol (Oxf), 2007. **190**(2): p. 151-61.
7. Akimoto, T., et al., *Skeletal muscle adaptation in response to voluntary running in Ca^{2+}/calmodulin-dependent protein kinase IV (CaMKIV) deficient mice.* Am J Physiol Cell Physiol, 2004. **287**(5): p. C1311-9.
8. Gramolini, A.O., et al., *Cardiac-specific overexpression of sarcolipin in phospholamban null mice impairs myocyte function that is restored by phosphorylation.* Proc Natl Acad Sci U S A, 2006. **103**(7): p. 2446-51.
9. Nair-Shalliker, V., et al., *Myofiber adaptational response to exercise in a mouse model of nemaline myopathy.* Muscle Nerve, 2004. **30**(4): p. 470-80.
10. Girard, I., et al., *Selection for high voluntary wheel-running increases speed and intermittency in house mice (Mus domesticus).* J Exp Biol, 2001. **204**(Pt 24): p. 4311-20.
11. De Bono, J.P., et al., *Novel quantitative phenotypes of exercise training in mouse models.* Am J Physiol Regul Integr Comp Physiol, 2005. **290**(4): p. R926-34.
12. Zhang, S.J., et al., *Limited oxygen diffusion accelerates fatigue development in mouse skeletal muscle.* J Physiol, 2006. **572**(Pt 2): p. 551-9.
13. Baylor, S.M. and S. Hollingworth, *Sarcoplasmic reticulum calcium release compared in slow-twitch and fast-twitch fibres of mouse muscle.* J Physiol, 2003. **551**(Pt 1): p. 125-38.
14. Cifelli, C., et al., *KATP channel deficiency in mouse flexor digitorum brevis causes fibre damage and impairs Ca2+ release and force development during fatigue in vitro.* J Physiol, 2007. **582**(Pt 2): p. 843-57.
15. Ter Veld, F., K. Nicolay, and J.A. Jeneson, *Increased resistance to fatigue in creatine kinase deficient muscle is not due to improved contractile economy.* Pflügers Arch, 2006. **452**(3): p. 342-348.
16. Haller, T., M. Ortner, and E. Gnaiger, *A respirometer for investigating oxidative cell metabolism: toward optimization of respiratory studies.* Anal Biochem, 1994. **218**(2): p. 338-42.
17. Crow, M.T. and M.J. Kushmerick, *Chemical energetics of slow- and fast-twitch muscles of the mouse.* J Gen Physiol, 1982. **79**(1): p. 147-66.

18. Srere, P.A. and G.C. Brooks, *The circular dichroism of glucagon solutions.* Arch Biochem Biophys, 1969. **129**(2): p. 708-10.
19. Bradford, M.M., *A rapid and sensitive method for the quantitation of microgram quantities of protein utilizing the principle of protein-dye binding.* Anal Biochem, 1976. **72**: p. 248-54.
20. Talmadge, R.J. and R.R. Roy, *Electrophoretic separation of rat skeletal muscle myosin heavy-chain isoforms.* J Appl Physiol, 1993. **75**(5): p. 2337-40.
21. Everts, M.E., et al., *Quantitative determination of Ca^{2+}-dependent Mg^{2+}-ATPase from sarcoplasmic reticulum in muscle biopsies.* Biochem J, 1989. **260**(2): p. 443-8.
22. De Preter, K., et al., *Quantification of MYCN, DDX1, and NAG gene copy number in neuroblastoma using a real-time quantitative PCR assay.* Mod Pathol, 2002. **15**(2): p. 159-66.
23. Livak, K.J. and T.D. Schmittgen, *Analysis of relative gene expression data using real-time quantitative PCR and the 2(-Delta Delta C(T)) Method.* Methods, 2001. **25**(4): p. 402-8.
24. Jemiolo, B. and S. Trappe, *Single muscle fiber gene expression in human skeletal muscle: validation of internal control with exercise.* Biochem Biophys Res Commun, 2004. **320**(3): p. 1043-50.
25. Rodnick, K.J., et al., *Variations in running activity and enzymatic adaptations in voluntary running rats.* J Appl Physiol, 1989. **66**(3): p. 1250-7.
26. Pellegrino, M.A., et al., *Effects of voluntary wheel running and amino acid supplementation on skeletal muscle of mice.* Eur J Appl Physiol, 2005. **93**(5-6): p. 655-64.
27. Momken, I., et al., *Voluntary physical activity alterations in endothelial nitric oxide synthase knockout mice.* Am J Physiol Heart Circ Physiol, 2004. **287**(2): p. H914-20.
28. Wernig, A., A. Irintchev, and P. Weisshaupt, *Muscle injury, cross-sectional area and fibre type distribution in mouse soleus after intermittent wheel-running.* J Physiol, 1990. **428**: p. 639-52.
29. Everts, M.E., et al., *Force development and metabolism in skeletal muscle of euthyroid and hypothyroid rats.* Acta Endocrinol (Copenh), 1981. **97**(2): p. 221-5.
30. Danieli-Betto, D., et al., *Deficiency of alpha-sarcoglycan differently affects fast- and slow-twitch skeletal muscles.* Am J Physiol Regul Integr Comp Physiol, 2005. **289**(5): p. R1328-37.
31. Everts, M.E., et al., *Fatigability and recovery of rat soleus muscle in hyperthyroidism.* Metabolism, 1987. **36**(5): p. 444-50.
32. Vangheluwe, P., et al., *Sarcolipin and phospholamban mRNA and protein expression in cardiac and skeletal muscle of different species.* Biochem J, 2005. **389**(Pt 1): p. 151-9.
33. Jorgensen, A.O. and L.R. Jones, *Localization of phospholamban in slow but not fast canine skeletal muscle fibers. An immunocytochemical and biochemical study.* J Biol Chem, 1986. **261**(8): p. 3775-81.
34. James, P., et al., *Nature and site of phospholamban regulation of the Ca2+ pump of sarcoplasmic reticulum.* Nature, 1989. **342**(6245): p. 90-2.
35. Tupling, A.R., M. Asahi, and D.H. MacLennan, *Sarcolipin overexpression in rat slow twitch muscle inhibits sarcoplasmic reticulum Ca2+ uptake and impairs contractile function.* J Biol Chem, 2002. **277**(47): p. 44740-6.

36. Asahi, M., et al., *Physical interactions between phospholamban and sarco(endo)plasmic reticulum Ca2+-ATPases are dissociated by elevated Ca2+, but not by phospholamban phosphorylation, vanadate, or thapsigargin, and are enhanced by ATP*. J Biol Chem, 2000. **275**(20): p. 15034-8.
37. Asahi, M., et al., *Sarcolipin inhibits polymerization of phospholamban to induce superinhibition of sarco(endo)plasmic reticulum Ca2+-ATPases (SERCAs)*. J Biol Chem, 2002. **277**(30): p. 26725-8.
38. Babu, G.J., et al., *Targeted overexpression of sarcolipin in the mouse heart decreases sarcoplasmic reticulum calcium transport and cardiac contractility*. J Biol Chem, 2006. **281**(7): p. 3972-9.
39. Babu, G.J., et al., *Ablation of sarcolipin enhances sarcoplasmic reticulum calcium transport and atrial contractility*. Proc Natl Acad Sci U S A, 2007. **104**(45): p. 17867-72.
40. Rolim, N.P., et al., *Exercise training improves the net balance of cardiac Ca2+ handling protein expression in heart failure*. Physiol Genomics, 2007. **29**(3): p. 246-52.
41. Kemi, O.J., et al., *Exercise-induced changes in calcium handling in left ventricular cardiomyocytes*. Front Biosci, 2008. **13**: p. 356-68.
42. Li, Y., et al., *Protein kinase A phosphorylation of the ryanodine receptor does not affect calcium sparks in mouse ventricular myocytes*. Circ Res, 2002. **90**(3): p. 309-16.
43. Wellman, G.C., et al., *Role of phospholamban in the modulation of arterial Ca(2+) sparks and Ca(2+)-activated K(+) channels by cAMP*. Am J Physiol Cell Physiol, 2001. **281**(3): p. C1029-37.
44. Freyssenet, D., M. Di Carlo, and D.A. Hood, *Calcium-dependent regulation of cytochrome c gene expression in skeletal muscle cells. Identification of a protein kinase c-dependent pathway*. J Biol Chem, 1999. **274**(14): p. 9305-11.
45. Ojuka, E.O., et al., *Intermittent increases in cytosolic Ca2+ stimulate mitochondrial biogenesis in muscle cells*. Am J Physiol Endocrinol Metab, 2002. **283**(5): p. E1040-5.

Chapter IV

The combined effect of aging and running wheel exercise on mouse soleus and EDL muscles

Submitted for publication

M.W. de Snoo
P.W.A. Cornelissen
M.E. Everts

ABSTRACT - The present study was performed to investigate the effects of age and exercise on the developing mouse, with a particular focus on SERCA and its regulatory proteins. Male C57Bl/6 mice, age 4 weeks, were randomly selected into 5 groups; three sedentary groups aged 4, 8, and 10 weeks, and two running wheel exercise groups aged 8 and 10 weeks. Slow-twitch soleus muscle demonstrated an age-dependent increase of SERCA2 in both mRNA as well as protein ($P<0.05$). The fast-twitch extensor digitorum longus (EDL) muscles demonstrated no changes in SERCA1 expression. Running wheel exercise significantly affected SERCA2 expression in EDL muscle. Ca^{2+} affected regulatory proteins sarcolipin and phospholamban mRNA expression were affected both by aging as well as exercise in soleus muscle ($P<0.05$), while calcineurin mRNA expression was slightly increased by aging only. In EDL, no changes were found in any of these regulatory proteins. These results demonstrate that a longitudinal study with appropriate control groups is essential in correctly interpreting and understanding results of mouse skeletal muscle adaptation.

4.1 Introduction

Regular endurance exercise leads to adaptations in the cardiovascular and musculoskeletal system, improving the aerobic capacity [1-3]. The exact pathways how these changes are induced are, however, still largely unknown. Rodents are regularly used to study these processes, either using treadmills or running wheels [2, 4]. Nowadays, mice seem the preferred choice, mainly due to the availability of genetically modified animals providing an opportunity to investigate the role of a selected gene or multiple genes [5, 6]. In addition, running wheels seem the preferred choice in this particular animal to study these processes, due to the natural running pattern of and the low stress impact on the animal. The focus of many exercise-related investigations has been on skeletal muscle, as it is the largest organ of the body.

We recently described the effects of six weeks running wheel exercise on mouse soleus muscle (de Snoo et al., submitted). Serial twitch stimulation of isolated slow-twitch soleus muscle demonstrated improved fatigue resistance and implications for improved Ca^{2+} handling capacity. We attributed the improved Ca^{2+} recovery to the observed decrease in phospholamban (PLB) mRNA and protein expression. As a negative regulator of SERCA2, this decrease would improve SERCA function and thus explain our results [7, 8]. This finding, however, was accompanied by an increase in sarcolipin (SLN) mRNA expression, a second negative regulator of both SERCA isoforms [9, 10]. This counteracts our hypothesis and suggests a compensatory mechanism. In another study using isolated fast-twitch EDL muscle we found only minor improvements in fatigue resistance at low stimulation frequencies [4], while at higher frequencies, i.e. 2 and 4 Hz, no implications for improved fatigue resistance were found [4]. Both studies were performed in mice starting at the age of 4 weeks ending at the age of 10 weeks. The mice in our studies started in their adolescent period and were presumably still developing, as male mice reach an adult stage at the age of approximately 8 weeks [11]. Surprisingly, little is known about developmental changes in mouse skeletal muscle. One study reported no changes in MyHC profile of sedentary control mice aged 6-10 weeks [6]. The same authors had previously focused on postnatal MyHC development, demonstrating that adult phenotype is reached 3 weeks after birth [12]. Another study demonstrated that adult MyHC phenotype at 3 weeks closely represents phenotype at 3 months, although some minor changes are ob-

served in this period [13]. This suggests that mouse skeletal muscle is adult at the MyHC level at the age of 3 weeks. The question is how aging of skeletal muscle affects other parameters, like SERCA. Changes in calcineurin (Cn) could be an indication of maturation state, as Cn is required for the maintenance, not development, of slow-twitch phenotype [14].

The present study was performed to investigate the effects of age and the interaction with exercise in the developing mouse, with a particular focus on SERCA and its Ca^{2+} affected regulatory proteins. Male C57Bl/6 mice, age 4 weeks, were randomly selected into 5 groups: Three sedentary groups sacrificed immediately, after 4 weeks, and after 6 weeks, and two exercise groups, subjected to running wheel exercise for 4 and 6 weeks, thus until the age of 8 and 10 weeks by the end of the experiment, respectively. The influence of development and running wheel exercise on SERCA mRNA and protein distribution was investigated along with mRNA expression of PLB, SLN and Cn.

4.2 Methods

Animal and experimental protocol

Male C57Bl/6 mice, age 4 weeks, were randomly selected into 5 groups; 3 sedentary control groups (SED0, SED4 and SED6), and 2 running wheel exercise groups (RWE4 and RWE6). Animals were housed individually at room temperature on a 12:12-h light-dark cycle with food and water provided *ad libitum*. Cages of the RWE groups were equipped with in-house made running wheels. SED0 (n=16) mice were sacrificed at the start of the experimental period. SED4 (n=8) and RWE4 (n=8) mice were sacrificed 4 weeks into the experimental period, thus at the age of 8 weeks. SED6 (n=8) and RWE6 (n=8) mice were sacrificed six weeks after the start of the experimental period, thus at the age of 10 weeks. The extensor digitorum longus (EDL) muscles and the soleus (SOL) were dissected, snap frozen in liquid nitrogen and stored at -80 °C for further use. One muscle was used for mRNA extraction, the contralateral muscle for protein isolation. However, two muscles of one mouse from the SED0 group were pooled, due to the small muscle size.

Experiments were performed in accordance with institutional and governmental guidelines after approval of the Animal Experimentation Ethics Committee, Utrecht University.

RT-PCR

Total RNA was isolated from soleus and EDL muscles using the Qiagen RNeasy fibrous tissue kit (Qiagen GmbH, Hilden, Germany). cDNA was prepared from 0.75 µg RNA in a total volume of 20 µl according to manufacturer's protocol (iScript cDNA synthesis kit; Biorad, Hercules, CA, USA). Primers were designed against SERCA 1, SERCA 2A, calcineurin (Cn), PLB, and SLN (Table 4.1). RT-PCR was performed in a MyiQ cycler (Biorad) at an annealing temperature of 57 °C; input of cDNA was 50 ng and the concentration of the primers (forward and reverse) was 10 µM. Product specificity during PCR was verified by melting curve analysis of the products. For each amount of RNA tested, duplicate Ct values were obtained and averaged. Quantification was performed using a mathematical model of relative expression ratio in real-time PCR, the $^{-\Delta\Delta Ct}$-method [15, 16]. GAPDH was used as a reference gene [17].

Name	Sequence	Product size (bp)
SERCA 1	*For* ACA GGC AGG TGG ATA AGC *Rev* CCC GAA ATA GGA CAA ACA TTC	144
SERCA 2	*For* TGC TGC TGG GAA AGC TAT GG *Rev* GTG TTC TCT CCT GTT CTG TTG C	101
PLB	*For* ACC GAA GCC AAG GTC TCC *Rev* CGA GCG AGT GAG GTA TTG C	149
SLN	*For* TTC ACA GTT GTC CTC ATC ACC *Rev* GCA CAC AGC AGT CAC TCC	101
Cn	*For* GAG ATG TCC GAG CCC AAG *For* GCT TTT AAG ATA TCC ACA CGA G	146
GAPDH	*Rev* GAA GGT CGG TGT GAA CGC *For* TGA AGG GGT CGT TGA TGG	101

Table 4.1 Sequences of selected RT-PCR-primers
Primer sequences are shown in 5' → 3' order. The length of the amplified product is indicated. Annealing temperature and number of cycles were 57°C and 40, respectively, for all primer sets. Product lengths are represented as numbers of base pairs.

Western blot
Soleus and EDL muscle were homogenized and centrifuged. Supernatant was collected in order to discard larger proteins like myosins. For SERCA1 and SERCA2, 10 µg of protein was run over a 10% running gel. Proteins were blotted to nitrocellulose membrane using a semi-dry blotting apparatus (Biorad). Membranes were blocked for 1 hour in 5% BSA. Membranes were incubated overnight at 4 °C with first antibody (**SERCA 1** catalog# MA3-912, **SERCA 2** catalog# PA1-21904l; Affinity Bioreagents, Golden, CO, USA) in blocking solution. Incubation with second HRP-conjugated antibody was done for 1 hour at room temperature. Membranes were developed with ECL (Pierce, Rockford, IL, USA). Alpha-tubulin (Catalog# T5168; Sigma Aldrich, St Louis, MO, USA) served as a reference protein.

Statistics
Data are presented as arithmetic means ± standard error (SE). Statistical analyses were performed using a one-way ANOVA, with Bonferroni as post-hoc test. Differences between groups were considered significant if $P<0.05$. When no significant changes were observed between SED and RWE groups of one age group, the two groups were combined to analyze the age effect.

4.3 Results

Animals
Mice with unlimited access to a running wheel typically ran 6.9 ± 0.3 km per day (n=12) during the dark cycle. For each mouse this distance was constant for the entire duration of the study. There was a significant increase in body weight over time observed in all groups (figure 4.1; $P<0.05$). Mice in SED0 weighed significantly less compared to mice of the same age in the other groups (figure 4.1; $P<0.05$).

mRNA expression in skeletal muscle
Soleus
No changes were found in the expression pattern of SERCA1 (figure 4.2A). Due to aging, SERCA2 expression was significantly upregulated after the six week experimental period (figure 4.2B; $P<0.05$), not after 4 weeks. SLN mRNA expression was significantly enhanced in both RWE groups ($P<0.05$), without developmental changes in the SED groups (figure 4.2C).

PLB was significantly upregulated after 4 weeks ($P<0.05$), while a further increase was seen in the SED6 group (figure 4.2D; $P<0.05$). Cn expression was upregulated after 4 weeks (figure 4.2E; $P<0.05$).

EDL

No changes were found in the mRNA expression patterns of any of the investigated genes (figures 4.3A-E).

Protein expression in skeletal muscle

Soleus

No significant changes were found in SERCA1 expression (figure 4A). SERCA2 protein expression was significantly upregulated in the RWE6 group, compared to SED0 mice as well as to its complementary SED6 group (figure 4B; $P<0.05$).

EDL

No significant changes were found in SERCA1 protein expression (figure 4C). SERCA2 protein expression was significantly lower in both RWE groups compared to SED4 (figure 4D; $P<0.05$).

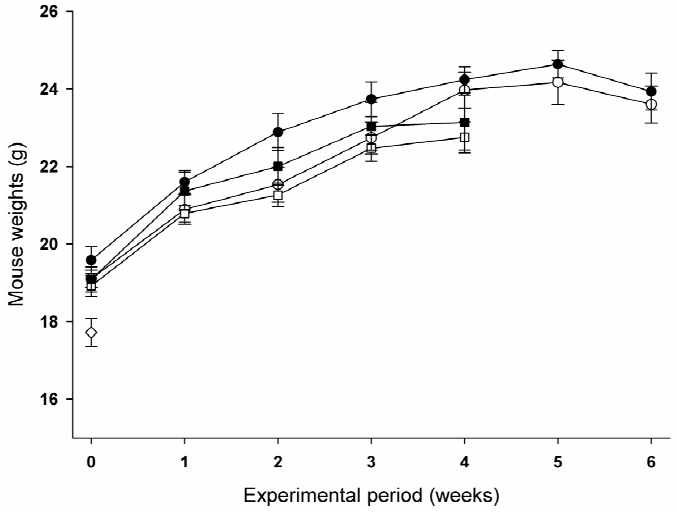

Figure 4.1 Mouse weights during the six-week experimental period. Sedentary mice are depicted as open symbols, RWE mice as closed symbols.
Diamonds: Mice aged 4 weeks (n=12), Squares: age 8 weeks (4 weeks experimental period; n=6 per group), Circles: age 10 weeks (6 weeks experimental period; n=6 per group)

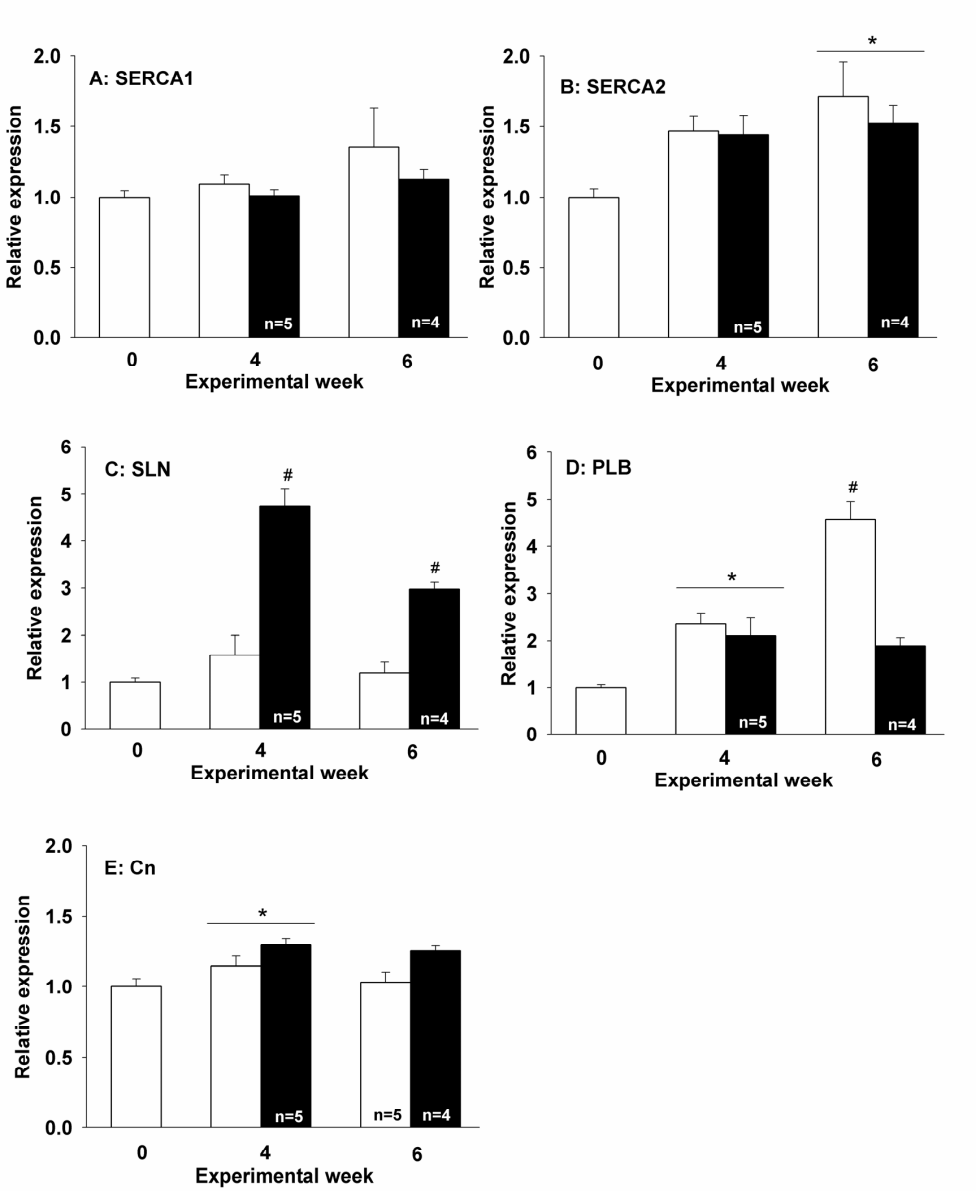

Figure 4.2 mRNA expression in mouse soleus muscle. SED mice are depicted as white bars, RWE mice as black bars. n=6 per group unless mentioned otherwise.
* $P<0.05$ versus SED0
# $P<0.05$ versus all other groups

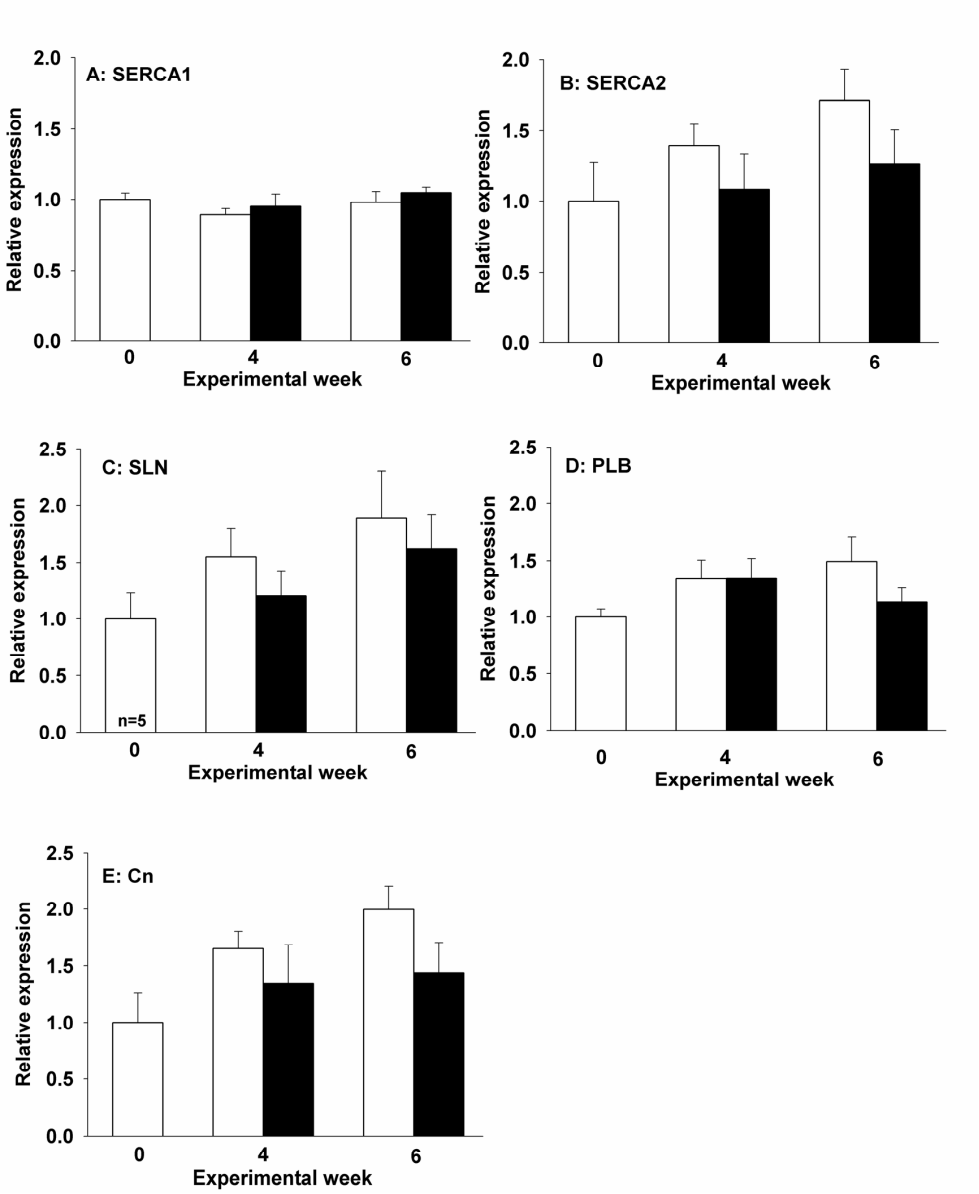

Figure 4.3 mRNA expression in mouse EDL muscle. SED mice are depicted as white bars, RWE mice as black bars. n=6 per group unless mentioned otherwise.

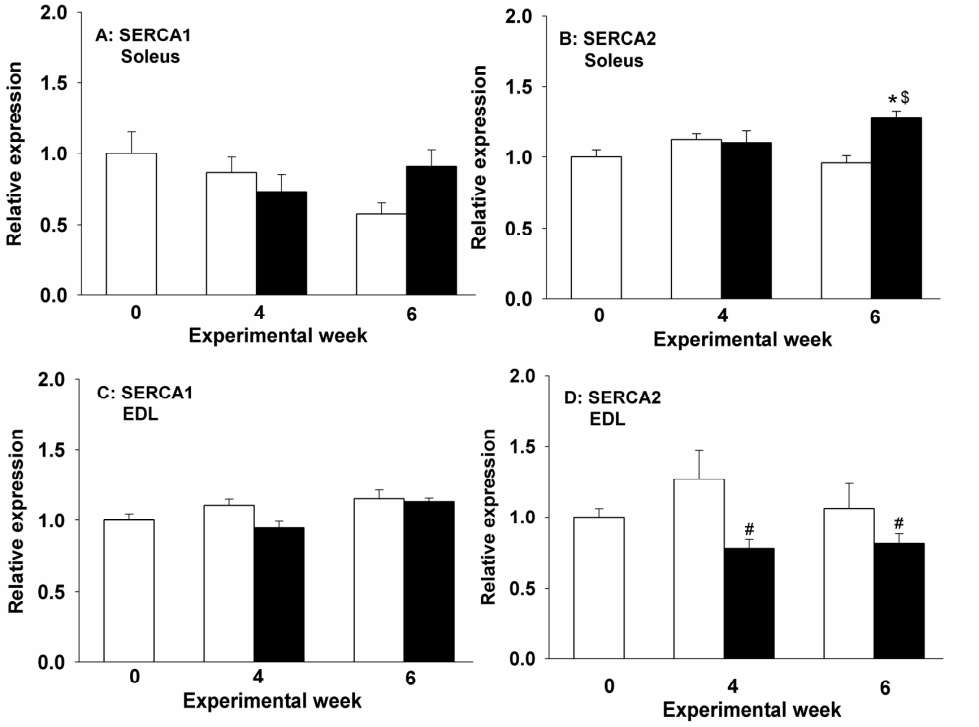

Figure 4.4 Protein expression in mouse soleus and EDL muscle. SED mice are depicted as white bars, RWE mice as black bars. n=6 per group
* $P<0.05$ versus SED0 $ $P<0.05$ versus SED6; # $P<0.05$ versus SED4

4.4 Discussion

Running wheel exercise is commonly used to study skeletal muscle adaptation in rodents. In the mouse slow-twitch soleus muscle, we previously found improved fatigue resistance and implications for improved Ca^{2+} handling, accompanied by alterations in Ca^{2+} pump regulatory proteins. In the fast-twitch EDL muscle, we found no indication of altered fatigue resistance. These results are from mice investigated at the age from 4 to 10 weeks, i.e. while mice are still developing.

During the six-week experimental period, mice demonstrated a significant increase in body weight, providing clear evidence that mice were still developing. Steady state body weight was reached after approximately four weeks of the experimental period, i.e. at the age of 8 weeks (figure 4.1). This

compares to previous studies [6, de Snoo et al. (submitted)], and corresponds to the age male mice reach sexual maturity [11]. Daily running distances were the same in both RWE groups, and compared to previous studies [6, 18]. The significant lower body weight in the SED0 group is remarkable, as mice were randomly selected into five groups prior to the experiment. However, mice were transported from the animal room to the laboratory at the day of sacrifice not to disturb the other animals, which might have caused stress to the animal. With the low body weights of these young animals (aged 4 weeks) a small –absolute- decrease of 1 g induces a huge –relative- difference in total body weight (figure 4.1). A similar tendency was observed at week 4 (age 8 weeks) between the SED+RWE groups that continued the experiment and those that were sacrificed. At these time-points there were no differences in body weight between SED and RWE groups. As such, we do not expect that the lower body weight due to sacrifice has influenced our results.

SERCA expression pattern

SERCA is responsible for re-uptake of Ca^{2+} into the SR after contractions. SERCA1 is the typical isoform present in fast-twitch fibers, while SERCA2 is predominantly expressed in slow-twitch muscle fibers [19-21]. In rat, SERCA2 isoform was significantly increased after both moderate and high intensity exercise [22]. In our mouse model, we found only minor effects of running wheel exercise on the expression of SERCA2 isoforms in either muscle, without changes in SERCA1 expression.

In soleus muscle, no significant changes were seen in SERCA1 mRNA and protein expression. SERCA2 mRNA expression in soleus muscle demonstrated an age-dependent increase. Like in soleus muscle, no significant changes were found in EDL SERCA1 mRNA and expression. An effect of running wheel exercise could be observed in SERCA2 protein expression. Protein expression closely resembled mRNA expression although no significant changes were found in the latter.

Previous studies demonstrated that the SERCA2 protein is dominant in the soleus muscle, while SERCA1 is the dominant isoform present in EDL muscle [9]. In the soleus muscle, development demonstrated a shift towards the slow-twitch isoform SERCA2, mainly at mRNA level. Such an effect was not seen in EDL muscle. Together, this demonstrates that the Ca^{2+} transport properties in mouse skeletal muscle are nearly fully developed at young age (i.e. 4 weeks) corresponding to previous studies [23, 24].

Ca^{2+} transport regulatory proteins

PLB inhibits SERCA2 function [7, 8], while phosphorylation of PLB relieves the inhibitory effect. In the EDL muscle we found no altered mRNA expression of PLB. On the other hand, SLN is described to inhibit both SERCA1 as well as SERCA2 [9, 10]. Again, no changes in SLN mRNA expression were found, although a minor non-significant increase in time might be observed.

In soleus muscle, however, major changes were seen in the SERCA regulatory proteins, SLN and PLB. SLN mRNA expression demonstrated a clear exercise effect; expression in SED groups was constant, while expression in both RWE groups was upregulated. The increased expression after the 4 week experimental period was decreased after 6 weeks. PLB mRNA expression was significantly enhanced after 4 weeks in both groups. After 6 weeks, PLB mRNA expression of SED mice demonstrated a near 2.5-fold increase compared to mice in the 4 weeks, while expression in RWE6 mice remained at expression levels similar to 4 weeks. The latter suggests that PLB is susceptible to developmental changes, and that running wheel exercise prevents the developmental increase in mRNA expression. SLN, on the other hand, is not influenced by development, while running wheel exercise has a major impact on its expression. Unfortunately, we were not able to measure PLB protein expression in SED0, SED4, and RWE4 mice. However, results of mRNA and protein expression after six weeks indicate that the decrease in PLB protein expression is proportional to its mRNA expression. SLN could not be detected at the protein level due to an unspecific antibody.

In our previous study we demonstrated that unstimulated –passive- force first is significantly affected during the first 30 s during serial stimulation of soleus muscle of mice at age 10 weeks. However, unstimulated force was lower and returned to its initial value more rapidly after 6 weeks of running wheel exercise in mice of the same age. Unstimulated force is an index of free Ca^{2+} within the cell and, as such, a reflection of Ca^{2+} handling [25]. We attributed this difference to improved SERCA2 function through relieve of the inhibitory effects of PLB, represented by a 60% decrease in both mRNA as well as protein expression [de Snoo et al. (submitted)]. The present study demonstrated that PLB mRNA expression in soleus muscle after 6 weeks of running wheel exercise (i.e. 10 weeks old) compares to expression in mice at age 8 weeks, both with and without running wheel exercise. Interestingly, preliminary data by our group demonstrated that unstimulated force in SED4 and RWE4 mice from a comparable experiment

was not affected (data not shown). Although preliminary, this strengthens the suggested role of PLB on Ca^{2+} handling after six weeks of running wheel exercise.

Calcineurin is a Ca^{2+} regulated gene involved in transcriptional regulation of slow-muscle fiber-type specificity [26]. More recent investigations, however, provide evidence that the development of slow-twitch fibers is independent of Cn, while maintenance of the adult phenotype does require Cn activity [14]. In this light, it is of interest to see that Cn mRNA expression in the fast-twitch EDL muscle was not altered during development or wheel running exercise. In the slow-twitch soleus muscle, a minor increase in Cn mRNA expression was seen in the 4^{th} experimental week. In the 6^{th} experimental week, Cn mRNA expression remained at the same level, suggesting maturation of the slow-twitch fibers.

Impact of the study

This study demonstrates that SERCA1 mRNA and protein expression is unaffected by aging and running wheel exercise in both EDL and soleus muscle. SERCA2 expression on the other hand, was altered during the adolescent life-span. Interestingly, aging seemed the predominant cause of alterations in the soleus muscle, while an effect of running wheel activity could be observed in the EDL muscle, most pronounced after 4 weeks. Likewise, previous studies demonstrated that mouse skeletal muscle MyHC in mice is remarkably robust and is not affected by voluntary exercise, or forced treadmill running [4, 27]. SERCA1 and 2 isoforms in adult muscles are specifically expressed in fast and slow-twitch MyHC myofibers, respectively, although it was previously demonstrated that expression of MyHC and SERCA is not completely co-regulated at birth [28]. The present study provides further evidence that the predominant SERCA isoform of each muscle is reached at relatively young age.

Further, the developmental and exercise-related adaptation of SERCA regulatory proteins in soleus but not EDL muscle is very interesting, but still not completely understood. As we were limited by the number of cages, further research is needed to elucidate this phenomenon, extended with data on the physiological contraction parameters.

Many studies investigating mouse skeletal muscle adaptation commence with mice aged 4 weeks for an experimental period of 6-8 weeks, with a particular interest at the end-point [18, 23, de Snoo et al. (submitted)]. The present study clearly demonstrates that a longitudinal setup with appro-

priate control groups is essential for correct interpretation of the results, and provides more insight in the resultant effects and adaptation processes.

4.5 Acknowledgements

Valuable discussions and manuscript proofreading by dr Karin Eizema are gratefully acknowledged. Further, the authors would like to thank Arend Schot and Iris ten Berge for their excellent technical assistance and animal handling.

4.6 References

1. Fuller, P.M., K.M. Baldwin, and C.A. Fuller, *Parellel and divergent adaptations of rat soleus and plantaris to chronic exercise and hypergravity.* Am J Physiol Regul Integr Comp Physiol, 2005. **290**(2): p. R442-8.
2. Kariya, F., et al., *Effects of prolonged voluntary wheel-running on muscle structure and function in rat skeletal muscle.* Eur J Appl Physiol, 2004. **92**(1-2): p. 90-7.
3. Pette, D. and G. Vrbova, *Adaptation of mammalian skeletal muscle fibers to chronic electrical stimulation.* Rev Physiol Biochem Pharmacol, 1992. **120**: p. 115-202.
4. Jeneson, J.A., et al., *Treadmill but not wheel running improves fatigue resistance of isolated extensor digitorum longus muscle in mice.* Acta Physiol (Oxf), 2007. **190**(2): p. 151-61.
5. Zhao, X., et al., *Enhanced resistance to fatigue and altered calcium handling properties of sarcalumenin knockout mice.* Physiol Genomics, 2005. **23**(1): p. 72-8.
6. Allen, D.L., et al., *Cardiac and skeletal muscle adaptations to voluntary wheel running in the mouse.* J Appl Physiol, 2001. **90**(5): p. 1900-1908.
7. Jorgensen, A.O. and L.R. Jones, *Localization of phospholamban in slow but not fast canine skeletal muscle fibers. An immunocytochemical and biochemical study.* J Biol Chem, 1986. **261**(8): p. 3775-81.
8. James, P., et al., *Nature and site of phospholamban regulation of the Ca2+ pump of sarcoplasmic reticulum.* Nature, 1989. **342**(6245): p. 90-2.
9. Vangheluwe, P., et al., *Sarcolipin and phospholamban mRNA and protein expression in cardiac and skeletal muscle of different species.* Biochem J, 2005. **389**(Pt 1): p. 151-9.
10. Tupling, A.R., M. Asahi, and D.H. MacLennan, *Sarcolipin overexpression in rat slow twitch muscle inhibits sarcoplasmic reticulum Ca2+ uptake and impairs contractile function.* J Biol Chem, 2002. **277**(47): p. 44740-6.
11. *Biology of the Laboratory Mouse. In: Earl. L. Green (editor).* By The Staff of The Jackson Laboratory. Dover Publications, Inc., New York, 1966(Second edition).
12. Allen, D.L. and L.A. Leinwand, *Postnatal myosin heavy chain isoform expression in normal mice and mice null for IIb or IId myosin heavy chains.* Dev Biol, 2001. **229**(2): p. 383-95.
13. Agbulut, O., et al., *Myosin heavy chain isoforms in postnatal muscle development of mice.* Biology of the Cell, 2003. **95**(6): p. 399-406.
14. Oh, M., et al., *Calcineurin is necessary for the maintenance but not embryonic development of slow muscle fibers.* Mol Cell Biol, 2005. **25**(15): p. 6629-38.
15. De Preter, K., et al., *Quantification of MYCN, DDX1, and NAG gene copy number in neuroblastoma using a real-time quantitative PCR assay.* Mod Pathol, 2002. **15**(2): p. 159-66.
16. Livak, K.J. and T.D. Schmittgen, *Analysis of relative gene expression data using real-time quantitative PCR and the 2(-Delta Delta C(T)) Method.* Methods, 2001. **25**(4): p. 402-8.
17. Jemiolo, B. and S. Trappe, *Single muscle fiber gene expression in human skeletal muscle: validation of internal control with exercise.* Biochem Biophys Res Commun, 2004. **320**(3): p. 1043-50.

18. Landisch, R.M., et al., *Adaptive and nonadaptive responses to voluntary wheel running by mdx mice.* Muscle Nerve, 2008. **38**(4): p. 1290-303.
19. Brandl, C.J., et al., *Two Ca2+ ATPase genes: homologies and mechanistic implications of deduced amino acid sequences.* Cell, 1986. **44**(4): p. 597-607.
20. Korczak, B., et al., *Structure of the rabbit fast-twitch skeletal muscle Ca2+-ATPase gene.* J Biol Chem, 1988. **263**(10): p. 4813-9.
21. Zarain-Herzberg, A., D.H. MacLennan, and M. Periasamy, *Characterization of rabbit cardiac sarco(endo)plasmic reticulum Ca2(+)-ATPase gene.* J Biol Chem, 1990. **265**(8): p. 4670-7.
22. Kubo, H., et al., *Differential effects of exercise training on skeletal muscle SERCA gene expression.* Med Sci Sports Exerc, 2003. **35**(1): p. 27-31.
23. Divet, A., A.M. Lompre, and C. Huchet-Cadiou, *Effect of cyclopiazonic acid, an inhibitor of the sarcoplasmic reticulum Ca-ATPase, on skeletal muscles from normal and mdx mice.* Acta Physiol Scand, 2005. **184**(3): p. 173-86.
24. Arai, M., et al., *Regulation of sarcoplasmic reticulum gene expression during cardiac and skeletal muscle development.* Am J Physiol, 1992. **262**(3 Pt 1): p. C614-20.
25. Cifelli, C., et al., *KATP channel deficiency in mouse flexor digitorum brevis causes fibre damage and impairs Ca2+ release and force development during fatigue in vitro.* J Physiol, 2007. **582**(Pt 2): p. 843-57.
26. Serrano, A.L., et al., *Calcineurin controls nerve activity-dependent specification of slow skeletal muscle fibers but not muscle growth.* Proc Natl Acad Sci U S A, 2001. **98**(23): p. 13108-13.
27. Pette, D. and R.S. Staron, *The malleability of skeletal muscle. In: Weibel, E., Taylor, C.R., Bolis, L. (Eds.).* Principles of Animal Design. Cambridge University Press, Cambridge, 1998: p. pp. 89-94.
28. Eizema, K., et al., *Differential expression of calcineurin and SR Ca2+ handling proteins in equine muscle fibers during early postnatal growth.* J Histochem Cytochem, 2007. **55**(3): p. 247-54.

Chapter V

Genetic profiling of wheel running exercise-induced adaptation of mouse soleus and extensor digitorum longus muscle

M.W. de Snoo
C.L.J.J. Kruitwagen
M. Strengers
P.W.A. Cornelissen
J.A.L. Jeneson
M.E. Everts

ABSTRACT - We previously reported improved Ca^{2+} handling and fatigue resistance in mouse soleus muscle after 6 weeks of voluntary wheel running exercise, while extensor digitorum longus (EDL) muscle demonstrated no such changes. To further investigate mechanisms underlying these results, mRNA profiling was performed on mRNA from soleus and EDL muscles isolated from animals in the running wheel (RWE; n=3) and sedentary control (SED; n=3) groups (male C57Bl/6 mice, age 10 weeks). The Affymetrix mouse 430 2.0 Genechip array was used. Data were analyzed with LIMMA (linear models for microarray data), an implementation in R. The top-50 of most likely up- and downregulated genes were selected and clustered according to their function. We found that genes responding to RWE soleus muscles fell into three major groups: (1) Ca^{2+} signaling, (2) Krebs cycle, and (3) cell cycle. The combination of up- and downregulated genes in group 1 (e.g. MARCKS↓, PLB↓, FK506BP↑) would enhance Ca^{2+} handling. Genes in group 2 (e.g. PDK4↓, Glut1↑) enhanced glucose metabolism and substrate oxidation (Krebs cycle). Genes in group (3) improved muscle cell differentiation (e.g. MyoD↑, cyclinD1↓). In EDL muscle, affected genes were mostly related to muscle cell differentiation.

5.1 Introduction

Skeletal muscle is an important tissue in posture maintenance, locomotion and skeletal support. Skeletal muscle is composed of bundles of fibers that are classified as slow-oxidative type I or as fast-glycolytic type II fibers, in a proportion that varies according to the specific functional role of the muscle. However, skeletal muscle is a highly plastic tissue, and its composition can change with altered functional demand (e.g. exercise, disuse, growth; for reviews see: [1-3]). Fiber type transformation comprises a cascade of events affecting ion channels, metabolic enzyme expression, and isoforms of contractile proteins. Although much research has focused on skeletal muscle plasticity [4-6], the exact mechanisms how skeletal muscles adapt towards altered functional demand are still largely unknown.

In rodents, studies on skeletal muscle adaptation are mostly performed in soleus and extensor digitorum longus (EDL) muscles, as representative slow-twitch and fast-twitch muscles respectively. In soleus muscle we recently demonstrated improved fatigue resistance after six weeks of voluntary wheel running exercise, and indications for improved Ca^{2+} handling capacity [de Snoo et al. (submitted)]. This was associated with changes in regulatory proteins (phospholamban and sarcolipin), rather than changes in 'hardware' (i.e. myosin heavy chain (MyHC) composition, sarcoplasmic reticulum Ca^{2+} ATPse (SERCA) content). Likewise, we found no changes in MyHC composition and mitochondrial density of running wheel exercised EDL muscle [7]. At the functional level these muscles demonstrated no changes. This suggests different adaptation processes in slow- versus fast-twitch muscles. However, the exact processes as to how these muscles respond to this type of exercise are still not completely understood.

To further investigate the mechanisms involved in mouse skeletal muscle adaptation, a genome-wide expression analysis was performed on soleus and EDL muscle of mice after six weeks of voluntary wheel running exercise. Microarray analysis revealed adaptation in soleus muscle to improve oxidative capacity/glycolysis, Ca^{2+} handling and cell cycle regulation and differentiation. In EDL muscle adaptations were associated with cell cycle regulation and differentiation. These results may give insight in the adaptation processes of both slow-twitch as well as fast-twitch muscles towards voluntary wheel running in mice.

5.2 Methods

Animals and experimental protocol

Animals for the microarray study were randomly chosen from a group described in a previous study [de Snoo et al. (submitted)]. In short, four-week old male C57Bl/6 mice were randomly assigned to a running wheel exercise group (n=12; RWE) or a sedentary control (n=10; SED) group. Animals were housed individually at room temperature on a 12:12-h light-dark cycle with food and water provided *ad libitum*. Cages of the RWE group were equipped with in-house made running wheels. Experiments were performed in accordance with institutional and governmental guidelines after approval of the Animal Experimentation Ethics Committee, Utrecht University.

Microarray

Mice were sacrificed by cervical dislocation at the age of ten weeks, i.e. six weeks after the start of the exercise protocol. The extensor digitorum longus (EDL) muscles and the soleus (SOL) were dissected, snap frozen in liquid nitrogen and stored at -80 °C for further use. Total RNA was isolated from mouse skeletal muscle using Trizol (Sigma-Aldrich, St. Louis, MO). The first step was homogenization of the muscles, which was performed in 300 µl lysis buffer RLT (containing 10 µl β-mercaptoethanol/ml) for 30 s at 10.000 rpm in a polytron (MagNAlyser; Roche, Indianapolis, IN, USA) using vials with MagNAlyser green beads (Roche). Next, RNA was isolated according to manufacturer's instructions and purified on RNeasy Mini Columns (Qiagen GmbH, Hilden, Germany). RNA quality control, amplification and labeling were performed by ServiceXS (ServiceXS, Leiden, the Netherlands). Likewise, microarray hybridization and scanning were performed on Affymetrix Mouse Genome 430 2.0 chip according to manufacturer's instruction by ServiceXS.

Microarray data analysis

Bayesian adjusted t-statistics from the linear models for Microarray data (LIMMA) package were used to test microarray data for differential expression between RWE and SED group utilizing R version 2.4.0 from Bioconductor (www.bioconductor.org) with R-packages 'limma', 'affy', and 'Biobase' [8]. Two soleus samples (one SED, one RWE) were analyzed as a pilot before the other samples. This resulted in a significantly different distribu-

tion of the raw data. This was compensated for by incorporating a 'day effect' in the analysis of soleus muscles.

Microarray validation: RNA isolation and Reverse transcription PCR

RT-PCR analysis was carried out on selected genes (table 5.1) to confirm microarray data. An additional running experiment (SED n=16; RWE n=16) was performed under the same conditions as the first experiment. Mice were sacrificed after six weeks, and soleus and EDL muscles were removed. Total RNA was isolated from frozen muscles using the Qiagen RNeasy Mini Columns (Qiagen), according to manufacturer's instructions with the first homogenization step performed with mortar and pestle under liquid nitrogen. Reverse transcription (RT) of 4 µg of total RNA sample was performed using the iScript cDNA synthesis kit (BioRad). RT products were diluted in nuclease-free mQ to a total concentration of 0.01 µg/µL.

PCR primers were designed against selected genes (table 5.1). RT-PCR was performed in a MyiQ cycler (Biorad, Hercules, CA, USA) at the indicated annealing temperature (table 5.1); input of cDNA was 50 ng and the concentration of the primers (forward and reverse) was 10 µM. Product specificity during PCR was verified by melting curve analysis of the products. For each amount of RNA tested, duplicate Ct values were obtained and averaged. Quantification was performed using a mathematical model of relative expression ratio in real-time PCR, the $^{-\Delta\Delta Ct}$-method [9, 10] was calculated with help of the Genex-software (Biorad). GAPDH was used as a reference gene [11]

Statistical analysis RT-PCR

Data are presented as arithmetic means ± standard error (SE). Statistical analyses were performed using a Student's unpaired *t*-test. Differences between SED and RWE muscles were considered significant if $P<0.05$.

Soleus		Primer sequence	Size (bp)	Temp (°C)
#5, table 5.3	cyclin D1	*For* CCC AAC CGA GAC CAC AGC *Rev* GTC GTT GAG GAG ATT GGT GTC	113	57
#33, table 5.3	myocyte enhancer factor 2C	*For* ATA GTA TGT CTC CTG GTG TAA C *Rev* GGT TGC CGT ATC CAT TCC	117	57
#23, table 5.2	myogenic differentiation 1	*For* ATT CCA ACC CAC AGA ACC *Rev* GCT CCA TAT CCC AGT TCC	114	57
#18, table 5.2	FK506 binding protein 5	*For* CAG GTC TTC TAC TTA CAA AGG *Rev* ACT CCT CTG TCT TTC TTC G	122	57
#1, table 5.3	pyruvate dehydrogenase kinase 4	*For* AGC CCA GAA GAC CAG AAA GC *Rev* GGA TGC CTT GAG CCA TTG TAG	100	58
#30, 50 table 5.2	3-phosphoglycerate dehydrogenase	*For* ATG AAG ACT GTA GGC TAT GAC C *Rev* GGT AGA GGG CAG GAG TGG	135	59
#5, table 5.2	major urinary protein 1	*For* ACC TAT CCA ATG CCA ATC G *Rev* ACT GGG GAT GCT GTA TGG	126	57
EDL		**Primer sequence**	**Size (bp)**	**Temp (°C)**
#5, 9 table 5.4	heat shock protein 110	*For* ATC CTT CTT CAC AGA TGC *Rev* TAT AAA TCC CAT AAT TCA AAG C	119	57
#22, table 5.5	TGFbeta inducible early growth response (TIEG)	*For* CCA ACC ATG CTC AAC TTC G *Rev* GCT TCC ACC GCT TCA AAG	134	57
#35, table 5.5	myocyte enhancer factor 2A	*For* AGG AAT TGG AGT TGA ATG C *Rev* GAG TAA TCA GTG TTG TAG GC	148	57
#46, table 5.4	DnaJ-like protein	*For* ACA AGG CGA GGA GAA GAC C *Rev* GGA TGA GAG GTG ATG ACT ATG G	119	57
#20, table 5.4	heat shock protein 90kDa alpha (cytosolic)	*For* TGA TTG GGC ACT GTT ATT TCC *Rev* ACA CAA GTT AAA ACA ACC TGA C	129	57
#25, table 5.4	phosphofructokinase, liver, B-type	*For* GTG AAG GAT CTG GTG GTT C *Rev* ATC TTG CTA CTC AGG ATT CG	113	57
#44, table 5.5	6-phosphofructo-2-kinase/fructose-2,6-biphosphatase 3	*For* CTG GAG AGG AGC AAG TGG *Rev* ACA CGA GAC AGA TGA GAG C	139	59
#8, table 5.5	sodium channel, voltage-gated, type IV, alpha	*For* CTT GAC CAA CTG CGT GTT C *Rev* TCT CGG AGG AAT GTG AAG TC	150	59
#34, table 5.5	transforming growth factor, beta 2	*For* GAG CGA GTG GGA GAG AAA G *Rev* CTC CAG AAT GGC TCT TTA AAC C	100	59
#3, table 5.4	G0/G1 switch gene 2	*For* GGA AGA AGA ACG CCA AAG C *Rev* AGC TCC TGC ACA CTT TCC	132	61

Table 5.1 Primer sequences and specifications for RT-PCR of selected genes

5.3 Results

Animals and experimental protocol

Selected RWE mice for microarray analysis (n=3) ran 6.7 ± 1.5 km/day. Food intake of SED and RWE mice was 6.1 ± 0.1 and 7.2 ± 0.2 g/day, respectively (n=3 per group; $P<0.05$ SED vs. RWE). Mice in the additional running experiment ran 6.1 ± 0.3 km per day (n=16). Food intake was 5.4 ± 0.2 g and 6.1 ± 0.1 g for SED (n=16) and RWE (n=16) mice, respectively ($P<0.05$ SED vs. RWE). Both distance run and food intake were significantly lower in the additional group than from the mice selected for microarray analysis ($P<0.05$).

Microarray analysis

The genome-wide analysis by LIMMA produced two gene lists for soleus and EDL muscle ranked in order of evidence for differential expression (i.e. the probability value). Both lists were split into upregulated and downregulated genes. The gene expression data of the first 50 differentially expressed genes according to LIMMA's probability value are listed in tables 5.2-5 for all groups. Genes in these lists were analyzed and combined according to function and/or signalling pathway. For the soleus muscle, this resulted in three functional clusters, i.e. Ca^{2+} homeostasis (#18 and 40 from table 5.2; #20 from table 5.3), glycolysis/Krebs cycle (# 2, 4, 11, 17, 27, 30, 35, 44, 49, and 50 from table 5.2; #1 from table 5.3), and cell cycle regulation/differentiation (#23 from table 5.2; #5, 33, and 40 from table 5.3). A schematic overview of these clusters is provided in figures 5.1-3, respectively. In EDL muscle, altered genes mostly included genes involved in cell cycle regulation/differentiation (#1, 2, 3, 22, and 42 from table 5.4; #34, 35, 41, and 48 from table 5.5) as well as several heat shock proteins (#5, 9, and 20 from table 5.4). A schematic overview of these clusters is provided in figure 5.4.

Microarray validation

Genes were selected from the lists in tables 5.2-5 (from page 101) to validate the microarray analysis outcome (see table 5.1). For soleus muscle, at least one up- and one downregulated gene was selected from each cluster, preferably with opposite functions. Further, the gene with the highest fold-change was selected, MUP-1 (#5 from table 5.2). For EDL muscle, primers were designed against heat shock proteins, and genes from the cell cycle cluster (table 5.1).

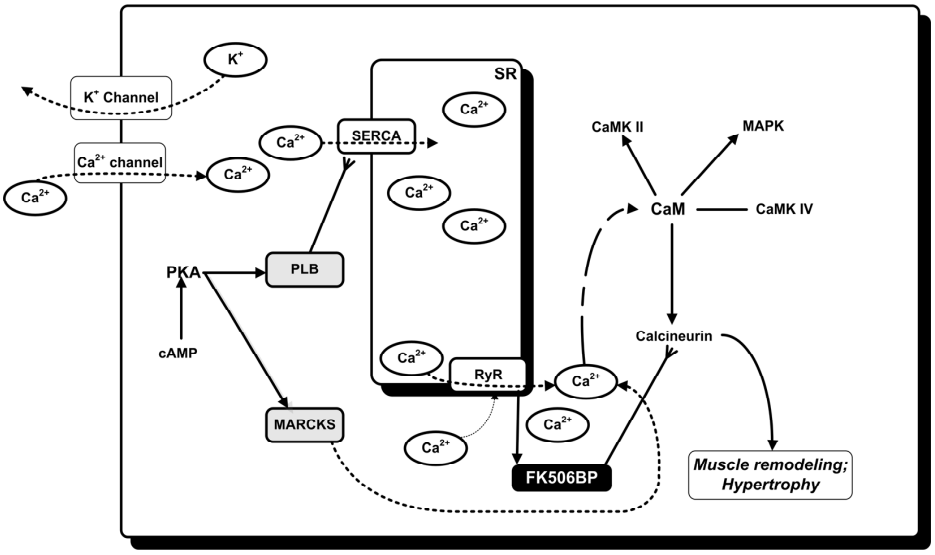

Figure 5.1 RWE affected genes involved in Ca^{2+} signalling in soleus muscle. Downregulated genes are depicted in grey, upregulated genes are depicted in black. *CaM: Calmodulin; CaMK: Calmodulin kinase; FK506BP: FK506 binding protein; MARCKS: myristoylated alanine rich protein kinase C substrate*

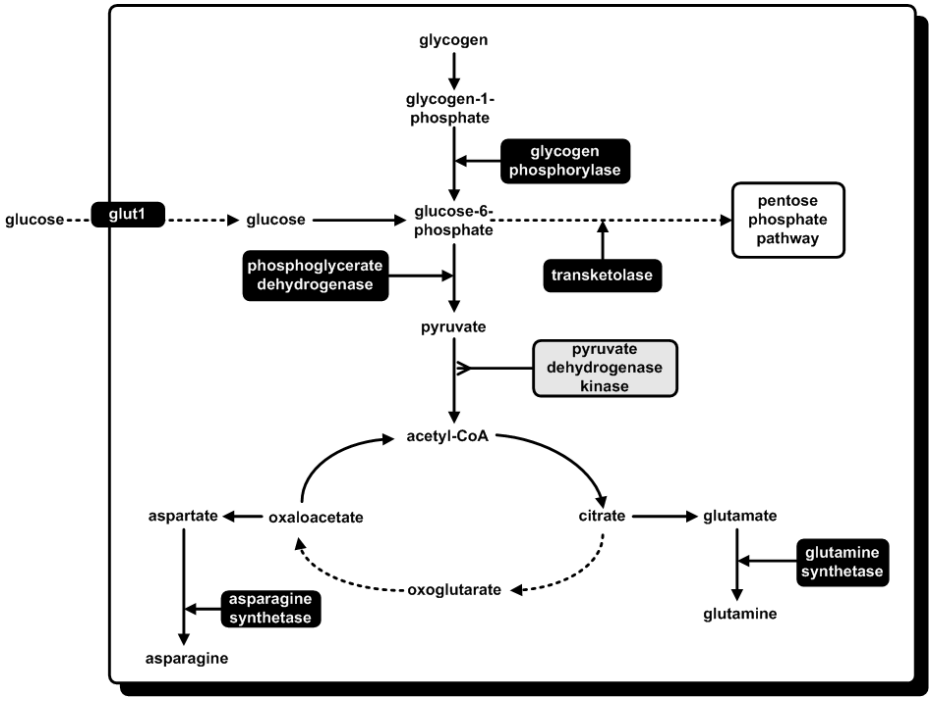

Figure 5.2 RWE affected genes involved in glycolysis.Krebs cycle in soleus muscle. Downregulated genes are depicted in grey, upregulated genes are depicted in black. *GLUT1: solute carrier family 2, member 1 (glucose transporter 1)*

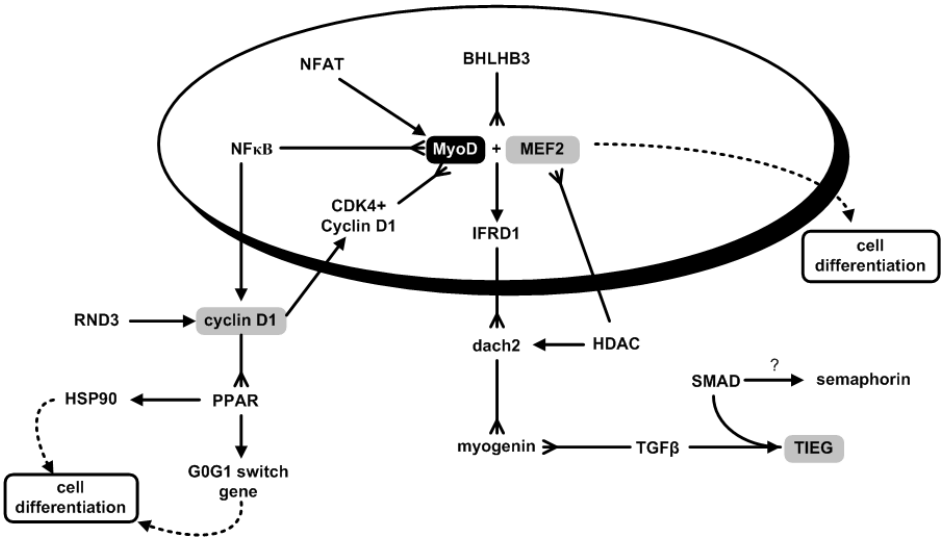

Figure 5.3 RWE affected genes involved in cell cycle regulation in soleus muscle. Downregulated genes are depicted in grey, upregulated genes are depicted in black.

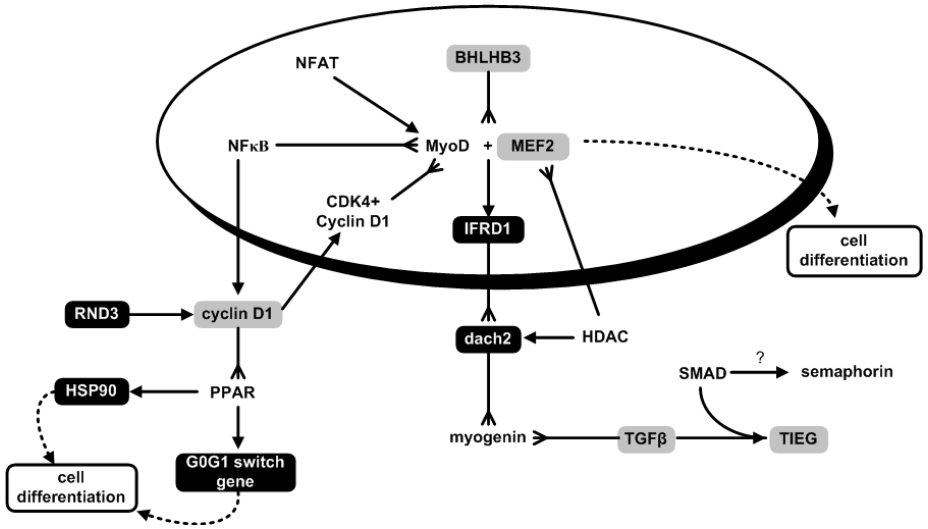

Figure 5.4 RWE affected genes involved in cell cycle regulation in EDL muscle. Downregulated genes are depicted in grey, upregulated genes are depicted in black.

BHLHB3: Basic helix loop helix, class B3; CDK4: cyclin dependent kinase 4; Dach2: Dachshund 2; HDAC: Histone deacetylase; HSP90: heat shock protein 90; IFRD1: interferon-related developmental regulator 1; MEF2: Myocyte enhancer factor 2; MyoD: Myogenic differentiation 1; NFAT: Nuclear factor of activated T-cells; NFκB: nuclear factor kappa B; PPAR: peroxisome proliferator-activated receptor; RhoE: Ras homolog gene family, member E; SMAD: small mothers against decapentaplegic; TIEG: TGBβ inducible early growth response; TGFβ: Transforming growth factor

Selected primers, and their alternatives, against Marcks, GT-1 and RGS4 did not result in specific product, and were thus not further analyzed.

In soleus muscle we did not find significantly altered expression in any of the selected genes from the three clusters. MUP-1, however, demonstrated a significant nearly six-fold increase in mRNA expression (SED 100 (n=8) ± 28, RWE (n=8) 583 ± 163; $P<0.05$; figure 5.6), while microarray analysis revealed a 12-fold increase (#5, table 5.2).

In EDL muscle we found a significant increase of G0s2 mRNA (SED (n=16) 100 ± 11% vs. RWE (n=16) 178 ± 33%; $P<0.05$), HSP110 mRNA (SED (n=16) 100 ± 6% vs. RWE (n=16) 141 ± 8%, $P<0.05$), and Pfkl mRNA (SED (n=16) 100 ±5% vs. RWE (n=16) 145 ± 9%, $P<0.05$), as depicted in figure 5.3. We were thus able to confirm only three altered expressed genes from the ten genes selected.

Name	'Reference'	SED	RWE	P-value
		Soleus		
CyclinD1	#5, table 5.3	100 ± 10	85 ± 10	0.29
Mef2C	#33, table 5.3	100 ± 6	104 ± 3	0.48
MyoD1	#23, table 5.2	100 ± 12	122 ± 10	0.15
FKBP5	#18, table 5.2	100 ± 8	98 ± 8	0.82
PDK4	#1, table 5.3	100 ± 12	121 ± 17	0.31
phgdh	#30, 50, table 5.2	100 ± 12	92 ± 10	0.60
MUP-1	#5, table 5.2	100 ± 28	583 ± 163	0.01
		EDL		
hsp110	#9, table 5.4	100 ± 6	141 ± 8	0.00
TIEG	#22, table 5.5	100 ± 9	93 ± 6	0.54
Mef2a	#35, table 5.5	100 ± 4	111 ± 5	0.11
HSJ2	#46, table 5.4	100 ± 7	104 ± 10	0.75
hsp90	#20, table 5.4	100 ± 12	119 ± 19	0.41
pfkl	#25, table 5.4	100 ± 5	145 ± 9	0.00
pfkfb3	#44, table 5.5	100 ± 7	127 ± 11	0.06
SCN4a	#8, table 5.5	100 ± 5	108 ± 4	0.22
TGFb2	#34, table 5.5	100 ± 6	97 ± 5	0.71
G0S2	#3, table 5.4	100 ± 11	178 ± 33	0.03

Table 5.6 Relative mRNA expression of selected genes, as detected by RT-PCR (n=16 per group for every selected gene; # n=8 per group)

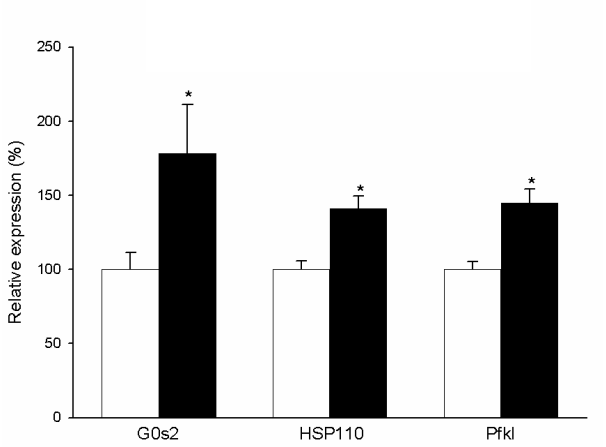

Figure 5.5 Relative mRNA expression in EDL muscle, as detected by RT-PCR. SED muscles are depicted in white bars, RWE muscles in black bars.
* $P<0.05$ versus SED muscles

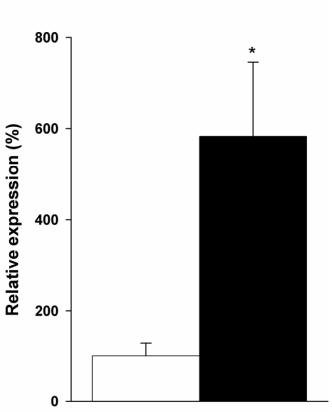

Figure 5.6 Relative expression of MUP-1 in soleus muscle, as detected by RT-PCR. SED muscles are depicted in white bars, RWE muscles in black bars.
* $P<0.05$ versus SED muscles

5.4 Discussion

Regular endurance exercise is known to have a beneficial effect on common well-being and skeletal muscle function in particular. Many studies employed wheel running exercise in mice to investigate the plasticity of skeletal muscle. However, to our knowledge, the present study is the first genome-wide study on mouse skeletal muscle adaptation on two different muscle types. The most prominent difference between the slow-twitch soleus and fast-twitch EDL muscle was the specific clustering. While voluntary exercise in soleus muscle affected genes in clusters of cell cycle regulation, Ca^{2+} homeostasis and Krebs cycle/Glycolysis, wheel running exercise in EDL muscle mostly affected genes of cell cycle regulation and heat shock proteins (HSP).

Soleus muscle

The first cluster as demonstrated by microarray data analysis revealed altered gene expression of genes associated with Ca^{2+} homeostasis (figure 5.1). We previously demonstrated implications for improved Ca^{2+} recovery into the SR in the soleus muscle during serial twitch contractions [de Snoo et al. (submitted)], supported by a 60% decrease in phospholamban (PLB) mRNA and protein expression. As an inhibitor of SERCA, a decrease in

PLB expression results in enhanced SERCA function [12, 13]. PLB expression is not listed in either table5., as it was at position 56 of downregulated genes and therefore only just fell out of the analysis in the present study. However, microarray data analysis revealed a 60% decrease in RWE soleus muscle. Together, these results suggest that not only a decrease in PLB improves Ca^{2+} recovery, but a combination of other genes contribute to this effect. This strengthens our hypothesis raised in our previous study that voluntary wheel running affects Ca^{2+} homeostasis due to intermittent running pattern [14, de Snoo et al. (submitted)].

The second cluster of altered genes results in improved Krebs cycle/glycolysis (figure 5.2). Interestingly, exercised soleus muscle consumed 1.3-fold more oxygen during serial twitch contractions ($P<0.05$; [de Snoo et al. (submitted)]) without changes in mitochondrial density. The combination of affected genes in the glycolysis/Krebs cycle cluster results in an improved oxygen metabolism, providing an explanation for our previous finding. Likewise, a report investigating two weeks of voluntary wheel running exercise on the mixed plantaris muscle demonstrated upregulated genes encoding mitochondrial proteins involved in oxidative phosphorylation [6]. The first in the list of downregulated genes is pyruvate dehydrogenase kinase-4 (PDK-4). PDK4 facilitates inactivation of pyruvate dehydrogenase, and downregulation thus promotes pyruvate dehydrogenase activity [15], resulting in improved oxidative capacity (figure 5.2). Interestingly, previous studies reported an increase in PDK-4 expression after high-intensity intermittent exercise in human [16], while downregulation was related to short-term endurance exercise [17].

Finally, one cluster of altered genes involved genes associated with cell cycle regulation (figure 5.3). MEF2 promotes myogenic differentiation during development and plays a role during skeletal muscle hypertrophy [18]. MEF2 functions in a cooperative manner with MyoD1, which is known as a muscle determination factor [19]. Likewise, it plays a role in muscle differentiation directing skeletal muscle repair and hypertrophy. Interestingly, MyoD1 was upregulated (#23, table 5.2), while MEF2c was found to be downregulated (#33, table 5.3), thus directing skeletal muscle differentiation in opposite directions. Further, cyclinD1 is a repressor of MyoD1 function [20]. Lowered expression of cyclinD1, as seen in our microarray (#5, table 5.3) would thus further improve differentiation. Together, this suggests equilibrium between genes in this cluster, thus not altering skeletal muscle differentiation. Interestingly, we found no changes in soleus muscle phenotype (MyHC) or in muscle size [de Snoo et al. (submitted)].

EDL

While soleus muscle demonstrated altered gene expression in three functional clusters, analysis of microarray data in EDL muscle revealed only one very distinct cluster. Interestingly, genes in this cluster were all associated with muscle cell differentiation and cell cycle regulation (figure 5.4), while we previously found no evidence for altered fiber type composition in EDL muscle after running wheel exercise [7], nor for changes in muscle size.

Like in soleus muscle, we found a downregulation of MEF2 mRNA expression, thus suppressing myofiber differentiation. Again, however, other affected genes in the cell cycle cluster direct muscle fibers in opposite directions; The G0G1 switch gene, for instance, induces a switch in the muscle cell between the G0 and G1 phase, thereby guiding the cells into cell cycle and resulting in muscle cell differentiation [21]. Also, TGF-β has been reported to regulate proliferation and differentiation of skeletal muscle myoblasts, suggesting a role in skeletal muscle adaptation [22]. How this protein fits in the complete cell cycle regulation pathway is, however, still unclear.

Further, four upregulated genes encoded for three different HSPs. HSPs are expressed in response to stress such as hypothermia, oxidative stress, and exercise, providing cellular protection [23]. Recently, HSP90 has further been described to co-interact with PPARα, which is associated with muscle fiber type differentiation [24]. This suggests that HSPs might play a role in muscle differentiation, expanding the cell differentiation cluster.

Validation

Taken as a whole, the real-time PCR results could not uniformly confirm differential expression of the selected genes, especially in the soleus muscle. Several explanations for the discrepancy between the microarray and PCR data should be taken into consideration. The first is related to the distance run; mice in the additional group ran 6.1 ± 0.3 km/day, which was significantly lower than the distance run by the mice selected for microarray analysis (6.7 ± 1.5 km/day; $P<0.05$). Microarray analysis revealed minor changes in the selected genes, as previously mentioned. It is likely that these changes are even smaller with a smaller total distance run, providing an explanation for our failure to confirm microarray results.

Second, LIMMA analysis is especially suitable for microarray analysis of groups with small sample sizes [8, 25]. Analysis results in a gene list based on the probability value and not on fold change. The gene with the greatest fold-change was Major Urinary Protein 1 (MUP-1), which demonstrated an increase of more than 12 times in soleus muscle by microarray

analysis, while RT-PCR analysis revealed a six-fold increase. MUP-1 is mainly secreted by the liver and is important for carrying pheromones through the body [26], and as such does not belong to any of the investigated clusters. In EDL muscles a comparable difference was found between fold changes detected by microarray and RT-PCR, which especially accounts for G0s2 (3.3 fold change by microarray, 1.8 fold change by RT-PCR). Interestingly, the previously mentioned data on soleus phospholamban mRNA –which was on position 56 of downregulated genes- demonstrated similar expressions detected by microarray and RT-PCR analysis (i.e. 60% decrease).

Finally, one could suggest that the housekeeping gene in RT-PCR might play a role. A suitable5. 'housekeeping' gene is used to normalize for internal control variations in RT-PCR. Ideally the housekeeping gene should not be regulated or influenced by the experimental procedure. Data in microarray analysis were compared without the use of a reference gene. However, GAPDH has proven a stable housekeeping gene in previous studies [11], and it was the most stable housekeeping gene present in our microarray data (variations between SED and RWE ± 1.0, data not shown). As such, we doubt that the choice of our reference gene has influenced the outcome of RT-PCR versus microarray data.

Together, this may imply that voluntary wheel running exercise induces minor changes in mouse skeletal muscle. However, all these small, non-significant changes in mRNA expression might result in a major additive effect, since most affected genes fall into functional clusters.

Overall conclusion

The results of this study demonstrate that the slow-twitch soleus and the fast-twitch EDL muscle respond differently to voluntary wheel running exercise. Both muscles demonstrate alterations in a cluster of genes regulating cell cycle and differentiation, which is most pronounced in EDL muscle. Soleus muscle further demonstrates alterations in genes improving glycolysis/Krebs cycle associated with increased oxygen consumption during serial stimulations, and improving Ca^{2+} regulation associated with enhanced Ca^{2+} recovery during serial stimulations.

Table 5.2 Top 50 of upregulated genes in RWE soleus muscle

#	Description	Affymetrix ID	Genbank ID	Fold change	Prob value
1	ESTs, Moderately similar to downregulated in renal cell carcinoma (Homo sapiens) (H.sapiens)	1434202_a_at	BF682848	3.06	0.81
2	ESTs	1458635_at	AV026232	2.98	0.71
3	Similar to hypothetical protein MGC2555, clone MGC:29018 IMAGE:3481880, mRNA, complete cds	1423835_at	BC018484.1	1.77	0.68
4	Solute carrier family 2 (facilitated glucose transporter), member 1	1426599_a_at	BM209618	1.67	0.65
5	major urinary protein 1 (Mup1)	1420465_s_at	NM_031188.1	12.66	0.61
6	solute carrier family 2 (facilitated glucose transporter), member 1	1434773_a_at	BM207588	1.51	0.59
7	kidney androgen regulated protein	1455961_at	AV174022	1.74	0.58
8	ESTs, Weakly similar to BETA-GALACTOSIDASE PRECURSOR (M.musculus)	1433727_at	AV025920	1.63	0.55
9	glutamine synthetase	1426236_a_at	AI391218	1.74	0.49
10	13 days embryo liver cDNA, RIKEN full-length enriched library, clone:2500003O20:Ank repeat containing protein, full insert sequence	1429300_at	AK010867.1	2.01	0.48
11	solute carrier family 7 (cationic amino acid transporter, y+ system), member 8 (Slc7a8)	1417929_at	NM_016972.1	1.68	0.39
12	ESTs, Moderately similar to transforming growth factor-beta type I receptor, ESK 2 precursor (M.musculus)	1443225_at	BB396526	1.89	0.38
13	RIKEN cDNA 4933428L19 gene	1453119_at	BB530087	2.17	0.35
14	ESTs, Moderately similar to Y779_HUMAN Hypothetical protein KIAA0779 (H.sapiens)	1455353_at	AV221889	1.59	0.35
15	ESTs	1436326_at	BB306272	1.40	0.35
16	talin	1436042_at	BI648366	1.56	0.34

17	transketolase	1451015_at	AI314476	1.65	0.32
18	FK506 binding protein 5 (51 kDa), clone MGC:18417	1416125_at	BC015260.1	1.81	0.32
19	ESTs	1456986_at	BB326368 1	1.67	0.30
20	immunoglobulin heavy chain 6 (heavy chain of IgM)	1427351_s_at	BB226392	1.51	0.30
21	period homolog 2 (Drosophila) (Per2)	1417602_at	NM_011066.1	1.60	0.30
22	ESTs, Highly similar to insulin receptor substrate-2 (M.musculus)	1443969_at	BE199054	1.48	0.30
23	myogenic differentiation 1 (Myod1)	1418420_at	NM_010866.1	1.75	0.30
24	18 days pregnant adult female placenta and extra embryonic tissue RIKEN	1428883_at	AK014449.1	1.35	0.29
25	ESTs	1456793_at	AV264055	1.35	0.29
26	ESTs	1444530_at	BE686339	1.45	0.29
27	asparagine synthetase	1433966_x_at	AV212753	1.40	0.28
28	paraoxonase 1 (Pon1)	1418190_at	NM_011134.1	1.88	0.27
29	transcription factor 3 (Tcf3), mRNA. /PROD=transcription factor 7-like 1	1450117_at	NM_009332.1	1.35	0.27
30	3-phosphoglycerate dehydrogenase (phgdh)	1437621_x_at	AV216768	1.56	0.26
31	EST AI448550	1434581_at	BB167663	1.32	0.25
32	ESTs	1457664_x_at	AV227574	1.47	0.25
33	DNA segment, Chr 3, ERATO Doi 330, expressed	1433640_at	BG070740	1.32	0.25
34	clone IMAGE:3708675, mRNA, partial cds	1434616_at	BB765308	1.38	0.24
35	glutamate-ammonia ligase	1426235_a_at	U09114.1	1.83	0.24
36	expressed sequence AW743275	1458145_at	BB520860	1.43	0.24
37	ESTs	1457121_at	AV271877	1.51	0.23

38	expressed sequence AW260363	1455090_at	BF681826	1.36	0.23
39	expressed sequence AW322671	1457266_at	BE447661	1.47	0.23
40	potassium voltage gated channel, shaker related subfamily, beta member 1, clone MGC:25284	1448468_a_at	NM_010597.1	1.40	0.23
41	RIKEN cDNA 1110050P16 gene	1430746_at	AI644298	1.30	0.22
42	expressed sequence C80731	1435091_at	BM207314	1.39	0.22
43	Nocturnin	1425837_a_at	AF199491.1	1.49	0.22
44	liver glycogen phosphorylase (Pygl)	1417741_at	NM_133198.1	1.66	0.21
45	cysteine dioxygenase 1, cytosolic (Cdo1)	1448842_at	NM_033037.1	2.85	0.21
46	RIKEN cDNA 1200006F02 gene, clone MGC:11938	1451486_at	BC006902.1	1.35	0.20
47	Similar to 10-formyltetrahydrofolate dehydrogenase, clone MGC:37834	1424400_a_at	BC025939.1	1.31	0.20
48	ESTs	1443801_at	BB376943	1.43	0.20
49	glycerol phosphate dehydrogenase 1, cytoplasmic adult (Gdc1)	1416204_at	NM_010271.1	1.67	0.19
50	3-phosphoglycerate dehydrogenase	1456471_x_at	BB204486	1.31	0.19

Table 5.3 Top 50 of downregulated genes in RWE soleus muscle

#	Description	Affymetrix ID	Genbank ID	Fold change	Prob value
1	pyruvate dehydrogenase kinase 4 (Pdk4)	1417273_at	NM_013743.1	-3.23	0.85
2	carboxypeptidase X2	1460248_at	NM_018867.2	-2.03	0.79
3	transmembrane 4 superfamily member 6 (Tm4sf6)	1448501_at	NM_019656.1	-1.88	0.79
4	angiotensin receptor-like 1	1438651_a_at	BB483357	-2.74	0.78
5	cyclin D1	1417420_at	NM_007631.1	-1.84	0.75
6	RIKEN cDNA 6720475J19	1423071_x_at	NM_026586.1	-2.10	0.74
7	thrombospondin 1	1460302_at	NM_011580.1	-2.11	0.73
8	ESTs, Weakly similar to TYROSINE-PROTEIN KINASE JAK3 (M.musculus)	1456046_at	AV319144	-1.79	0.72
9	RIKEN cDNA 2610028K12 gene	1452661_at	AK011596.1	-1.64	0.68
10	carbonic anhydrase-related polypeptide	1427482_a_at	X61397.1	-1.58	0.66
11	RIKEN cDNA 2210403K04 gene	1428562_at	AK008813.1	-1.90	0.65
12	mutant fibrillin-1 (Fbn1)	1425896_a_at	AF007248.1	-2.10	0.65
13	expressed sequence AA407270	1455180_at	BG063148	-1.70	0.64
14	RIKEN cDNA 1100001H23 gene (1100001H23Rik)	1448786_at	NM_025806.1	-1.61	0.63
15	ESTs	1438577_at	BB376947	-3.07	0.63
16	RIKEN cDNA 5730408C10 gene	1430527_a_at	AK017523.1	-1.51	0.61
17	ESTs, Moderately similar to G01936 Abl binding protein 3 (H.sapiens)	1436984_at	BG261647	-1.68	0.61
18	ESTs	1442562_at	BB346556	-1.57	0.61

19	ESTs	1458012_at	BB175077	-1.74	0.58
20	myristoylated alanine rich protein kinase C substrate	1415973_at	NM_008538.1	-1.69	0.58
21	RIKEN cDNA 2700063G02 gene	1427293_a_at	AW556180	-1.50	0.57
22	RIKEN cDNA 5430401H09 gene	1454193_at	AK017255.1	-2.71	0.57
23	ESTs	1456603_at	BG070087	-1.51	0.56
24	fibromodulin (Fmod)	1415939_at	NM_021355.1	-1.71	0.56
25	BTBPOZ zinc finger protein DPZF	1422064_a_at	NM_019778.1	-1.59	0.55
26	thrombospondin 1	1450377_at	NM_011580.1	-1.74	0.55
27	a disintegrin-like and metalloprotease (reprolysin type) with thrombospondin type 1 motif, 8 (Adamts8)	1418270_at	NM_013906.1	-1.67	0.54
28	RIKEN cDNA 1110001I24 gene	1423456_at	NM_025840.1	-1.52	0.54
29	Similar to hypothetical protein FLJ11110, clone MGC:11734	1424374_at	BC005577.1	-1.61	0.53
30	Sel1 (suppressor of lin-12) 1 homolog (C. elegans)	1425188_s_at	BI691849	-1.68	0.53
31	cytosolic acyl-CoA thioesterase 1 (Cte1)	1449065_at	NM_012006.1	-1.52	0.53
32	phosphatidic acid phosphatase 2a (Ppap2a)	1422620_s_at	NM_008903.1	-1.46	0.52
33	myocyte enhancer factor 2C (Mef2c)	1451507_at	BB280300	-1.51	0.52
34	lectin, galactose binding, soluble 9 (Lgals9)	1421217_a_at	NM_010708.1	-1.46	0.52
35	ESTs	1441058_at	BB434111	-1.48	0.52
36	viral hemorrhagic septicemia virus(VHSV) induced gene 1	1421009_at	NM_021384.1	-1.71	0.52
37	RIKEN cDNA 2310067L22 gene	1428785_at	BG917015	-1.64	0.51
38	ESTs	1455554_at	BB269387	-1.46	0.51

39	ESTs	1440975_at	BB275943	-1.52	0.51
40	TGFB inducible early growth response (Tieg)	1416029_at	NM_013692.1	-1.60	0.50
41	RIKEN cDNA 4933404I11 gene	1454341_at	AV278881	-1.75	0.49
42	expressed sequence AI595338	1447927_at	BG092512	-1.46	0.49
43	interferon-inducible GTPase	1419043_a_at	NM_021792.1	-2.52	0.49
44	interferon-inducible GTPase (Iigp-pending)	1419042_at	NM_021792.1	-2.09	0.49
45	sorting nexin 4 (Snx4)	1460182_at	NM_080557.1	-1.78	0.49
46	ESTs	1434102_at	BB100463	-1.58	0.48
47	mitochondrial acyl-CoA thioesterase 1 (Mte1-pending)	1422997_s_at	NM_134188.1	-1.58	0.48
48	RIKEN cDNA 6230401I02 gene	1428939_s_at	W41916	-1.53	0.47
49	ESTs	1441233_at	BM240795	-1.71	0.47
50	lectin, galactose binding, soluble 4	1451336_at	NM_010706	-1.57	0.46

Table 5.4 Top 50 of upregulated genes in RWE EDL muscle

#	Description	Affymetrix ID	Genbank ID	Fold change	Prob value
1	EGL nine homolog 3 (C. elegans) (Egln3)	1418648_at	NM_028133.1	2.45	0.45
2	EGL nine homolog 3 (C. elegans)	1418649_at	NM_028133.1	3.16	0.41
3	G0G1 switch gene 2 (G0s2)	1448700_at	NM_008059.1	3.30	0.39
4	ESTs	1435292_at	AF023098	2.27	0.37
5	heat shock protein 105 kDa beta (42 degrees C-specific heat shock protein)	1425993_a_at	D67017.1	1.75	0.35
6	Mus musculus, clone MGC:35978	1426471_at	BM225280	1.69	0.35
7	FMS-like tyrosine kinase 1 (Flt1)	1419300_at	NM_010228.1	1.84	0.31
8	ESTs	1443299_at	BB480432	1.55	0.28
9	heat shock protein, 105 kDa (Hsp105)	1423566_a_at	NM_013559.1	1.86	0.26
10	heterogeneous nuclear ribonucleoprotein D-like	1424251_a_at	BC021374.1	1.56	0.26
11	Wrch-1	1449028_at	AF378088.1	2.21	0.25
12	translocase of inner mitochondrial membrane 8 homolog a (yeast) (Timm8a)	1416345_at	NM_013898.1	1.56	0.25
13	dachshund 2 (Drosophila) (Dach2)	1449823_at	NM_033605.1	2.28	0.24
14	expressed sequence AW539457	1433453_a_at	BB621938	1.84	0.24
15	ESTs	1455418_at	BM119433	2.06	0.24
16	RIKEN cDNA 2410005O16 gene	1438034_at	BB115225	1.55	0.23
17	ESTs	1438862_at	BB227434	1.68	0.22
18	ESTs	1444343_at	BB475564	1.60	0.22

19	ESTs	1446182_at	BB451412	1.42	0.21
20	heat shock protein, 86 kDa 1 (Hsp86-1)	1438902_a_at	C77287	1.68	0.20
21	ESTs, Highly similar to S12207 hypothetical protein (M.musculus)	1439840_at	BB208426	1.59	0.20
22	interferon-related developmental regulator 1 (Ifrd1)	1416067_at	NM_013562.1	1.89	0.20
23	corticotropin releasing hormone receptor 2 (Crhr2)	1422012_at	NM_009953.1	1.53	0.20
24	ESTs	1445900_at	BG066962	1.60	0.20
25	phosphofructokinase, liver, B-type (pfkl-1)	1439148_a_at	BE914497	1.62	0.19
26	RIKEN cDNA C330027G06 gene	1429558_a_at	BI104294	1.43	0.19
27	ESTs	1447830_s_at	BB034265	2.13	0.19
28	RIKEN cDNA 8430438D04 gene	1429809_at	AK018506.1	1.36	0.18
29	ras homolog gene family, member E (Arhe)	1416700_at	NM_028810.1	1.48	0.18
30	RIKEN cDNA 1300012C15 gene	1416424_at	BC011116.1	1.96	0.18
31	ESTs	1458635_at	AV026232	2.82	0.18
32	expressed sequence R75501	1434935_at	BG067888	1.37	0.18
33	ESTs	1455506_at	BE650825	1.77	0.17
34	clusterin (Clu)	1418626_a_at	NM_013492.1	1.52	0.17
35	ESTs Similar to mannosyl (alpha-1,3-)-glycoprotein beta-1,4-N-acetylglucosaminyltransferase, isoenzym	1455002_at	AV331223	1.53	0.17
36	expressed sequence AI528491	1440830_at	AW547876	1.35	0.17

37	Mus musculus, clone IMAGE:4007705, mRNA, partial cds	1455475_at	AV317245	1.90		0.17
38	regulator of G-protein signaling 4	1416286_at	BC003882.1	1.76		0.17
39	RIKEN cDNA 4432404J10 gene	1429454_at	AK014474.1	1.31		0.17
40	EST AI447490	1433671_at	BI149851	1.42		0.16
41	Mus musculus, clone IMAGE:4216135	1427533_at	BM022919	1.35		0.16
42	WDR9 protein (Wdr9 gene), form B	1452321_at	BB491154	1.42		0.16
43	expressed sequence AI118064	1457721_at	AI118064	1.88		0.16
44	ESTs	1440977_at	BB201490	1.47		0.16
45	RIKEN cDNA 2900063A19 gene	1452973_at	AK013741.1	1.45		0.16
46	DnaJ (Hsp40) homolog, subfamily A, member 1	1416288_at	BF141076	1.44		0.16
47	ESTs	1441346_at	BB162465	1.41		0.16
48	ESTs	1440952_at	BM123777	1.43		0.16
49	RIKEN cDNA C430045I18 gene	1430633_s_at	BG066234	1.38		0.16
50	RIKEN cDNA 1110058B13 gene (1110058B13Rik)	1416400_at	NM_025412.1	1.38		0.15

Table 5.5 Top 50 of downregulated genes in RWE EDL muscle

#	Description	Affymetrix ID	Genbank ID	Fold change	Prob value
1	collagen pro-alpha-1 type I chain	1423669_at	U08020.1	-1.83	0.43
2	expressed sequence AW743275	1458145_at	BB520860	-0.80	0.39
3	ESTs	1441946_at	AV239969	-0.56	0.32
4	thioredoxin interacting factor	1415997_at	AF173681.1	-1.10	0.31
5	ESTs	1441908_x_at	BB483759	-0.50	0.31
6	RIKEN cDNA 2310004G06 gene	1429639_at	AK009137.1	-0.81	0.30
7	tissue inhibitor of metalloproteinase 2 (Timp2)	1420924_at	NM_011594.1	-0.71	0.29
8	sodium channel, voltage-gated, type IV, alpha polypeptide (Scn4a)	1450557_at	NM_133199.1	-0.52	0.28
9	RIKEN cDNA C330007M08 gene	1428921_at	AK021189.1	-0.47	0.27
10	junctophilin 1 (Jph1)	1421520_at	NM_020604.1	-0.64	0.27
11	RIKEN cDNA 5730543C08 gene	1431164_at	AK017818.1	-0.55	0.26
12	stromal cell derived factor 1, clone MGC:6119	1448823_at	BC006640.1	-0.41	0.25
13	expressed sequence AV009181	1455948_x_at	AV009181	-0.55	0.24
14	DNA segment, Chr 4, ERATO Doi 76, expressed (D4Ertd76e)	1457901_at	BB244812	-0.70	0.24
15	expressed sequence AI323528	1449773_s_at	AI323528	-1.54	0.24
16	ESTs	1440286_at	BM232403	-0.69	0.23
17	angiopoietin-like 2 (Angptl2)	1421002_at	NM_011923.1	-0.52	0.22

18	DNA segment, Chr 16, ERATO Doi 266, expressed (D16Ertd266e)	1441466_at	BG066615	-0.84	0.22
19	Mus musculus, clone IMAGE:4952594	1452185_at	AW413962	-0.41	0.22
20	procollagen, type I, alpha 2 (Col1a2)	1423110_at	AW545978	-1.43	0.21
21	expressed sequence AI317158	1445481_at	BM125070	-0.46	0.21
22	TGFB inducible early growth response (Tieg)	1416029_at	NM_013692.1	-0.88	0.21
23	ATP-binding cassette, sub-family D (ALD), member 2 (Abcd2)	1419748_at	NM_011994.1	-0.73	0.21
24	RIKEN cDNA 5730455P16 gene	1453735_at	BF535440	-0.49	0.21
25	RIKEN cDNA 2610529H08 gene	1420523_at	NM_026202.1	-0.39	0.20
26	ESTs	1446536_at	BB482394	-0.35	0.20
27	scavenger receptor class B1	1437378_x_at	BB224405	-0.75	0.20
28	sema domain, immunoglobulin domain (Ig), short basic domain, secreted, (semaphorin) 3C (Sema3c)	1420696_at	NM_013657.1	-0.37	0.20
29	ESTs	1446145_at	BB327170	-0.40	0.20
30	expressed sequence AA409502	1434282_at	BB029886	-0.69	0.19
31	ESTs	1443675_at	BM118780	-0.47	0.19
32	ESTs	1442569_at	BM206269	-0.48	0.19
33	RIKEN cDNA 2510010B09 gene	1429448_s_at	BM240219	-0.43	0.19
34	transforming growth factor, beta 2 (TGFβ2)	1450922_a_at	AW049938	-0.73	0.19
35	myocyte enhancer factor 2A (Mef2a)	1421252_a_at	NM_013597.1	-0.38	0.18

36	ESTs, Moderately similar to S12207 hypothetical protein (M.musculus)	1457529_x_at	BB066943	-0.39	0.18
37	ESTs, Highly similar to S12207 hypothetical protein (M.musculus)	1439655_at	BG064372	-0.49	0.18
38	thymus cell antigen 1, theta	1423135_at	NM_009382.1	-0.73	0.17
39	ESTs	1437422_at	AV375653	-0.34	0.17
40	Mus musculus, clone IMAGE:4506466	1426993_at	AV369396	-0.89	0.17
41	CArG box-binding factor	1426114_at	L36663.1	-0.68	0.17
42	ESTs	1439033_at	AV341907	-0.50	0.17
43	CXC chemokine MIP-2gamma precursor	1418457_at	AF252873.1	-0.50	0.17
44	inducible 6-phosphofructo-2-kinase (Pfkfb3)	1456676_a_at	AV282911	-0.50	0.16
45	procollagen, type I, alpha 2 (Col1a2)	1450857_a_at	NM_007743.1	-0.78	0.16
46	RIKEN cDNA 1200015K23 gene	1434949_at	AW456859	-0.41	0.16
47	RIKEN cDNA 2310045N14 gene	1433296_at	AK009831.1	-2.06	0.16
48	basic helix-loop-helix domain containing, class B3 (Bhlhb3)	1421099_at	NM_024469.1	-0.40	0.16
49	RIKEN cDNA 1700086G08 gene	1453605_s_at	AK007017.1	-0.47	0.15
50	ESTs, Moderately similar to KIAA0878 protein (H.sapiens)	1447869_x_at	AV047988	-0.86	0.15

5.5 References

1. Hoppeler, H. and M. Fluck, *Normal mammalian skeletal muscle and its phenotypic plasticity.* J Exp Biol, 2002. **205**(Pt 15): p. 2143-52.
2. Potthoff, M.J., E.N. Olson, and R. Bassel-Duby, *Skeletal muscle remodeling.* Curr Opin Rheumatol, 2007. **19**(6): p. 542-9.
3. Salmons, S. and J. Henriksson, *The adaptive response of skeletal muscle to increased use.* Muscle Nerve, 1981. **4**(2): p. 94-105.
4. Allen, D.L., et al., *Cardiac and skeletal muscle adaptations to voluntary wheel running in the mouse.* J Appl Physiol, 2001. **90**(5): p. 1900-1908.
5. Akimoto, T., et al., *Skeletal muscle adaptation in response to voluntary running in Ca^{2+}/calmodulin-dependent protein kinase IV (CaMKIV) deficient mice.* Am J Physiol Cell Physiol, 2004. **287**(5): p. C1311-9.
6. Wu, H., et al., *Transcriptional analysis of mouse skeletal myofiber diversity and adaptation to endurance exercise.* J Muscle Res Cell Motil, 2003. **24**(8): p. 587-92.
7. Jeneson, J.A., et al., *Treadmill but not wheel running improves fatigue resistance of isolated extensor digitorum longus muscle in mice.* Acta Physiol (Oxf), 2007. **190**(2): p. 151-61.
8. Smyth, G.K., *Limma: linear models for microarray data.* In: *Bioinformatics and Computational Biology Solutions using R and Bioconductor*, R. Gentleman, V.Carey, S. Dudoit, R. Irizarry, W. Huber (eds), Springer, New York, 2005: p. 397-420.
9. De Preter, K., et al., *Quantification of MYCN, DDX1, and NAG gene copy number in neuroblastoma using a real-time quantitative PCR assay.* Mod Pathol, 2002. **15**(2): p. 159-66.
10. Livak, K.J. and T.D. Schmittgen, *Analysis of relative gene expression data using real-time quantitative PCR and the 2(-Delta Delta C(T)) Method.* Methods, 2001. **25**(4): p. 402-8.
11. Jemiolo, B. and S. Trappe, *Single muscle fiber gene expression in human skeletal muscle: validation of internal control with exercise.* Biochem Biophys Res Commun, 2004. **320**(3): p. 1043-50.
12. James, P., et al., *Nature and site of phospholamban regulation of the Ca2+ pump of sarcoplasmic reticulum.* Nature, 1989. **342**(6245): p. 90-2.
13. Jorgensen, A.O. and L.R. Jones, *Localization of phospholamban in slow but not fast canine skeletal muscle fibers. An immunocytochemical and biochemical study.* J Biol Chem, 1986. **261**(8): p. 3775-81.
14. De Bono, J.P., et al., *Novel quantitative phenotypes of exercise training in mouse models.* Am J Physiol Regul Integr Comp Physiol, 2005. **290**(4): p. R926-34.
15. Sugden, M.C. and M.J. Holness, *Recent advances in mechanisms regulating glucose oxidation at the level of the pyruvate dehydrogenase complex by PDKs.* Am J Physiol Endocrinol Metab, 2003. **284**(5): p. E855-62.
16. Nordsborg, N., J. Bangsbo, and H. Pilegaard, *Effect of high-intensity training on exercise-induced gene expression specific to ion homeostasis and metabolism.* J Appl Physiol, 2003. **95**(3): p. 1201-6.
17. Vissing, K., J.L. Andersen, and P. Schjerling, *Are exercise-induced genes induced by exercise?* Faseb J, 2005. **19**(1): p. 94-6.

18. Black, B.L. and E.N. Olson, *Transcriptional control of muscle development by myocyte enhancer factor-2 (MEF2) proteins.* Annu Rev Cell Dev Biol, 1998. **14**: p. 167-96.
19. Weintraub, H., *The MyoD family and myogenesis: redundancy, networks, and thresholds.* Cell, 1993. **75**(7): p. 1241-4.
20. Muscat, G.E. and U. Dressel, *Not a minute to waste.* Nat Med, 2000. **6**(11): p. 1216-7.
21. Joulia, D., et al., *Mechanisms involved in the inhibition of myoblast proliferation and differentiation by myostatin.* Exp Cell Res, 2003. **286**(2): p. 263-75.
22. Schabort, E.J., et al., *TGF-beta's delay skeletal muscle progenitor cell differentiation in an isoform-independent manner.* Exp Cell Res, 2009. **315**(3): p. 373-84.
23. Li, Z. and P. Srivastava, *Heat-shock proteins.* Curr Protoc Immunol, 2004. **Appendix 1**: p. Appendix 1T.
24. Sumanasekera, W.K., et al., *Evidence that peroxisome proliferator-activated receptor alpha is complexed with the 90-kDa heat shock protein and the hepatitis virus B X-associated protein 2.* J Biol Chem, 2003. **278**(7): p. 4467-73.
25. Wettenhall, J.M. and G.K. Smyth, *limmaGUI: a graphical user interface for linear modeling of microarray data.* Bioinformatics, 2004. **20**(18): p. 3705-6.
26. Stopka, P., K. Janotova, and D. Heyrovsky, *The advertisement role of major urinary proteins in mice.* Physiol Behav, 2007. **91**(5): p. 667-70.

Chapter VI

The effect of wheel running exercise on plasma IL-6 and muscle IL-6 mRNA levels in mice

Submitted for publication

M.W. de Snoo
C.E. van den Brom
J.A.L. Jeneson
M.E. Everts

ABSTRACT - Interleukin-6 –a cytokine involved in the immune response- has also been described to play an important role in exercise paradigms. In mice, plasma cytokine levels were upregulated 1.5 and 3 hours after cessation of forced treadmill fatigue runs. However, as running wheels are the preferred devices to study skeletal muscle adaptations in mice, we focused on IL-6 protein and mRNA levels in plasma and muscles, respectively, during and after six weeks of voluntary wheel running. Ten C57Bl/6 mice were randomly assigned to either a sedentary control group or an exercise group. Mice in the exercise group had unlimited access to a running wheel, running 8.8 ± 0.4 km/day for the entire duration of the study. After six weeks, mice were sacrificed, blood samples were taken and hindlimb muscles were isolated. We found no exercise-related changes of IL-6 levels plasma levels. We did, however, find a six-fold increase over time ($P<0.05$) in both control and running wheel group. Only in soleus muscle we found a minor -twofold- increase in IL-6 mRNA expression ($P<0.05$). These results suggest that IL-6 only plays a minor –if any- role in this particular exercise model.

6.1 Introduction

Cytokines are a class of regulatory proteins involved in the immune response. However, cytokines have also been demonstrated to play a role during exercise without muscle damage [1-3], thus under noninflammatory conditions. In this respect, interleukin-6 (IL-6) has been well documented; in human, IL-6 plasma protein and muscle mRNA levels were increased after several forms of endurance exercise, e.g. rowing, biking and running [4, 5]. The study by Ostrowksi et al. suggested a correlation between exercise intensity and plasma IL-6 levels [5]. In rat, both tetanic as well as eccentric contractions of *in situ* stimulated calf muscles induced IL-6 mRNA expression, followed by IL-6 protein upregulation [6]. Moreover, endurance capacity of IL-$6^{-/-}$ mice was significantly reduced during fatiguing treadmill running in both 4-month-old pre-obese and 8-month-old obese animals [7].

It is suggested that endurance exercise promotes production of IL-6 in skeletal muscle, which is subsequently released into the circulation, promoting lipolysis and glucose output from adipose tissue and liver [8, 9, 10]. Direct effects on skeletal muscle would increase fatty acid and glucose uptake and utilization. As such, it serves a beneficial role in energy metabolism by providing additional substrates during exercise.

Numerous studies in mice employ exercise models to study adaptation processes in skeletal muscle [11-14]. To our knowledge, only one of these studies has focused on the role of cytokines in response to exercise [14]. This study demonstrated a significant increase of plasma IL-6 levels directly as well as 1.5 and 3 h after fatiguing, but not moderate, running on a treadmill. Treadmill running, however, forces continuous running at a set speed for a sustained period. We recently demonstrated that voluntary wheel running in mice involves periods of burst activity (de Snoo et al., submitted) at a typically higher speed. In the light of this specific running pattern, we proposed that adaptations in mouse soleus muscle were associated with repetitive bursts of free Ca^{2+} increases. Interestingly, recent studies have attributed Ca^{2+} as an important stimulator for IL-6 expression [15, 16].

The purpose of the present study was to elucidate whether voluntary exercise behavior in mice would lead to increases in IL-6 expression. Mice were randomly assigned to either a control group or an exercise group, and were housed individually. Blood samples were taken at regular intervals during the experimental period. Mice were sacrificed after the six week experimental period and hindlimb muscles were isolated for IL-6 mRNA analysis. We could not demonstrate any exercise-related changes in plasma

or mRNA IL-6 expression levels. This suggests that the load or the intermittent pattern associated with voluntary wheel running is not high sufficient enough to induce IL-6 expression.

6.2 Methods

Animals and workload characterization

Four-week old male C57Bl/6 mice were randomly assigned to a running wheel exercise (RWE; n=5) or a sedentary control (SED; n=5) group and housed individually on a 12:12-h light-dark cycle with food and water provided *ad libitum*.

Cages (28.8 cm x 28.8 cm x 24.5 cm) were custom built and made from Plexiglas. Cages of the RWE group were equipped with in-house made running wheels with a diameter of 12.1 cm. Treads on the wheel were 1.2 cm apart. For each cage, the running wheel was equipped with a small magnet. Juxtaposed on the outside of the Plexiglas cage, a magnetic relais was attached and hooked up to a PC. The analog output of the relais was sampled at a frequency exceeding 10 kHz using dedicated homebuilt Labview software (National Instruments, Austin, Texas, NI). Ordinary bicycle speedometers (Hema, Amsterdam, the Netherlands) served as a backup control to measure total accumulated running distance.

Blood samples were collected via tail vein sampling under isoflurane anesthesia at weeks 0, 1, 2, and 6 of the experimental period. Mice were sacrificed by cervical dislocation at the age of ten weeks, i.e. six weeks after the start of the protocol. The hindlimb soleus, plantaris, gastrocnemius, tibialis anterior and extensor digitorum longus (EDL) muscles were dissected, snap frozen in liquid nitrogen and stored at -80 °C.

Experiments were performed in accordance with institutional and governmental guidelines after approval of the Animal Experimentation Ethics Committee, Utrecht University.

IL-6 ELISA

Blood samples were centrifuged at maximum speed. Supernatant was collected and stored as plasma. IL-6 plasma levels were assayed using CytoSet ELISA kit (Biosource, Camarillo, Ca, USA), according to manufacturer's instructions. In short, microplates coated with capture antibody were incubated with plasma samples, and incubated with Biotin-conjugated IL-6 antibody. After excessive washing, wells were incubated with Streptavidin-HRP. Reactions were stopped with Stop Solution, and microplate optical

densities were read at 450 nm. Concentrations of samples were read from a standard curve constructed from standard samples. Experiments were performed in duplo.

RNA isolation

Total RNA was isolated from each isolated hindlimb muscle using RNeasy Fibrous Tissue Mini Kit (Qiagen, Venlo, the Netherlands) according to manufacturer's protocol. Muscles were homogenized in 300 µl lysis buffer RLT (containing 10 µl β-mercaptoethanol/ml) for 30 s at 10.000 rpm in a polytron (MagNAlyser; Roche, Indianapolis, IN, USA) using vials with MagNAlyser green beads (Roche). Next, the protocol was followed according to manufacturer's instructions. Following isolation, RNA concentration was determined spectrophotometrically.

First-strand cDNA synthesis

Reverse transcription of total RNA was performed using SuperScript II Reverse Transcriptase (Invitrogen, Carlsbad, CA, USA) according to manufacturer's instructions. Shortly, 5 µg of RNA was incubated with 500 ng of random hexamer primers. The sample was mixed with 5x First-strand Buffer and 10 mM dNTP mix, and incubated for 10 minutes at 42°C. Superscript II Reverse Transcriptase was added and incubated for 1 hour at 42 °C, followed by 15 min at 72 °C to inactivate the transcriptase.

Quantitative real-time PCR

Real-time PCR was performed on a MyiQcycler (Biorad, Hercules, CA, USA) using SYBR Green Supermix (Biorad). cDNA input was 1.25 ng and the concentration of the primers (forward and reverse) used was 10 µM. Primer sequences are listed in table 6.1. Product specificity during PCR was verified by melting curve analysis of the products. For each sample tested, duplicate Ct values were obtained and averaged. Quantification was performed using a mathematical model of the relative expression ratio in real-time PCR, the $2^{-\Delta\Delta Ct}$-method [17, 18] and was calculated with the help of Genex software (Biorad). GAPDH served as a reference gene [19].

Statistics
Data are presented as arithmetic means ± standard error (SE). Statistical analyses to analyze the age-effect in IL-6 plasma levels were performed using a one-way ANOVA, with Bonferroni as post-hoc test. Statistical analyses on mRNA data were performed using a Student's unpaired *t*-test. Differences between groups were considered significant if $P<0.05$.

Name	Sequence	Product size (bp)
GAPDH	*For* GAA GGT CGG TGT GAA CGG *Rev* TGA AGG GGT CGT TGA TGG	101
IL-6	*For* TTC CAT CCA GTT GCC TTC TTG *Rev* AGG TCT GTT GGG AGT GGT ATC	108

Table 6.1 The primer sequences are shown in 5' → 3' order. The length of the amplified product is indicated. Annealing temperature and number of cycles were 57 °C and 40, respectively, for all primer sets. Product lengths are represented as numbers of base pairs.

6.3 Results

Animals
Mice with unlimited access to a running wheel typically ran 8.8 ± 0.4 km per day (n=5; range: 8.1– 9.9 km) during the dark cycle at an average speed of 2.5 ± 0.1 km per hour. For each mouse this distance was constant for the entire duration of the study. There were no differences in body weight between both groups, with both showing a significant increase over the six-week experimental period (data not shown).

IL-6 in plasma
IL-6 protein concentration in plasma demonstrated a six-fold increase during the six-week experimental period ($P<0.05$). Steady state was reached after 2 weeks, i.e. at the age of 6 weeks. No differences were seen between SED and RWE groups (Figure 6.1).

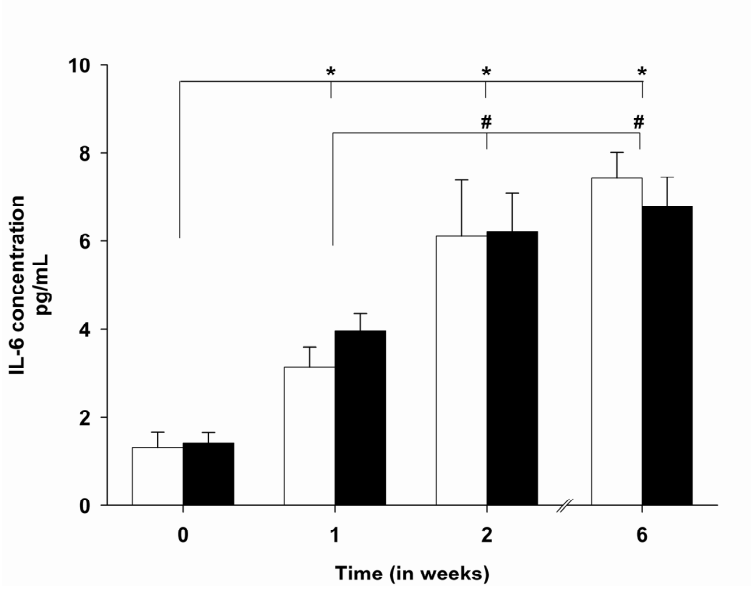

Figure 6.1 Mouse plasma IL-6 concentration in SED (white bars; n=5) and RWE (black bars; n=5) mice during the six week experimental period. * $P<0.05$ Weeks 1, 2, and 6 vs. week 0; # $P<0.05$ Weeks 2 and 6 vs. week 1

IL-6 mRNA in skeletal muscle

IL-6 mRNA expression was analyzed in all hindlimb muscle, i.e. soleus, gastrocnemius, plantaris, EDL, and tibialis anterior muscle. CT-values in all muscle samples were very high (data not shown), reflecting low expression levels and resulting in high error bars (figure 6.2A). None of the muscles demonstrated significant changes, although a trend toward upregulated IL-6 mRNA was seen in soleus and EDL muscle. We therefore also analyzed IL-6 mRNA expression in soleus and EDL muscles from an additional experiment. Together, this resulted in a twofold increase in soleus muscle (**SED** 1.0 ± 0.14, **RWE** 2.1 ± 0.5; $P<0.05$, figure 6.2B), while no significant changes were found in EDL muscle.

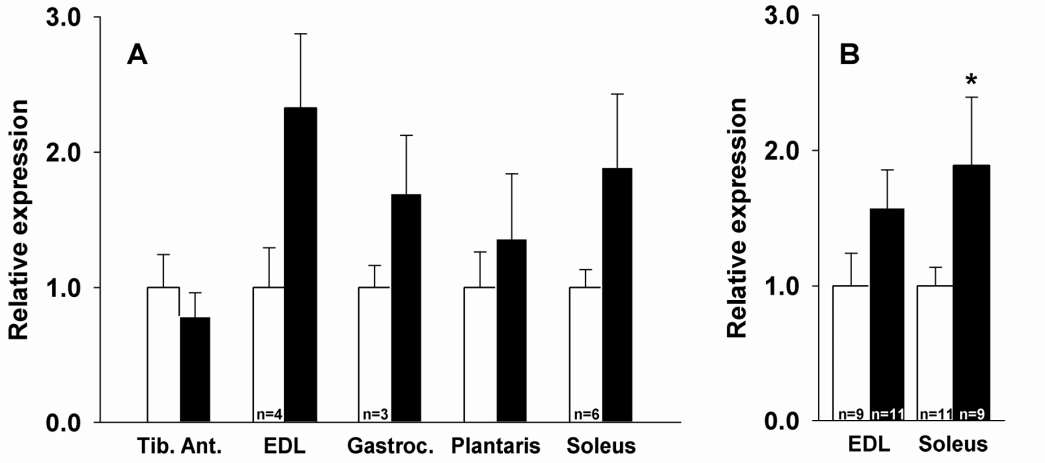

Figure 6.2 A Relative mRNA expression in SED (white bars) and RWE (black bars) hindlimb muscles after the six week experimental period. Relative expression is related to the corresponding muscle of SED mice. n=5 unless mentioned otherwise. **B** A trend towards upregulated IL-6 mRNA expression was found in soleus and EDL muscles as seen in figure 6.2a. Data represent mRNA expression of soleus and EDL muscles from figure 6.2a and an additional experiment.
* $P<0.05$

6.4 Discussion

Endurance exercise is associated with increases in IL-6 plasma levels. It is suggested that this free IL-6 stimulates fat metabolism and glycogenolysis, thus promoting energy metabolism during endurance exercise. Mouse models have for long been used to study the effects on skeletal muscle adaptation and the effects of endurance exercise. To our knowledge, only one of these studies focused on cytokine release. In that particular study, treadmill running was used to induce changes in mouse skeletal muscle. However, wheel running exercise in mice more closely represents the natural activity of the mouse and is the preferred method to study exercise-related changes in this animal. Therefore, we investigated the effects of six weeks of mouse wheel running exercise on plasma IL-6 protein, as well as skeletal muscle IL-6 mRNA levels.

Mice with free access to a running wheel ran 8.8 ± 0.4 km per day during the entire six-week experimental period. This distance was substantially higher than distances run in the study by Colbert et al. [14]. In that study mice that demonstrated an increase in IL-6 plasma levels ran approximately 6 km during a single forced fatiguing treadmill experiment. Moderately

exercised mice that did not demonstrate such an increase ran approximately 1 km. We, however, found no increase in plasma IL-6 during voluntary wheel running exercise. One explanation for this discrepancy could be related to the type of exercise. Mice in our study had free access to a running device, and could therefore run and stop *ad libitum*. Typically, mice demonstrate an intermittent running pattern, consisting of short bouts of high-speed running taking small pauses of approximately 1.8 seconds [de Snoo et al. (submitted)], corresponding to their natural behavior as prey animals [20]. During treadmill running, however, mice are forced to run continuously for substantially longer periods, typically at a lower speed than during voluntary exercise. IL-6 plasma concentration is suggested to correlate to exercise duration and intensity [21]. The present data and the data by Colbert et al, suggest a more dominant effect of exercise intensity compared to duration.

Interestingly, we found increases in plasma IL-6 levels over time in both groups during the experimental period. This age-related effect has previously been demonstrated in human [22], and has been attributed to increased IL-6 production by peripheral blood mononuclear cells [23].

The precise source of exercise-induced IL-6 in plasma is still not completely understood, although recent investigations have demonstrated a role for the skeletal muscle as a source for IL-6. During strenuous metabolic challenges, like heavy exercise, skeletal muscle becomes the predominant source of IL-6. More particular, IL-6 during exercise is produced by myocytes [24]. This leads to an increase in plasma IL-6, which is suggested to induce the beneficial effects of physical exercise on glucose and fatty acid metabolism. We found no evidence for increased plasma IL-6 levels in the running wheel exercise group (figure 6.1). Recent investigations, however, also demonstrated an autocrine function for IL-6 in skeletal muscle [25]. Specifically, strenuous exercise leads to IL-6 production by skeletal muscle, which stimulates further IL-6 production by an autocrine effect, resulting in the beneficial effect on energy metabolism. This could be reflected in an upregulation of IL-6 production in skeletal muscle, reflected in increased mRNA expression. We therefore measured mRNA expression in hindlimb muscles after the six-week experimental period. Only in the slow-twitch soleus muscle we found a minor, twofold upregulation of IL-6 mRNA expression (figure 6.2B), while previous studies in rat calf muscles reported up to 60 fold increases after eccentric as well as concentric *in situ* contractions [6].

Impact of the study

This study has evaluated the role of IL-6 in voluntarily running mice. It demonstrated that during six weeks of running wheel exercise no exercise-related changes were found in plasma IL-6 levels. Further, IL-6 mRNA expression was unchanged in four of five hindlimb muscles analyzed after the six week experimental period. This compares to treadmill trained mice, where no changes were seen in plasma IL-6 levels in moderately trained mice [14]. An upregulation of plasma was only seen immediately, 1.5 and 3 hours after strenuous exercise. Together, these data suggest that the exercise load in voluntarily running mice was not sufficient to induce increases in IL-6 production. Likewise, we previously found no changes in citrate synthase also suggesting that the exercise load was not sufficient enough to expand mitochondrial density [de Snoo et al. (submitted)].

As stated before, a rise in $[Ca^{2+}]_i$ has been described as an important stimulator for IL-6 production. Voluntary exercising mice demonstrate an intermittent running pattern of bouts of high speed. Interestingly, large transient increases in $[Ca^{2+}]_i$ selectively activate NF-κB [26] -a Ca^{2+}-sensitive transcriptional regulator- that is known to exert its transcriptional effect on a.o. IL-6 [reviewed in [27]. We previously proposed that the specific running pattern of mice is associated with repetitive bursts of free Ca^{2+} concentration increases (de Snoo et al., submitted). As such, it is likely that the NF-κB pathway is stimulated. In human, this specific pathway is not activated upon skeletal muscle contraction and is therefore suggested not to be related to IL-6 production [reviewed in [28]. In rodents, however, the NF-κB signaling pathway is stimulated upon skeletal muscle contraction [29]. Further investigation is needed to elucidate the significance of this particular pathway in mouse skeletal muscle during exercise.

Together, our data suggest that IL-6 plays –if any- only a limited role in our running model, either due to the specific running pattern, or due to the low exercise load during voluntary running wheel exercise.

6.5 Acknowledgements

The authors would like to thank Arend Schot, Peter Cornelissen, and Peter Tooten for their technical assistance.

6.6 References

1. Steinacker, J.M., et al., *New aspects of the hormone and cytokine response to training.* Eur J Appl Physiol, 2004. **91**(4): p. 382-91.
2. Febbraio, M.A. and B.K. Pedersen, *Muscle-derived interleukin-6: mechanisms for activation and possible biological roles.* FASEB J., 2002. **16**(11): p. 1335-1347.
3. Croisier, J.L., et al., *Effects of training on exercise-induced muscle damage and interleukin 6 production.* Muscle Nerve, 1999. **22**(2): p. 208-12.
4. Nielsen, H.B., et al., *Lymphocytes and NK cell activity during repeated bouts of maximal exercise.* Am J Physiol, 1996. **271**(1 Pt 2): p. R222-7.
5. Ostrowski, K., et al., *Evidence that interleukin-6 is produced in human skeletal muscle during prolonged running.* J Physiol (Lond), 1998. **508**(3): p. 949-953.
6. Jonsdottir, I.H., et al., *Muscle contractions induce interleukin-6 mRNA production in rat skeletal muscles.* J Physiol (Lond), 2000. **528**(1): p. 157-163.
7. Faldt, J., et al., *Reduced exercise endurance in interleukin-6-deficient mice.* Endocrinology, 2004. **145**(6): p. 2680-6.
8. Glund, S. and A. Krook, *Role of interleukin-6 signalling in glucose and lipid metabolism.* Acta Physiol (Oxf), 2008. **192**(1): p. 37-48.
9. Bruce, C.R. and D.J. Dyck, *Cytokine regulation of skeletal muscle fatty acid metabolism: effect of interleukin-6 and tumor necrosis factor-alpha.* Am J Physiol Endocrinol Metab, 2004. **287**(4): p. E616-21.
10. Carey, A.L., et al., *Interleukin-6 increases insulin-stimulated glucose disposal in humans and glucose uptake and fatty acid oxidation in vitro via AMP-activated protein kinase.* Diabetes, 2006. **55**(10): p. 2688-97.
11. Kemi, O.J., et al., *Intensity-controlled treadmill running in mice: cardiac and skeletal muscle hypertrophy.* J Appl Physiol, 2002. **93**(4): p. 1301-9.
12. Nair-Shalliker, V., et al., *Myofiber adaptational response to exercise in a mouse model of nemaline myopathy.* Muscle Nerve, 2004. **30**(4): p. 470-80.
13. Akimoto, T., et al., *Skeletal muscle adaptation in response to voluntary running in Ca^{2+}/calmodulin-dependent protein kinase IV (CaMKIV) deficient mice.* Am J Physiol Cell Physiol, 2004. **287**(5): p. C1311-9.
14. Colbert, L.H., et al., *Tissue expression and plasma concentrations of TNFalpha, IL-1beta, and IL-6 following treadmill exercise in mice.* Int J Sports Med, 2001. **22**(4): p. 261-7.
15. Holmes, A.G., et al., *Ionomycin, but not physiologic doses of epinephrine, stimulates skeletal muscle interleukin-6 mRNA expression and protein release.* Metabolism, 2004. **53**(11): p. 1492-5.
16. Juretic, N., et al., *Depolarization-induced slow Ca2+ transients stimulate transcription of IL-6 gene in skeletal muscle cells.* Am J Physiol Cell Physiol, 2006. **290**(5): p. C1428-36.
17. Livak, K.J. and T.D. Schmittgen, *Analysis of relative gene expression data using real-time quantitative PCR and the 2(-Delta Delta C(T)) Method.* Methods, 2001. **25**(4): p. 402-8.
18. De Preter, K., et al., *Quantification of MYCN, DDX1, and NAG gene copy number in neuroblastoma using a real-time quantitative PCR assay.* Mod Pathol, 2002. **15**(2): p. 159-66.

19. Jemiolo, B. and S. Trappe, *Single muscle fiber gene expression in human skeletal muscle: validation of internal control with exercise.* Biochem Biophys Res Commun, 2004. **320**(3): p. 1043-50.
20. Edut, S. and D. Eilam, *Protean behavior under barn-owl attack: voles alternate between freezing and fleeing and spiny mice flee in alternating patterns.* Behav Brain Res, 2004. **155**(2): p. 207-16.
21. Pedersen, B.K., T. Rohde, and K. Ostrowski, *Recovery of the immune system after exercise.* Acta Physiol Scand, 1998. **162**(3): p. 325-32.
22. Ferrucci, L., et al., *The origins of age-related proinflammatory state.* Blood, 2005. **105**(6): p. 2294-9.
23. Roubenoff, R., et al., *Monocyte cytokine production in an elderly population: effect of age and inflammation.* J Gerontol A Biol Sci Med Sci, 1998. **53**(1): p. M20-6.
24. Hiscock, N., et al., *Skeletal myocytes are a source of interleukin-6 mRNA expression and protein release during contraction: evidence of fiber type specificity.* Faseb J, 2004. **18**(9): p. 992-4.
25. Weigert, C., et al., *Upregulation of IL-6 mRNA by IL-6 in skeletal muscle cells: role of IL-6 mRNA stabilization and Ca2+-dependent mechanisms.* Am J Physiol Cell Physiol, 2007. **293**(3): p. C1139-47.
26. Dolmetsch, R.E., et al., *Differential activation of transcription factors induced by Ca^{2+} response amplitude and duration.* Nature, 1997. **386**(6627): p. 855-8.
27. May, M.J. and S. Ghosh, *Signal transduction through NF-kappa B.* Immunol Today, 1998. **19**(2): p. 80-8.
28. Pedersen, B.K. and M.A. Febbraio, *Muscle as an endocrine organ: focus on muscle-derived interleukin-6.* Physiol Rev, 2008. **88**(4): p. 1379-406.
29. Ho, R.C., et al., *Regulation of IkappaB kinase and NF-kappaB in contracting adult rat skeletal muscle.* Am J Physiol Cell Physiol, 2005. **289**(4): p. C794-801.

Chapter VII

General discussion

In the present thesis, we investigated skeletal muscle adaptation using a mouse exercise model. Mice were subjected to six weeks of forced or voluntary running. After this period, mice were sacrificed and hindlimb muscles were isolated. Data on contraction parameters of these isolated skeletal muscles were combined with proteomic and genomic analyses. This provided us with physiological data on intact, isolated skeletal muscle function after complete body performance in an *in vivo* trained animal. In this chapter we will provide answers to the questions raised in the introduction and link the outcomes of the individual experimental chapters.

1) How do forced treadmill and voluntary running wheel exercise modalities affect mouse skeletal muscle mechanical performance, and 2) what is the running pattern of voluntarily running mice?

In chapter two, we compared the effects of six weeks of forced treadmill with voluntary running wheel exercise on the fast-twitch extensor digitorum longus (EDL) muscle. Both exercise regimes induced adaptations at the functional level during serial contractions. At low stimulation frequencies, fatigue resistance was improved in EDL muscles of both exercise groups. However, when stimulated at higher frequencies only treadmill exercised EDL muscle continued demonstrating improved fatigue resistance compared to SED and RWE muscles. Interestingly, mice in the voluntary exercise group had run as much as four times the distance as mice in the forced exercise group. We attributed the differences between these two groups to a difference in running pattern; mice subjected to treadmill exercise are forced to run for a set amount of time (typically 1-2 hours in one continuous period), while mice with access to a running wheel can run at their own pace, speed and time. Running pattern analysis in chapter three clearly demonstrated that mice with unlimited access to a running wheel run in periods of very short bouts of high speed, resulting in an activity time that was 'spread out' over the day.

Both continuous and high speed interval training are regarded as endurance exercise. Only few studies directly compared these two typical exercise regimes. These studies involved human subjects and rats and demonstrated that both regimes were associated with improved exercise capacity and increased muscle oxidative capacity [1-4]. Interestingly, the greatest improvements were seen in the interval trained groups both in humans and

rats [3, 4], although total time and distances spent on this exercise regime were smaller than in the endurance trained groups. This is in contrast to our study where we demonstrated greatest improvement on fatigue resistance in the forced continuous running group (chapter 2). This suggests that in mice, treadmill running is more intense than wheel running exercise, likely due to the forced character of the first, as mice are forced to run beyond their natural performance. Further, although the voluntary running in mice compares to high intensity interval exercise in human and rat, there is one major difference. The exercise load and duration are precisely determined in human studies, while total distance and time spent running in running wheel exercised mice varies between individual animals. This results in larger standard deviation, and might therefore also introduce larger variability in resulting adaptations.

Differences between running wheel exercised soleus and EDL muscles

Table 7.1 summarizes details on contractile properties of wheel running exercised EDL and soleus muscle, as obtained in chapters 2 and 3, respectively. Typically, twitch and tetanic forces produced by EDL muscles are approximately 2-3 times higher than forces produced by soleus muscles. This difference is remarkable, as previous studies demonstrated no such differences between these two muscles [5, 6]. The significant higher contraction and relaxation times in soleus muscle are typical for this slow-twitch muscle compared to the fast-twitch EDL muscle. As becomes clear from these data, soleus muscle does not demonstrate any differences in contractile twitch and tetanic properties in response to wheel running exercise. If any, this muscle becomes slower -detectable from tetanus contractile properties- suggesting an adaptation associated with endurance capacity. From EDL tetanus contractile properties it becomes clear that this specific muscle further develops its fast-twitch characteristics in response to voluntary wheel running exercise.

Despite the greater effect of treadmill running in EDL muscle, further studies with soleus muscle were performed with the voluntary exercise model; it requires less handling of the animals and will thus be associated with less stress to the animal.

	Soleus		EDL	
	SED	RWE	SED	RWE
General parameters	**n=4**	**n=6**	**n=8**	**n=8**
Muscle weight (mg)	13.1 ± 1.3	13.0 ± 0.6	10.1 ± 0.3	11.0 ± 0.3
Twitch	**n=4**	**n=6**	**n=6**	**n=8**
Force (N/g muscle)	1.4 ± 0.2	1.6 ± 0.1	4.2 ± 0.3	3.7 ± 0.6*
Contraction time (ms)	36.0 ± 1.3	37.9 ± 2.5	12.7 ± 0.1	13.4 ± 0.8
Relaxation time (ms)	352 ± 19	335 ± 36	97 ± 10	74 ± 36
Tetanus	**n=4**	**n=6**	**n=6**	**n=8**
Force (N/g muscle)	13.1 ± 2.0	11.9 ± 0.8	25.4 ± 1.5	19.4 ± 1.7*
Contraction time (ms)	455 ± 134	492 ± 88	226 ± 10	138 ± 33*
Relaxation time (ms)	97 ± 11	114 ± 10	63 ± 6	68 ± 4

Table 7.1: Contractile properties of wheel running exercised soleus and EDL muscles.
* $P<0.05$ versus sedentary control for the same muscle.

3) Does aging affect skeletal muscle adaptation and how is this influenced by running wheel exercise?

Postnatal development of skeletal muscle involves growth as well as changes in the structural composition, including changes in MyHC content. Skeletal muscle contractile properties in our studies –and of others- were investigated in mice at the age of 10 weeks, thus at adult stage [7]. However, during the previous six week experimental period, mice were still developing. As such, it is logically to assume that aging has an influence on the resultant outcome. The combined effects of aging and running wheel exercise were studied in chapter 4, and demonstrated that SERCA distribution is nearly fully developed in mice age 4 weeks, while major changes were found in its regulatory proteins both under influence of aging as well as running wheel exercise. To our knowledge, this was the first study analyzing SERCA1 and 2 expression at mRNA as well as protein level in maturing mice.

Previous studies demonstrated an increase in SR volume as function of age in both mouse soleus and EDL muscle, with the largest increase seen in the latter, accompanied by a decrease in mitochondrial volume [8]. Soleus contraction time decreased from 4 to 8 weeks of age, while relaxation times increased. In EDL muscles, both contraction and relaxation times decreased [9]. The decrease in contraction times in soleus and EDL were simi-

lar. This demonstrates that contractile properties of developing skeletal muscle differentiate during aging. Differences between slow-twitch and fast-twitch muscle development mostly affects relaxation times. The increased relaxation time in soleus muscle suggests slower Ca^{2+} reuptake into the SR, which corresponds to increased SERCA2 expression (chapter 4) relative to SERCA1 expression. In EDL muscle, we found no such corresponding differences in SERCA expression.

4) What genes, or subset of genes, are affected by running wheel exercise?

Calcium regulation

Serial contractions demonstrated improved fatigue resistance in both slow-twitch (soleus) and fast-twitch (EDL) muscles after running wheel exercise (chapters 3 & 2, respectively). Soleus muscle contractile properties were studied after wheel running exercise only and further demonstrated significant improved unstimulated force dynamics, which suggests improved Ca^{2+} recovery. Interestingly, unstimulated force was mostly attenuated during the first 20 seconds of stimulation. The improved unstimulated force recovery in soleus muscle was associated with improved SERCA function, demonstrated by changes in its regulatory proteins, PLB and SLN (chapters 3 & 4). Interestingly, microarray analysis also revealed a signaling pathway associated with improved Ca^{2+} handling capacity (chapter 5). This cluster was only found in soleus muscle and not in EDL muscle, suggesting that running wheel exercise specifically affects Ca^{2+} signaling in slow-twitch muscle only.

Energy metabolism

Running wheel exercised soleus muscle further demonstrated a 1.3 increase in oxygen consumption during serial contractions at 3 Hz (chapter 3). We found no evidence for an enlarged mitochondrial pool and attributed the increase to the 1.3-fold higher residual force compared to SED soleus muscles. In EDL muscle, we found no differences in oxygen consumption between RWE and SED muscles at none of the stimulation frequencies (chapter 2). Likewise, we found no changes in mitochondrial density, represented by citrate synthase.

Interestingly, microarray data revealed changes in regulatory proteins improving oxygen and energy metabolism in the slow-twitch soleus muscle. Like the Ca^{2+} regulatory signaling pathway, no such changes were seen in

the fast-twitch EDL muscle. The combination of increased oxygen consumption during serial contractions and microarray data revealing improvements in the oxygen/energy metabolism in soleus muscle provide further evidence for different involvement and adaptation of the two investigated hindlimb muscles.

Cell cycle regulation

Microarray data also demonstrated that major changes in soleus and EDL muscle are to be found at the cell cycle regulatory level (chapter 5). It is reasonable to assume that skeletal muscle responds to increased physiological demand by adapting 'regulatory mechanisms', eventually resulting in changes in MyHC profile. It has been demonstrated that especially mouse skeletal muscle is rather robust in its MyHC profile [10] compared to larger animals. Indeed, we found no evidence for altered MyHC profile in both muscles after six weeks of wheel running exercise (Chapters 2 & 3) [11].

Interestingly, there is evidence that the cell cycle pathway is initially stimulated in a Ca^{2+} dependent manner. As shown in figures 5.3 and 5.4, MyoD function is regulated through NFκB [12, 13] or NFAT [14]. Both NF-κB and NFAT are in turn activated by increases in $[Ca^{2+}]_i$, as seen during skeletal muscle contractions. The speed and height of Ca^{2+} influx finally determines which pathway is activated [15]. This could provide an explanation for differences between soleus and EDL muscle in the genes that are affected in this pathway.

A rise in $[Ca^{2+}]_i$ has also been described as an important stimulator for IL-6 production. More specifically, activation of NF-κB is known to exert its transcriptional effect on a.o. IL-6 [16]. Interestingly, large transient increases in $[Ca^{2+}]_i$ selectively activate NF-κB [15]. The specific running pattern of mice is most likely associated with repetitive bursts of free Ca^{2+} concentration increases (chapter 3). As such, it is expected that the NF-κB pathway is stimulated. We previously concluded that soleus muscle adaptation is primarily associated with Ca^{2+} handling pathways, not in EDL muscle (chapters 3 & 5). Likewise, a running wheel exercise induced increase in IL-6 mRNA expression was only detected in soleus muscle, not in EDL or other hindlimb muscle (chapter 6). As such, it seems tempting to assume that the NF-κB pathway is selectively stimulated in this specific muscle.

Overall, it seems impossible to conclude from our data which of the two pathways (NFAT or NF-κB) is exactly stimulated. We can conclude that the major adaptation in mouse skeletal muscle affects regulatory proteins,

and that each muscle responds differently. Soleus muscle mostly demonstrates altered Ca^{2+} handling, cell cycle regulation and energy expenditure. EDL muscle adaptation is associated with cell cycle regulation.

Extrapolation of our data

Transgenic animals have proven an excellent animal model to provide insight in the involvement of specific genes and signaling pathways. The involvement of endurance exercise in these animals has been extensively investigated to study influence of exercise on heart and skeletal muscle. Altogether, data in the present thesis demonstrate that an endurance exercise mouse model is suitable to study adaptations in skeletal muscle. However, in order to extract the data of these studies to human, one must take into account several important differences between humans and mice.

First, it seems likely that forced continuous running in mice is more enduring to the animal than its voluntary running behavior, while continuous running is the most 'accepted' form of running in humans. Even high intensity sprint interval training protocols in human are not completely comparable to the normal running pattern in mice. Whereas interval training induced the greatest improvements in human [3], mice demonstrated greatest fatigue resistance in response to forced continuous running (chapter 2). The dissimilar outcome of compared continuous and interval training suggests different adaptations of human and mice.

Second, the present thesis -together with previous studies- demonstrates that a MyHC fast-to-slow transition can not be uniformly demonstrated in running mice (chapters 2 & 3) [17]; both treadmill and running wheel exercised mice did not demonstrate changes MyHC isoforms. Further, no increase in mitochondrial pool was found (chapters 2 & 3). Interestingly, data in chapter 5 (Microarray) demonstrated changes in oxygen and energy regulation suggesting improvement at the regulatory level. In human studies, large fast-to-slow MyHC transitions and increases in mitochondrial content have regularly been described, even with less enduring exercise protocols [1, 18-20]. This suggests that mice are rather robust in their MyHC profile and are already well adapted to endurance performance.

Mice need to move around quickly while observing their surroundings. This natural behavior is reflected in their running pattern, as described in chapter 3, and makes an appropriate control group difficult to obtain. In our studies, we kept animals in special cages to prevent unregistered ex-

treme movement, although animals could still move around freely. In human studies "normal active persons' are often used as control group.

Concluding remarks

The present thesis demonstrates that mouse skeletal muscle is affected by endurance exercise, although to a lesser extent when compared to other mammals, like rats and humans. We found different responses in the fast-twitch EDL muscle to forced treadmill and voluntary wheel running exercise, although both are associated with endurance exercise. Further research is needed in order to compare the effect of these exercise modalities on the slow-twitch soleus muscle.

The combination of functional, proteomic and genomic analysis demonstrates different adaptations to voluntary wheel running exercise of fast-twitch and slow-twitch muscles. Although we had expected to find most changes in a fast-twitch muscle, the slow-twitch soleus muscle was more prone to adapt towards enhanced physical demands than the EDL muscle. In soleus muscle the most remarkable changes were seen in Ca^{2+} affected signaling pathways, while major changes in the EDL muscle were seen in cell cycle regulation.

Finally, for future studies focusing on contractile function in skeletal muscle, wheel running has proven a low-invasive, low-time consuming model to induce endurance-exercise related adaptations.

7.1 References

1. Gibala, M.J., et al., *Short-term sprint interval versus traditional endurance training: Similar initial adaptations in human skeletal muscle and exercise performance.* J Physiol, 2006.
2. Rakobowchuk, M., et al., *Sprint interval and traditional endurance training induce similar improvements in peripheral arterial stiffness and flow-mediated dilation in healthy humans.* Am J Physiol Regul Integr Comp Physiol, 2008. **295**(1): p. R236-42.
3. Helgerud, J., et al., *Aerobic high-intensity intervals improve VO2max more than moderate training.* Med Sci Sports Exerc, 2007. **39**(4): p. 665-71.
4. Haram, P.M., et al., *Aerobic interval training vs. continuous moderate exercise in the metabolic syndrome of rats artificially selected for low aerobic capacity.* Cardiovasc Res, 2009. **81**(4): p. 723-32.
5. Ter Veld, F., K. Nicolay, and J.A. Jeneson, *Increased resistance to fatigue in creatine kinase deficient muscle is not due to improved contractile economy.* Pflügers Arch, 2006. **452**(3): p. 342-348.
6. Leijendekker, W.J., W.J. van der Laarse, and G. Elzinga, *The production of initial heat and recovery heat by isolated EDL and soleus muscles of euthyroid and hypothyroid mice.* Prog Clin Biol Res, 1989. **315**: p. 233-4.
7. *Biology of the Laboratory Mouse. In: Earl. L. Green (editor).* By The Staff of The Jackson Laboratory. Dover Publications, Inc., New York, 1966(Second edition).
8. Luff, A.R. and H.L. Atwood, *Changes in the sarcoplasmic reticulum and transverse tubular system of fast and slow skeletal muscles of the mouse during postnatal development.* J Cell Biol, 1971. **51**(21): p. 369-83.
9. Bressler, B.H., et al., *Changes in isometric contractile properties of fast-twitch and slow-twitch skeletal muscle of C57BL/6J dy2J/dy2J dystrophic mice during postnatal development.* Exp Neurol, 1983. **80**(2): p. 457-70.
10. Pette, D. and R.S. Staron, *The malleability of skeletal muscle. In: Weibel, E., Taylor, C.R., Bolis, L. (Eds.).* Principles of Animal Design. Cambridge University Press, Cambridge, 1998: p. pp. 89-94.
11. Jeneson, J.A., et al., *Treadmill but not wheel running improves fatigue resistance of isolated extensor digitorum longus muscle in mice.* Acta Physiol (Oxf), 2007. **190**(2): p. 151-61.
12. Bakkar, N., et al., *IKK/NF-kappaB regulates skeletal myogenesis via a signaling switch to inhibit differentiation and promote mitochondrial biogenesis.* J Cell Biol, 2008. **180**(4): p. 787-802.
13. Muscat, G.E. and U. Dressel, *Not a minute to waste.* Nat Med, 2000. **6**(11): p. 1216-7.
14. Armand, A.S., et al., *Cooperative synergy between NFAT and MyoD regulates myogenin expression and myogenesis.* J Biol Chem, 2008. **283**(43): p. 29004-10.
15. Dolmetsch, R.E., et al., *Differential activation of transcription factors induced by Ca^{2+} response amplitude and duration.* Nature, 1997. **386**(6627): p. 855-8.
16. May, M.J. and S. Ghosh, *Signal transduction through NF-kappa B.* Immunol Today, 1998. **19**(2): p. 80-8.

17. Pette, D. and G. Vrbova, *Adaptation of mammalian skeletal muscle fibers to chronic electrical stimulation*. Rev Physiol Biochem Pharmacol, 1992. **120**: p. 115-202.
18. Short, K.R., et al., *Changes in myosin heavy chain mRNA and protein expression in human skeletal muscle with age and endurance exercise training*. J Appl Physiol, 2005. **99**(1): p. 95-102.
19. Holloszy, J.O. and E.F. Coyle, *Adaptations of skeletal muscle to endurance exercise and their metabolic consequences*. J Appl Physiol, 1984. **56**(4): p. 831-8.
20. O'Neill, D.S., et al., *Effect of endurance exercise on myosin heavy chain gene regulation in human skeletal muscle*. Am J Physiol, 1999. **276**(2 Pt 2): p. R414-9.

Chapter VIII

NL

Samenvatting in het Nederlands

IN DIT PROEFSCHRIFT wordt het effect van verschillende vormen van duurtraining op spieren van de muis beschreven. Daarnaast is onderzocht welke mechanismen verantwoordelijk zouden kunnen zijn voor de aanpassingen in skeletspieren ten gevolge van duurtraining.

Skeletspieren zijn van groot belang voor lichaamshouding en motoriek. Alle skeletspieren samen vormen het grootste orgaansysteem van het lichaam. Tijdens inspanning wordt de meeste energie verbruikt door skeletspieren. Spieren kunnen grofweg in twee soorten worden verdeeld: 1) snelle, glycolytische spieren en 2) langzame, oxidatieve spieren. De eerste soort levert veel kracht, maar kan dit slechts een beperkte tijd volhouden. Spieren in de tweede groep hebben juist een groot uithoudingsvermogen, maar kunnen slechts een beperkte hoeveelheid kracht leveren. Het verschil tussen de twee groepen spieren wordt o.a. verklaard door een verschil in samenstelling van de contractiele eiwitten. De belangrijkste hiervan is de zware myosine keten (Myosin Heavy Chain: MyHC). MyHC eiwitten van volwassen spieren worden onderverdeeld in I, IIa, IIx en IIb. Spieren voornamelijk opgebouwd uit type IIb zijn de krachtspieren, terwijl spieren met een hoog gehalte aan type I een groot uithoudingsvermogen hebben.
Een ander verschil tussen de twee groepen is de bloed- en zuurstofvoorziening. Spieren die gebruikt worden tijdens langdurige inspanning zijn afhankelijk van zuurstof voor de aanmaak van ATP als energiebron. In spieren met een goede doorbloeding wordt veel zuurstof aangeleverd. Het eiwit myoglobine bindt zuurstof in het bloed en zorgt voor de rode kleur van deze spieren. Tijdens korte, explosieve krachtsinspanning is er echter geen tijd energie te maken met behulp van zuurstof. Deze spieren hebben dan ook een niet-oxidatieve energiehuishouding, gebaseerd op de anaerobe omzetting van glycogeen en glucose.
Regelmatige krachttraining zal over het algemeen leiden tot een toename van de omvang van de spieren en van de hoeveelheid kracht die een spier kan leveren; een extreem voorbeeld hiervan zijn natuurlijk de spieren van een bodybuilder of gewichtheffer. Regelmatige duurtraining leidt juist tot een groter uithoudingsvermogen met vaak slanke spieren, zoals bij marathonlopers. De eigenschappen van skeletspieren zijn genetisch bepaald, maar tegelijkertijd zijn spieren ook erg dynamisch. Zij kunnen zich aanpassen aan veranderende omstandigheden, zoals training en belasting. Hoewel al veel onderzoek is gedaan naar de processen die plaatsvinden in skeletspieren tijdens verhoogde activiteit, is het mechanisme dat verantwoordelijk is voor de aanpassingen in de spier nog steeds niet opgehelderd.
Het in dit proefschrift beschreven onderzoek was gericht op de aanpassingen in spieren tijdens duurtraining, omdat duurtraining niet alleen van belang is voor een groter uithoudingsvermogen per se (de fysieke conditie), maar ook in algemene zin leidt tot aangenamer en gezonder leven; regelmatige duurtraining is belangrijk voor de preventie van hart- en vaatziekten

en ziekten als diabetes. Typische voorbeelden van duurtraining zijn hardlopen en wielrennen. Om tijdens het beoefenen van deze sporten spieronderzoek te kunnen doen is het nodig spierbiopten te nemen, een ingreep die belastend is voor proefpersonen. Bovendien zullen de verkregen resultaten alleen inzicht geven in een beperkt deel van de te onderzoeken spier, terwijl onbekend blijft wat er in de rest van de spier gebeurt. Om dit 'probleem' op te lossen, wordt in spieronderzoek veel gebruik gemaakt van proefdieren, vooral van ratten en muizen. Met de introductie van technieken voor het modificeren of onwerkzaam maken van individuele genen is vooral de muis een populair proefdier geworden om het effect van training op ziekten/ziekteprocessen te bestuderen. Om de resultaten correct te kunnen interpreteren is het van belang het loopgedrag van een 'normale' (wild-type) muis te kennen en te begrijpen in combinatie met de veranderingen en aanpassingen in de muizenspier.

In **hoofdstuk 2** wordt het effect van de twee meest gangbare trainingsmethodes bij muizen op de contractieparameters van de *extensor digitorum longus* (EDL) spier met elkaar vergeleken. De eerste trainingsmethode behelst het gedwongen lopen op een loopband, wat vergelijkbaar is met een continue duurloop bij mensen. De tweede methode geeft muizen vrij toegang tot een loopwiel, waarbij de dieren in hun eigen tempo kunnen lopen wanneer zij willen. Muizen uit de eerste groep (TRE) liepen zo 1,9 km per 24 uur, terwijl muizen in de tweede groep (RWE) gemiddeld 8,8 ± 0,2 km per 24 uur aflegden, wat een significant langere afstand was. Na zes weken werden de muizen opgeofferd en werd de snelle EDL spier vrij geprepareerd uit de achterpoot. Deze spieren werden daarna via een electrode gestimuleerd gedurende zes minuten bij frequenties oplopend van 0,5 tot 2,0 Hz. Bij lage stimulatie frequenties lieten de spieren in beide getrainde groepen een significant hogere krachtontwikkeling zien en een groter uithoudingsvermogen in vergelijking met een controle groep (CON). Echter, bij hogere frequenties was er geen verschil tussen de CON en RWE groep, terwijl de spieren in de TRE groep nog wel een beter uithoudingsvermogen lieten zien. Dit was opvallend aangezien de muizen uit de TRE groep slechts één derde van de afstand van de RWE groep hadden afgelegd. Vermoedelijk wordt dit verschil verklaard door het verschil in looppatroon; het gedwongen karakter van loopbandtraining lopen lijkt een zwaardere belasting voor muizen te zijn dan het vrijwillig lopen in een loopwiel.

Hoofdstuk 3 beschrijft het loopgedrag van muizen tijdens zes weken vrijwillige loopwiel training en het effect hiervan op de langzame *soleus* spier. Analyse van het loopgedrag toonde aan dat muizen gemiddeld 7,3 ± 0,5 km per nacht aflegden en een activiteitspatroon lieten zien vergelijkbaar met sprint-interval training bij de mens; intervallen die bestaan uit meerdere snelle sprintjes op hoge snelheid (2.4 km/h) van ongeveer 4 seconden. De gemiddelde snelheid was echter lager tijdens de eerste dagen van de studie wat kan duiden op gewenning aan het loopwiel.
Na zes weken werden de muizen opgeofferd en werd de *soleus* spier geïsoleerd. Seriële twitch contracties lieten ook nu weer een groter uithoudingsvermogen van de getrainde (RWE) spieren zien in vergelijking met spieren van de controle groep (SED). Opvallendst was echter dat de passieve, ongestimuleerde kracht bij aanvang van het stimulatieprotocol opliep in SED spieren en na ongeveer 30 seconden weer terug ging naar de nul-waarde. In RWE spieren liep deze kracht echter veel minder hoog op en bereikte ook sneller weer de uitgangswaarde. Verder was het zuurstofverbruik tijdens dit stimulatieprotocol 30% hoger in RWE spieren. Dit lijkt verband te houden met de 30% hogere kracht die geleverd wordt door deze spieren vergeleken met SED spieren. Het verhoogde zuurstofgebruik werd echter niet verklaard door een toegenomen mitochondriële capaciteit, wat erop duidt dat deze reeds ruim voldoende is.
De lagere ongestimuleerde kracht in RWE spieren duidt op een grotere capaciteit te ontspannen en dus op een verbetering van het mechanisme calcium terug te pompen in het sarcoplasmatisch reticulum (SR). De hoeveelheid en/of samenstelling van de Ca^{2+} pompen die ervoor zorgen dat Ca^{2+} naar het SR wordt terug gepompt (SERCA) was echter niet veranderd in de RWE spieren. SERCA wordt negatief gereguleerd door phospholamban (PLB) en sarcolipine (SLN). Onze studie liet een 60% afname van PLB mRNA en eiwit in de soleus spieren van RWE muizen zien. De remmende werking van PLB op SERCA wordt zo dus opgeheven, waardoor SERCA beter zal kunnen werken. Aan de andere kant zagen we juist een toename van SLN mRNA. Aangezien SLN op eenzelfde manier werkt als PLB, lijkt dit een compensatoir mechanisme, hoewel een stijging van SLN het effect van de daling in PLB op de snelheid van Ca^{2+} handling weer teniet zou doen.
Samenvattend lijkt het er dus op dat het discontinue looppatroon van muizen in de soleus spier zorgt voor herhaaldelijke afgifte van Ca^{2+} uit het SR die leidt tot een stijging van de Ca^{2+} concentratie in de cel en een toename

van de activiteit om dit terug te pompen in het SR. Loopwieltraining leidt dus tot veranderingen in Ca^{2+} huishouding van de langzame spieren.

In de voorafgaande studies werden steeds mannelijke C57Bl/6 muizen getraind vanaf de leeftijd van 4 tot en met 10 weken. Mannelijke muizen bereiken echter pas een 'volwassen' leeftijd rond 8 weken. Dit betekent dus dat de muizen tijdens de training nog in de ontwikkelingsfase waren. In **hoofdstuk 4** zijn daarom de gecombineerde effecten van leeftijd en loopwieltraining op de EDL en de soleus spieren bestudeerd. De studieopzet was gelijk aan die van hoofdstuk 3, alleen werden muizen nu ook opgeofferd aan het begin van de studie (SED0, leeftijd 4 weken) en tijdens de studie na 4 weken (SED4 en RWE4, leeftijd 8 weken) en na 6 weken (SED6 en RWE6, leeftijd 10 weken).
SERCA1, de meest voorkomende isovorm in snelle spieren, werd in geen van beide spieren beïnvloed door leeftijd of training. SERCA2 expressie veranderde in de soleus spier met name ten gevolge van het ouder worden, terwijl in de EDL spier veranderingen konden worden toegeschreven aan de training. In de EDL spieren werden geen veranderingen in PLB en SLN expressie waargenomen. In de soleus spier werd de verandering in SLN toegeschreven aan een leeftijdseffect onafhankelijk van training, terwijl PLB expressie werd beïnvloed door zowel leeftijd als training. Zodoende lijkt training de leeftijdsgebonden veranderingen tegen te gaan.
Veel studies naar spieradaptatie als gevolg van duurtraining maken gebruik van muizen die bij de start van het experiment 4 weken oud zijn. De resultaten in dit hoofdstuk tonen echter aan dat zowel leeftijd als training de spierontwikkeling beïnvloeden. Voor een correcte interpretatie van de gegevens is een longitudinale studie met de juiste controle groepen essentieel.

In **hoofdstuk 5** hebben we een uitgebreid genomisch profiel gemaakt van soleus en EDL spieren na 6 weken vrijwillige looptraining. mRNA geïsoleerd uit deze spieren werd met behulp van een affymetrix microarray chip gescreend. Dit resulteerde in een expressiepatroon van 45.000 genen die met behulp van een specifieke analyse methode (LIMMA) geanalyseerd werden. Dit resulteerde in een lijst van genen gerangschikt op basis van 'de waarschijnlijkheid dat de expressie veranderd was'. Van deze lijst werd de top 50 van de verhoogde en top 50 van de verlaagde genen geselecteerd. Aan de hand van hun functie werden deze voor zover mogelijk vervolgens ingedeeld in functionele clusters.

In RWE soleus spieren waren 3 functionele clusters te onderscheiden: 1) verhoogde Ca^{2+} signalering, 2) verbeterd glucosemetabolisme en energiehuishouding en 3) veranderde spiercel differentiatie. De veranderde genen in RWE EDL spieren hielden voornamelijk verband met spiercel differentiatie.
Deze resultaten tonen aan dat snelle en langzame spieren anders reageren op loopwieltraining. De clusters die we vonden in soleus spier (Ca^{2+} huishouding en energiemetabolisme) komen overeen met eerdere resultaten beschreven in hoofdstuk 3. In beide spieren behelsden de veranderingen ook genen geassocieerd met spiercel differentiatie. Hoewel wij eerder geen directe aanwijzingen vonden voor fenotypische veranderingen (omvang, MyHC profiel) in deze spieren tonen deze resultaten dat er toch veranderingen plaatsvinden, vermoedelijk meer op een regulatoir niveau.

Interleukine-6 (IL-6) is een cytokine dat een rol speelt bij de immuun respons. Recentelijk is echter gesuggereerd dat dit cytokine ook een rol zou kunnen spelen tijdens duurtraining, zonder dat er spierschade optreedt. In dit verband wordt gespeculeerd over het verbeteren van het energie metabolisme door het vrijmaken van substraten. In **hoofdstuk 6** wordt het effect van 6 weken vrijwillige looptraining op IL-6 plasma productie en mRNA expressie in achterpootspieren van de muis beschreven.
In het plasma vonden wij geen effecten van training op de expressie van IL-6. Wel vonden wij een zesvoudige toename van het IL-6 in plasma met het toenemen van de leeftijd. Deze leeftijdsafhankelijke toename is eerder ook beschreven bij de mens en wordt toegeschreven aan een toegenomen IL-6 productie door perifere mononucleaire cellen in het bloed.
Hoewel alle 5 de achterpootspieren (tibialis, EDL, gastrocnemius, soleus en plantaris) van de muis werden geanalyseerd, vonden wij alleen in de soleus spier een significante toename van IL-6 mRNA expressie na training. In alle andere spieren bleef de expressie dus gelijk.
In een eerdere studie werd een verhoogde plasma IL-6 concentratie in muizen alleen gevonden na intensieve, verplichte loopbandtraining, terwijl dit niet werd gevonden na een milde training. De data in onze studie lijken aan te tonen dat vrijwillige loopwieltraining een milde vorm van training is en dat IL-6 expressie slechts een beperkte rol speelt in dit trainingsmodel.

In **hoofdstuk 7**, ten slotte, worden alle bevindingen uit de eerdere hoofdstukken op een rij gezet en bediscussieerd. Als eerste concluderen we –zoals ook al duidelijk werd in hoofdstuk 2- dat gedwongen, continu rennen meer

effect heeft op de snelle EDL spier dan vrijwillige looptraining in muizen. Zoals uit hoofdstuk 3 duidelijk werd, bestaat vrijwillige loopwieltraining uit meerdere korte sprints met zeer hoge snelheden. Het lijkt dus dat het gedwongen karakter meer belasting oplevert dan vrijwillige beweging. In eerdere studies bij mensen blijkt juist dat sprint interval training meer positieve effecten heeft op de spieren en op het uithoudingsvermogen dan een training bestaande uit langdurige, continue belasting. Verder vertoont de soleus spier adaptaties op het gebied van Ca^{2+} huishouding, energie metabolisme en cel cyclus regulatie, terwijl in de EDL spier voornamelijk aanpassingen plaatsvinden in de regulatie van de celcyclus.
Al met al kunnen we concluderen dat het extrapoleren van data op het gebied van duurtraining in muizen naar de mens voorlopig nog niet goed mogelijk is. De resultaten tussen sprint-interval en continue looptraining in mens en muis laten een dusdanige discrepantie zien dat aangenomen mag worden dat adaptatieprocessen in skeletspieren van deze zoogdieren ook zal verschillen. Verder konden wij geen verschillen in myosine expressie en mitochondriële capaciteit aantonen, terwijl dit in humane studies vrijwel altijd wordt gevonden. Het lijkt dat het myosine profiel van skeletspieren van muizen vrij robuust is en dat de spieren reeds zijn aangepast aan intensieve duurtraining. Ten slotte speelt het verschil in controle groep mogelijk een rol; in onze studies werden de controle muizen relatief beperkt in hun mogelijkheden tot natuurlijk loopgedrag, terwijl in humane studies vaak gebruik wordt gemaakt van 'normaal actieve personen'.
Samenvattend kunnen wij aan de hand van deze studie concluderen dat achterpoot spieren van muizen wel degelijk veranderen gedurende duurtraining, maar in mindere mate dan andere zoogdieren. Verplichte loopband en vrijwillige loopwiel training lieten verschillende uitkomsten zien op de snelle EDL spier, maar verder onderzoek is nodig naar de effecten van beide op de langzame soleus spier. De combinatie van functionele, metabole en genetische analyses liet een verschillende adaptatie zien van deze twee spieren aan loopwieltraining. Hoewel wij anders hadden verwacht, vertoonde de langzame soleus spier de meeste aanpassing aan deze training. Al met al blijkt de vrijwillige loopwieltraining in muizen een effectieve, laagintensieve methode om duurtraining-geassocieerde adaptatie in skeletspieren van dit specifieke dier te induceren.

Dankwoord

‘Eeuwige roem’

HET DANKWOORD; het meest gelezen onderdeel van een proefschrift. Al jaren denk je er over na wat er in moet komen te staan, maar nu het eenmaal zo ver is, is het een uitdaging iedereen in een aantal woorden tot zijn of haar recht te laten komen. De afgelopen vijf jaar is er zo veel gebeurd dat het onmogelijk zal worden alles en/of iedereen op te noemen en te bedanken. Maar een wetenschapper zoekt altijd weer naar mogelijkheden.

Allereerst dr. Jeneson. Beste Jeroen, zonder jou zou dit boekje er nooit zijn gekomen. Jij hebt het onderzoeksvoorstel geschreven en mij de eerste anderhalf jaar uitstekend voorbereid op het leven als onderzoeker. Velen hebben het al gezegd en ook ik wil hier weer benadrukken dat jouw enthousiasme een bijzondere gave is. Met jouw vertrek naar de Technische Universiteit Eindhoven heb je helaas een grote leegte achter gelaten, maar ik blijf gelukkig met goede herinneringen achter waaronder een beperkt wetenschappelijke: Surfing the Pacific!
Daarnaast mijn promotor prof. dr. Everts. Beste Marjanne, met het vertrek van Jeroen kwam de druk steeds meer op jouw schouders te liggen. Het was voor ons beide even wennen aan de veranderde situatie en rolverdeling, maar ik geloof dat we ons hier goed doorheen hebben geslagen. Enkele wijze lessen zullen mij altijd bij blijven en mijn verdere carrière ten goede komen.

Dan de anatomen&fysiologen en in het bijzonder de 'muizenmensen' van het eerste uur op de faculteit. Arend, met een klassiek muziekje op de achtergrond spieren prepareren en alle 'actualiteiten' doornemen: mocht je ooit een andere baan willen dan zou je het bij de Story goed doen. Los hiervan is het geweldig hoe je altijd voor iedereen klaar staat, al dan niet voorzien van een goede grap. Dank voor al je steun bij de verzorging van onze muizen en meer. Arie, ook al heeft onze samenwerking veel te kort geduurd, zonder jou zou ik nooit zover zijn gekomen. Bedankt voor alle Labview analyses en verfijning van de software. Jouw bijdrage was van essentieel belang bij mijn boekje. Brian, ook jij was juist in het begin van essentiële waarde voor alle essays. Jouw precisie is een ongekend goed. Peter, al ben je natuurlijk meer bekend als de PCR man, de meeste herinneringen heb ik aan onze western blots. Hoeveel pech hebben wij daar wel niet mee gehad. Maar ik ben blij dat je meedacht en altijd maar weer meeging in nog meer pogingen. Ingrid, officieel werkten we natuurlijk niet samen, maar het is fantastisch hoe je altijd met iedereen meedenkt; zelfs op je 'mama-dag' nog links sturen naar interessante artikelen met weer nieuwe ideeën!

Naast deze 'muizenmensen' zijn er vele andere lieve collega's die deze vijf jaar verrijkt hebben. Ineke, vooral de laatste paar maanden ben jij weer eens van onschatbare waarde gebleken voor mijn boekje. Maar de overige jaren waren minstens zo bijzonder. Dank dat je die kronkel bij me hebt weten te ontdekken. Ik hoop dat ik er in mijn latere leven nog veel aan zal hebben, al zal dat vast wel niet.

Eva: Jammer dat het varen in de Amsterdamse grachten er niet meer van gekomen is, maar wie weet wat de toekomst nog brengt. Bier drinken in Göttingen is een prima alternatief!
Sander en Richard: Nooit zal ik ons wadloopavontuur vergeten. Memory spelen, bedorven Liga's eten en om 5 uur 's morgens op de dijk staan. Je moet wel erg gek zijn daar nog van te genieten ook. En Richard: ik kom zeker nog een keer het grint aanharken!

Als laatste genoemd van de collega's, en toch het belangrijkst: mijn kamergenoten en mede-lotgenoten Nancy, Maarten en Miriam: Wat hebben wij een bijzondere tijd gehad. Het was fijn lief en leed te kunnen delen, alle ups & downs samen te beleven en er vooral voor elkaar te zijn. De mooiste herinneringen zijn gelukkig de leukste: Het M-team in München… Geweldig! Stropdas los, bril af en gaan. Het blijkt maar weer: soms loont het om eigenwijs te zijn!

Natuurlijk ben ik de overige collega's niet vergeten, maar het zijn/waren er teveel om allemaal persoonlijk op te noemen. Gelukkig woon ik nog om de hoek, dus ik kom gewoon een paar keer een kop thee drinken voor jullie gezelligheid!

'Mijn' stagiaires: Charissa en Marjolein. Wat heb ik een geluk met jullie gehad! Allebei hebben jullie een geweldige bijdrage aan mijn onderzoek weten te leveren, maar jullie hebben ook een hoop gezelligheid op het lab gebracht. Charissa, nog even doorbikkelen en dan ben jij ook zover. Alvast heel veel succes met de laatste loodjes. Marjolein, voor drie maanden een project, maar daarna nog bedelen om meer werk. Heel bijzonder!
De stagiaires die *en passant* ook even mijn muizen verzorgden: Krista, Iris en Gaby. Bedankt voor alles!

Cas, zonder jou zou het microarray hoofdstuk een grote rotzooi zijn, als het me al zou zijn gelukt hier iets van te maken. Geweldig hoeveel tijd je voor me wist vrij te maken om zo al die duizenden genen te analyseren. Natuurlijk altijd met een kop 'T' bij 'R' ;-)

Anton: niet *echt* een collega, maar wel van onschatbare waarde! Niet alleen voor de gezelligheid op borrels en de muzikale omlijsting bij het kerstdiner, maar vooral de aller, allerlaatste fase: De afronding van het boekje. Nu ik

dit schrijf weet ik natuurlijk nog niet hoe het uiteindelijke resultaat is geworden, maar de ervaring leert dat het de verwachting overtreft!

En dan natuurlijk nog een hele rij vrienden die er altijd waren voor de nodige ontspanning. De beste methode om alle zorgen overboord te gooien!
P-mannen en –vrouwen: Van wintersport tot koninginnedag, van terrasjes en etentjes tot Lokaal 9 (what's next?). Heerlijk om zo'n club vrienden om je heen te hebben. Els en Meg: Nog maar een paar maanden en dan kunnen we weer aan de Unagi en Hup Sake!
Nienke en Jurgen: 'Beter een goede buur dan een verre vriend'. Wat als die vrienden gewoon om de hoek wonen?
Henriëtte: Van Buuf tot vriendin… We wonen niet meer samen, maar je blijft gewoon een schat.
Het Argilla team in al haar samenstellingen. Van trio tot kwintet en 'alles' wat daar maar tussenvalt. "We zijn eigenlijk een (trio /kwartet/symfonieorkest) maar de tweede viool is ziek". Het lukt niet veel gezelschappen zo regelmatig te spelen, maar wij hebben heel wat afreageeruurtjes doorgebracht. Hopelijk lukt het in 2009 ook nog een keer samen te spelen ;-) Sowieso wordt het nog een keer tijd voor een Westmalle-met-tijgernoten-en-hachee-date.
De 'prutsers' voor de nodige ontspanning op het water. Elk jaar in wisselende samenstelling het water op. Van Friese dorpjes tot Almere Haven, we kunnen het allemaal aan. Want: "Prutsers kunnen beter in de haven blijven"!

Mijn nieuwe collega's bij NWO-CW/ACTS. Het balletje bleek weer eens raar te kunnen lopen, maar ik ben blij dat ik bij jullie terecht kwam. Nog maar net bij jullie aan het werk en nu al voel ik me helemaal 'thuis'.

Mijn paranimfen!
Marieke: Al leer je nog zoveel tijdens studies en opleidingen, die paar maanden met jou Down Under waren pas echt een leerervaring. Wat er ook gebeurt: She'll be 'right, mate en natuurlijk bugger all! Wat een fijn idee dat je achter me zult staan. En komende jaren kruipen we in februari gewoon weer in die tent, ondanks de steeds warmere winters: hebben we daarvoor een donzen slaapzak gekocht…
Anne: Wat heb jij de afgelopen 5 jaar met me meegeleefd in zware en mooie tijden! Hoe ver weg je ook was, altijd weer een SMSje of een kaartje. En dan ook nog elke week afreageren en bijkletsen op de fiets. Tandje hoger! En

Haakon, je wilde ook graag een keer in een dankwoord genoemd worden, dus bij deze: Bedankt dat je je die avond in de Kosten Koper liet koppelen!

En dan mijn familie. Al zwerven we allemaal over de wereld, we vinden altijd wel een momentje om elkaar een keer te zien. Waar dan ook. Eva, Ryan & Nils: de 'verplichte' reisjes naar New York maken een hoop goed. Ik ben blij dat jullie er deze belangrijke dag ook bij zullen zijn! Femke, Ties, Arvid & Lasse: in jullie drukke bestaan ook nog tijd vrijmaken voor 'de jongste'. Avondjes/weekendjes oppassen blijkt heerlijk ontspannend (???) en in elk geval erg relativerend. Ik bouw graag nog snel wat credits op…
Pap & mam: Rotsen in de branding. Jullie hebben me altijd de vrijheid gegeven (of heb ik die gewoon genomen?), maar op de cruciale momenten zijn jullie er altijd. Hopelijk breken nu iets rustiger tijden aan en lukt het me wat vaker langs te komen. En pap: Medische biologie bleek toch een goed alternatief :-)

Tjerk, guapo, waar moet ik beginnen? Dank voor alles wat je bent, wie je bent en wat je doet. Je hulp bij dip(je)s, je morele steun, de mooie discussies, de PWPtjes. Ik zou willen zeggen dat rustiger tijden vanaf nu aanbreken, maar we weten wel beter… Als jij zover bent, ben ik er voor jou! Al hebben we dan wel versterking ☺

Appendix

Curriculum Vitae
List of publications

A

MAARTJE DE SNOO was born May 13th 1978 in Groningen. She graduated from the Praedinius Gymnasium in Groningen in 1996, and continued at Utrecht University to study biomedical sciences. Her first internship investigated the role of the interleukin-4-recepter in heart transplantation under supervision of dr. Roel de Weger and dr. Femke Bijlsma at Pathology of the UMC Utrecht. Her final internship focused on the role of pneumococcal immune adherence in neonatal erythrocytes under supervision of dr. André Fleer and dr. Jeanne-Marie Hament at the Eykman Winkel for microbiology at UMC Utrecht. She obtained her doctoral exam in 2002. After several months of travelling, she worked at the educational department of the UMC Utrecht. In June 2004 she commenced her PhD project on mouse skeletal muscle adaptation in response to endurance exercise under supervision of prof. dr. Marjanne Everts and dr. Jeroen Jeneson at the department of animal science at Utrecht University. In 2009 the finished this project with her thesis defence on June 24th of that same year. At present, Maartje works as programme manager at NWO, the Netherlands Organisation for Scientific Research.

MAARTJE DE SNOO werd op 13 mei 1978 geboren te Groningen. Na het behalen van haar diploma aan het Praedinius Gymnasium te Groningen in 1996, vertrok ze naar de Universiteit van Utrecht om Medische Biologie te studeren. Haar eerste onderzoeksstage naar de rol van de interleukine-4-receptor bij harttransplantaties deed zij bij dr. Roel de Weger en dr. Femke Bijlsma bij de afdeling Pathologie van het UMC Utrecht. Haar afstudeerstage naar de rol van pneumococcen adherentie bij neonatale kinderen deed zij bij dr. André Fleer en dr. Jeanne-Marie Hament bij het Eijkman Winkler voor microbiologie bij het UMC Utrecht. In 2002 sloot ze deze opleiding af met het doctoraal examen. Na enkele maanden over de wereld te hebben rondgetrokken, heeft ze bij het onderwijsinstituut van het UMC Utrecht gewerkt. In juni 2004 begon ze haar promotieonderzoek aan de faculteit diergeneeskunde van de Universiteit Utrecht. Dit onderzoek naar skeletspieradaptatie bij muizen ten gevolge van duurtraining voerde zij uit onder begeleiding van prof. dr. Marjanne Everts en dr. Jeroen Jeneson. Dit project werd in 2009 afgerond met de eigenlijke promotie op 24 juni van datzelfde jaar. Op dit moment werkt Maartje als beleidsmedewerker bij NWO, de Nederlandse Organisatie voor Wetenschappelijk Onderzoek.

Publications

Treadmill but not wheel running improves fatigue resistance of isolated extensor digitorum longus muscle in mice.
JAL Jeneson, MW de Snoo, NA Verlinden, BJLJ Joosten, A Doornenbal, A Schot, ME Everts. Acta Physiol 2007; **190(2)**: 151-161

Crucial role of the Interleukin-4 receptor in acute rejection after clinical heart transplantation
FJ Bijlsma, MW de Snoo, J van Kuik, DF van Wichen, N de Jonge, MGJ Tilanus, FH Gmelig-Meyling, RA de Weger. In: "T-helper 2 cytokines in acute allograft rejection after heart transplantation", Thesis dr. ir. F.J. Bijlsma, chapter 5

Pneumococcal immune adherence to human erythrocytes
JM Hament, H van Dijk, A Fleer, PC Aerts, M Schoenmakers, MW de Snoo, BH Dekker, JL Kimpen, TF Wolfs. Eur J Clin Invest 2003; **33(2)**: 169-175. Further in: "The pathogenesis of *S. pneumoniae* infections", Thesis dr. J.M. Hament, chapter 7

Conferences

Phospholamban expression in mouse soleus muscle is downregulated after chronic running wheel exercise
MW de Snoo, ME Everts, BJLJ Joosten, A Doornenbal, A Schot, JAL Jeneson. FASEB J 2008; **22 (meeting abstracts)**: 961.9 (Oral + Poster presentation)

Genetic profiling of wheel running exercise-induced adaptation of mouse soleus muscle
MW de Snoo, C Kruitwagen, PWA Cornelissen, JAL Jeneson, ME Everts. FASEB J 2008; **22 (meeting abstracts)**: 962.11 (Poster presentation)

Electrical interval stimulation improves calcium handling rapidly but transiently in isolated mouse soleus muscle
MW de Snoo & JAL Jeneson. FASEB J 2006; **20(4)**: A807 (Poster presentation)

Voluntary wheel-running exercise in mice involves periodic burst activity and causes muscle adaptations supporting cation homeostasis
MW de Snoo, BJLJ Joosten, A Doornenbal, A Schot, ME Everts, JAL Jeneson (Oral + Poster presentation). Acta Physiologica 2006; **186(1)**: 64

Wheel-running in mice involves periodic burst activity and causes muscle adaptation supporting cation homeostasis
MW de Snoo, BJLJ Joosten, A Doornenbal, A Schot, ME Everts, JAL Jeneson. FASEB J 2005; **19(4)**: A132 (Poster presentation)